RESEARCH AND DEVELOPMENT ON APPLICATION OF BIOLOGICAL NANO TECHNOLOGY FOR ORGANIC CITRUS AND DURIAN

PHEAKTRA PHAL

A THESIS SUBMITTED IN FULFILLMENT OF THE REQUIREMENT FOR THE DEGREE OF DOCTOR OF PHILOSOPHY IN AGRICULTURE

SCHOOL OF AGRICULTURAL TECHNOLOGY

KING MONGKUT'S INSTITUTE OF TECHNOLOGY LADKRABANG

2024

KMITL-2024-AG-D-064-046

This material is reserved for educational use only, not allowed for commercial use.
Forbidden to modify the content, and cite the document when use.

COPYRIGHT 2024
SCHOOL OF AGRICULTURAL TECHNOLOGY
KING MONGKUT'S INSTITUTE OF TECHNOLOGY LADKRABANG

This material is reserved for educational use only, not allowed for commercial use.
Forbidden to modify the content, and cite the document when use.

หัวข้อวิทยานิพนธ์	การวิจัย และ พัฒนาการประยุกต์ใช้เทคโนโลยีชีวภาพสำหรับ การปลูกส้ม และ ทุเรียนอินทรีย์
นักศึกษา	Pheaktra Phal
รหัสประจำตัว	62604009
ปริญญา	ปรัชญาดุษฎีบัณฑิต
สาขา	เกษตรศาสตร์
พ.ศ.	2567
อาจารย์ที่ปรึกษาวิทยานิพนธ์	รศ.ดร. เกษม สร้อยทอง
อาจารย์ที่ปรึกษาวิทยานิพนธ์ร่วม	รศ.ดร. สุพัตรา โพธ์เอี่ยม

บทคัดย่อ

Phytophthora palmivora PYSC01 เป็นเชื้อราสาเหตุของโรคเน่าของทุเรียน และ *Colletotrichum gloeosporioides* เป็นเชื้อราสาเหตุโรคแอนแทรคโนสของทุเรียน และ ส้ม ที่ถูกแยกจากทุเรียน และ ส้มที่ติดเชื้อ และได้รับการพิสูจน์ว่าเป็นเชื้อราสาเหตุโรคทุเรียนและส้มด้วยวิธี Koch's postulate โดยเชื้อปฏิปักษ์ ได้แก่ *Chaetomium lucknowense* CL *Trichoderma hamatum* K01 และเชื้อราสาเหตุโรคพืช ได้แก่ *P. palmivora* PYSC01 *C. gloeosporioides* C01และ *C. gloeosporioides* C02 ได้รับการพิสูจน์โดยสัณฐานวิทยาและโมเลกุล

Ch. lucknowense CL และ *T. hamatum* K01 เป็นปฏิปักษ์ต่อเชื้อรา *P. palmivora* PYSC01 และ *C. gloeosporioides* ในการทดลองเลี้ยงเชื้อร่วมกันบนอาหารเลี้ยงเชื้อ *T. hamatum* K01 สามารถยับยั้งการเจริญของเส้นใย เละ ยับยั้งการสร้างสปอร์ของ *P. palmivora* PYSC01 และ *C. gloeosporioides* มีค่าระหว่าง 58% ถึง 70% และ 79% ถึง 92% ตามลำดับ และ *Ch. lucknowense* CL สามารถยับยั้งการเจริญของเส้นใยมีค่าระหว่าง 48% ถึง 52% และ ยับยั้งการสร้างสปอร์มีค่าระหว่าง 64% ถึง 94% และพบว่าสารสกัดจาก *T. hamatum*

This material is reserved for educational use only, not allowed for commercial use.
Forbidden to modify the content, and cite the document when use.

K01 ที่สกัด ด้วยเมทานอล แสดงผลที่ดีที่สุดในการยับยั้ง *P. palmivora* PYSC01 และ *C. gloeosporioides* โดยเส้นใยถูกยับยั้งที่ค่า ED_{50} ระหว่าง 288 ถึง 273 ppm และ การสร้างสปอร์ถูกยับยั้งที่ค่า ED_{50} ระหว่าง 355 ถึง 118 ppm สำหรับสารสกัดจาก *Ch. lucknowense* CL ที่สกัดด้วย เอทิล อะซิเตรท แสดงการยับยั้ง *P. palmivora* และ *C. gloeosporioides*ได้ดีที่สุด โดยยับยั้งการเจริญของเส้นใยมีค่า ED_{50} อยู่ในช่วง 197 ถึง 95 ppm และ ยับยั้งการสร้างสปอร์มีค่า ED_{50} อยู่ในช่วง 37 ถึง 13 ppm

นอกจากนี้ ผลิตภัณฑ์ธรรมชาตินาโนไฟเบอร์ที่ได้จาก *T. hamatum* K01 และ *Ch. lucknowense* CL แสดงฤทธิ์ต้านทานต่อ *C. gloeosporioides* และ *P. palmivora* โดยเฉพาะนาโนไฟเบอร์จาก *T. hamatum* K01 ที่ได้จากสารสกัดหยาบจากตัวทำละลายเมทานอล แสดงผลยับยั้งการเจริญของเส้นใย และยับยั้งการสร้างสปอร์ดีที่สูงสุดต่อทั้ง *C. gloeosporioides* และ *P. palmivora* ด้วยค่า ED_{50} ตั้งแต่ 14 ถึง 11 ppm และ 3 ถึง 2 ppm ตามลำดับ รวมทั้งประสิทธิภาพ นาโนไฟเบอร์จาก *Ch. lucknowense* CL ในการยับยั้ง *C. gloeosporioides* และ *P. palmivora* โดยนาโนไฟเบอร์ที่ได้จากสารสกัดหยาบจากตัวทำละลายเอทิล อะซิเตรท มีประสิทธิภาพดีที่สุด ในการยับยั้งการเจริญเติบโตของเส้นใย และ ยับยั้งการสร้างสปอร์ของเชื้อสาเหตุโรคทั้งหมดถึง 100% ที่ความเข้มขนเพียง 3 ppm เท่านั้นโดยมีค่า ED_{50} สำหรับการยับยั้งการเจริญ และ ยับยั้งการสร้างสปอร์เท่ากับ 2 ppm

การทดลองในโรงเรือน ด้วยการใช้สารสกัดหยาบและนาโนไฟเบอร์ (สารสกัดหยาบจาก *Ch. lucknowense* CL และ *T. hamatum* K01 และ นาโนไฟเบอร์จาก *Ch. lucknowense* CL และ *T. hamatum* K01) พบว่าพืชสามารถสร้าง phytoalexins ได้แก่ scopoletin ที่มีค่า R_f ที่ 0.77 ใน 12% กรดอะซิติก ของทุเรียน และ scoparone ที่มีค่า R_f เท่ากับ 0.58 ใน toluene:ethyl acetate (1:1) ของส้ม ซึ่งเป็นสารกระตุ้นให้เกิดระบบภูมิคุ้มกันของพืช

This material is reserved for educational use only, not allowed for commercial use.
Forbidden to modify the content, and cite the document when use.

นอกจากนี้การใช้สารสกัดหยาบและนาโนไฟเบอร์ยังสามารถลดความรุนแรงของโรคแอนแทรคโนสในส้ม และ ทุเรียนที่เกิดจาก *C. gloeosporioides* และ โรคเน่าของทุเรียนที่เกิดจาก *P. palmivora* อย่างมีนัยสำคัญเช่นเดียวกับสาร metalaxyl นาโนไฟเบอร์จาก *T. hamatum* K01 มีประสิทธิภาพในการลดความรุนแรงของโรคแอนแทรคโนสและโรคเน่าทุเรียนถึง 99.16% และ โรคแอนแทรคโนสส้ม 99.13% ตามด้วยสาร metalaxyl 92.08% และ 96.6% นาโนไฟเบอร์จาก *Ch. lucknowense* CL ที่ 95.41% และ 98.72%, ผลิตภัณฑ์จาก *T. hamatum* K01 90% และ 97.50% และผลิตภัณฑ์จาก *Ch. lucknowense* CL ที่ 86.66% และ 93.30% ตามลำดับ

รวมทั้งการใช้สารสกัดหยาบและนาโนไฟเบอร์ยังสามารถเพิ่มปริมาณเม็ดสีที่เกี่ยวข้องกับการสังเคราะห์แสงในส้มและทุเรียนได้ โดยนาโนไฟเบอร์จาก *T. hamatum* K01 มีประสิทธิภาพดีที่สุด โดยมีค่าปริมาณคลอโรฟิลเท่ากับ 25.98 ไมโครกรัมต่อกรัม และ ปริมาณแคโรทีนอยด์ที่มีค่าที่ 3.70 ไมโครกรัมต่อกรัม โดยที่ปริมาณคลอโรฟิล และ แคโรทีนอยด์ที่ต่ำที่สุดในกลุ่ม negative control ที่มีค่า 8.07 ไมโครกรัมต่อกรัม และ 1.65 ไมโครกรัมต่อกรัม ตามลำดับ อย่างไรก็ตาม การสังเคราะห์แสงของส้มได้รับผลโดยตรงจากการได้รับของนาโนไฟเบอร์จาก *T. hamatum* K01 ซึ่งมีปริมาณคลอโรฟิลเท่ากับ 15.98 ไมโครกรัมต่อกรัม และ แคโรทีนอยด์คำนวณได้เป็น 0.78 ไมโครกรัมต่อกรัม ในเวลาเดียวกัน ปริมาณคลอโรฟิลและแคโรทีนอยด์ที่ต่ำที่สุดในกลุ่ม negative control มีค่า 6.13 ไมโครกรัมต่อกรัม และ 0.16 ไมโครกรัมต่อกรัม ตามลำดับ

ในการศึกษาด้านการการเจริญเติบโตของพืชเกี่ยวกับความสูงของต้นทุเรียนพบว่าต้นมีความสูงเพิ่มมากขึ้นอย่างมีนัยสำคัญหลังจากการใช้สารป้องกันทางการเกษตรแล้วในวันที่ 120 โดยพืชที่ได้รับนาโนไฟเบอร์จาก *T. hamatum* K01 แสดงผลดีที่สุดสามารถเพิ่มความสูงของต้นทุเรียนที่ 82 ซม ตามด้วยนาโนไฟเบอร์จาก *Ch. lucknowense* CL ที่ 81 ซม ผลิตภัณฑ์จาก *Ch.*

This material is reserved for educational use only, not allowed for commercial use.
Forbidden to modify the content, and cite the document when use.

lucknowense CL มีค่าความสูงที่ 76.75 ซม สาร metalaxyl 76 ซม ผลิตภัณฑ์จาก *T. hamatum* K01 ที่74 ซม และ positive control มีความสูง72 ซม เมื่อเปรียบเทียบกับ negative control ที่มีค่ามีความสูงน้อยที่สุดคือ 53.25 ซม อย่างไรก็ตาม ความสูงของต้นส้มไม่แตกต่างกันย่างมีนัยสำคัญ โดยนาโนไฟเบอร์จาก *T. hamatum* K01 ให้ผลดีที่สุดต่อความสูงของต้นส้มที่ 76.50 ซม ในขณะเดี่ยวกันผลกระทบต่ำสุดสังเกตเห็นได้ใน negative control ที่มีความสูง 51.75 ซม

กลไกการควบคุมทั้งความสามารถในการยับยั้งการเจริญของเชื้อสาเหตุโรคในพืช และการส่งเสริมการเจริญเติบของพืชได้รับการยืนยันจากเมตาบอไลต์ของ *T. hamatum* K01 โดยพบการผลิต pyrone (6-pentyl-2H-Pyran-2-one) sorbicillin และ fatty acid และ สารเมตาบอไลต์ของ *Ch. lucknowense* CL ที่พบสารออกฤทธิ์ทางชีวภาพ เช่น aliphatic volatile (hexadecanoic acid, 9, 12-Octadecadienoic acid (Z), and Octadecanoic acid) และการศึกษานี้เป็นการรายงานครั้งแรกว่า pyrone (6-pentyl-2H-Pyran-2-one) sorbicillin และ fatty acid และ hexadecanoic acid, 9, 12-Octadecadienoic acid (Z) และ Octadecanoic acid จากเมตาบอไลต์ของ *Ch. lucknowense* CL สามารถยับยั้งการเจริของ *P. palmivora* และ *C. gloeosporioides* ได้ นอกจากนี้ นาโนไฟเบอร์จาก *T. hamatum* K01 ได้รับการรายงานครั้งแรกว่าสามารถยับยั้งการเจริญของ *P. palmivora* และ *C. gloeosporioides* ที่เป็นสาเหตุของโรคเน่าและ โรคแอนแทรคโนสทุเรียน

This material is reserved for educational use only, not allowed for commercial use.
Forbidden to modify the content, and cite the document when use.

Thesis	Research and Development on Application of Biological Nano Technology for Organic Citrus and Durian
Student	Mr. Pheaktra Phal
Student ID	62604009
Degree	Doctor of Philosophy
Program	Agriculture
Year	2024
Thesis Advisor	Assoc. Prof. Dr. Kasem Soytong
Thesis Co-Advisor	Assoc. Prof. Dr. Supattra Poeaim

ABSTRACT

Phytophthora palmivora is known as a causal agent of durian rot, and *Colletotrichum gloeosporioides* is known as a causal agent of durian and citrus anthracnose, which were isolated from infect durian and citrus, and they were proved to be a serious threat to durian and citrus plantations, which were confirmed by the Koch's postulate. Morphology and molecular phylogenetic identification confirmed the antagonistic species *Chaetomium lucknowense* CL and *Trichoderma hamatum* K01 and pathogenic isolates, *C. gloeosporioides* C01, *C. gloeosporioides* C02 and *P. palmivora* PYSC01. Antagonistic fungi, *T. hamatum* K01 and *Ch. lucknowense* CL, were proved to have antagonistic activities against *P. palmivora* PYSC01and *C. gloeosporioides* in the bi-culture test. *T. hamatum* K01 inhibited colony growth and reduced sporulation of *P. palmivora* and *C. gloeosporioides* between 58% to 70% and 79% to 92%, respectively. *Ch. lucknowense* Cl suppressed colony growth between 48% and 52% and suppressed sporulation between 64% and 94%. Metabolites crude methanol extract from *T. hamatum* K01 showed the best inhibitory effect against *P. palmivora* PYSC01 and *C. gloeosporioides*, in which the colony growth was inhibited at ED_{50} values ranging from 288 to 273 ppm, and sporulation was inhibited at ED_{50} values ranging from 355 to 118 ppm. The crude metabolites from *Ch. lucknowense* Cl extracted by ethyl acetate exhibited the highest antifungal activity against *P. palmivora* and *C. gloeosporioides*, the ED_{50}

This material is reserved for educational use only, not allowed for commercial use.
Forbidden to modify the content, and cite the document when use.

values were computed at ranging from 197 to 95 ppm on colony growth inhibition, and the ED_{50} values were computed at ranging from 37 to 13 ppm, on sporulation inhibition.

Furthermore, natural product nanofibers derived from *T. hamatum* K01 and *Ch. lucknowense* CL exhibited antibiotic activity against *C. gloeosporioides* and *P. palmivora*. Specifically, nanofibers derived from *T. hamatum* K01, loaded with crude methanol, demonstrated the highest potency in inhibiting the colony growth and sporulation of *C. gloeosporioides* and *P. palmivora*, with ED_{50} values ranging from 14 to 11 ppm and 3 to 2 ppm, respectively. Additionally, nanofibers from *Ch. lucknowense* CL exhibited excellent antimicrobial activity against *C. gloeosporioides* and *P. palmivora*. Notably, nanofibers loaded with crude ethyl acetate displayed the most effective spectrum of antifungal activity, inhibiting the colony growth and sporulation of all test pathogens by 100% at a concentration of only 3 ppm. The ED_{50} values for colony growth and sporulation suppression of the pathogens were computed at 2 ppm or even lower.

Under greenhouse trials, applying of agricultural inputs (*Ch. lucknowense* CL and *T. hamatum* K01 products and nanofibers from *Ch. lucknowense* Cl and *T. hamatum* K01) were found to produce phytoalexins, namely scopoletin with R_f values of 0.77 in 12% acetic acide of durian and scoparone with R_f value of 0.58 in toluene:ethyl acetate (1:1) of citrus which is known the defense mechanism or elicitor for plant immunity. Moreover, treatment of agricultural inputs (*Ch. lucknowense* CL and *T. hamatum* K01's products and nanofibers from *Ch. lucknowense* Cl and *T. hamatum* K01) significantly reduced the disease severity of citrus and durian anthracnose caused by *C. gloeosporioides* and durian rot caused by *P. palmivora*, same as chemical metalaxyl compared to negative control. Nanofiber from *T. hamatum* K01 was effective in reducing disease severity of durian anthracnose and durian rot by 99.16% and citrus anthracnose 99.13%, followed by chemical metalaxyl 92.08% and 96.67%, nanofiber from *Ch. lucknowense* CL 95.41 and 98.72%, *T. hamatum* K01 products 90% and 97.50%, and *Ch. lucknowense* CL product 86.66% and 93.30%, respectively.

Additionally, the application of agricultural inputs significantly affected citrus and durian photosynthesis pigments. Among these, Nanofiber from

This material is reserved for educational use only, not allowed for commercial use.
Forbidden to modify the content, and cite the document when use.

T. hamatum K01 was the most effective on chlorophyll content at 25.98 µg/g, carotenoids and content at 3.70 µg/g, the lowest chlorophyll content, and carotenoid content was recorded with negative control 8.07 µg/g, 1.65 µg/g, respectively. However, the photosynthesis of citrus was significantly affected by the treatment of nanofiber from *T. hamatum* K01, in which the chlorophyll content was computed 15.98 µg/g and carotenoid was computed 0.78 µg/g. At the same time, a lesser effect was also recorded in negative control 6.13 µg/g and 0.16 µg/g, respectively.

The plant growth parameter, regarding the plant height of durian, was significantly enhanced after applying agricultural inputs on day 120. Treatment nanofiber from *T. hamatum* K01 showed the best in enhancement of plant height of durian 82 cm, followed by nanofiber from *Ch. lucknowense* CL 81 cm, *Ch. lucknowense* CL's product 76.75 cm, chemical metalaxyl 76 cm, *T. hamatum* K01 product 74 cm and positive control 72 cm. The lowest effect was observed in the negative control, 53.25 cm. The plant height of citrus was not significantly different in all treatments. However, the nanofiber from *T. hamatum* K01 had the highest effect on plant height at 76.50 cm, while the lesser effect was observed in the negative control 51.75 cm.

The control mechanism as antibiosis and plant growth promotion were proved by metabolites of *T. hamatum* K01 through the production of pyrone (6-pentyl-2H-Pyran-2-one), sorbicillin and fatty acid and *Ch. lucknowense* CL produced bioactive compounds namely aliphatic, volatile compounds. It is reported for the first time that pyrone and sorbicillin from *T. hamatum* K01 and hexadecanoic acid, 9, 12-Octadecadienoic acid (Z), and Octadecanoic acid from *Ch. lucknowense* CL could be expressed as bioactive compounds to inhibit *P. palmivora* and *C. gloeosporioides*. Moreover, the constructed nanofibres from *T. hamatum* K01 and *Ch. lucknowense* CL were first discovered to inhibit *P. palmivora and C. gloeosporioides,* causing durian rot and durian anthracnose.

This material is reserved for educational use only, not allowed for commercial use.
Forbidden to modify the content, and cite the document when use.

ACKNOWLEDGEMENTS

First, I would like to acknowledge my advisor, Prof. Dr. Kasem Soytong, from the Department of Plant Production Technology, School of Agricultural Technology, King Mongkut's Institute of Technology Ladkrabang (KMITL), who has accepted me as his student and supported me to make this thesis wholly done. Thanks for his excellent guidance for doing research. He is the best manner to inspire me to be the best scientist.

I would like to express my sincerest gratitude to Assoc. Prof. Dr. Supattra Poeaim at the Department of Biology, School of Science, King Mongkut's Institute of Technology Ladkrabang (KMITL) offered me to conduct molecular phylogeny work, support materials, facilities, and the opportunity to learn molecular techniques.

I would like to acknowledge the KMITL Doctoral Scholarships from King Mongkut's Institute of Technology Ladkrabang (KMITL) to provide the scholarship and research cost [KDS 2019] for the PhD degree.

I am also thankful to all my best friends, Dr. Harry Jay Cavite, Dr. Christopher Llones, Dr. Norden Lepcha, and Dr. Naphat Somala, who are very good friends and always help all things during my studies with their best suggestions.

Lastly, I would like to thank to all members in my family, Their presence in my life is a constant source of strength and comfort, shaping the person I am today. Through the highs and lows, their encouragement and understanding have been forwarded to my pillars of resilience.

Pheaktra Phal

This material is reserved for educational use only, not allowed for commercial use.
Forbidden to modify the content, a[illegible]te the document when use.

CONTENTS

This material is reserved for educational use only, not allowed for commercial use.
Forbidden to modify the content, and cite the document when use.

This material is reserved for educational use only, not allowed for commercial use.
Forbidden to modify the content, and cite the document when use.

This material is reserved for educational use only, not allowed for commercial use.
Forbidden to modify the content, and cite the document when use.

LIST OF TABLES

This material is reserved for educational use only, not allowed for commercial use.
Forbidden to modify the content, and cite the document when use.

LIST OF TABLES (CONTINUED)

This material is reserved for educational use only, not allowed for commercial use.
Forbidden to modify the content, alte the document when use.

LIST OF FIGURES

This material is reserved for educational use only, not allowed for commercial use.
Forbidden to modify the content, a[illegible]ite the document when use.

LIST OF FIGURES (CONTINUED)

This material is reserved for educational use only, not allowed for commercial use.
Forbidden to modify the content, and cite the document when use.

LIST OF FIGURES (CONTINUED)

This material is reserved for educational use only, not allowed for commercial use.
Forbidden to modify the content, alte the document when use.

LIST OF FIGURES (CONTINUED)

This material is reserved for educational use only, not allowed for commercial use.
Forbidden to modify the content, adapte the document when use.

LIST OF FIGURES (CONTINUED)

This material is reserved for educational use only, not allowed for commercial use.
Forbidden to modify the content, the document when use.

LIST OF FIGURES (CONTINUED)

This material is reserved for educational use only, not allowed for commercial use.
Forbidden to modify the content, alter the document when use.

LIST OF FIGURES (CONTINUED)

This material is reserved for educational use only, not allowed for commercial use.
Forbidden to modify the content, and cite the document when use.

LIST OF FIGURES (CONTINUED)

This material is reserved for educational use only, not allowed for commercial use.
Forbidden to modify the content, a[illegible]te the document when use.

LIST OF FIGURES (CONTINUED)

This material is reserved for educational use only, not allowed for commercial use.
Forbidden to modify the content, adapt the document when use.

CHAPTER 1

INTRODUCTION

1.1 Introduction to citrus

Citrus (*Citrus reticulata*) is a species of small and evergreen shrub crops belonging to the Rutaceae. This crop grows in tropical and sub-tropical climates and temperate regions (Abobatta, 2019). Citrus fruits are considered economically essential crops due to their valuable component and health-related benefits (e.g., soluble, and insoluble fibers) (Pragasam & Rasool, 2013). Citrus cultivation is also one of the major agricultural livelihoods of small-scale farmers; hence, policies that support citrus farmers help to increase employment opportunities and income (Nguyen *et al.*, 2020). The crop is native to several countries like China, the Philippines, Myanmar, Thailand, and Indonesia. In 2016, the total citrus production worldwide was 242.46 million tons. FAO reported that China, Brazil, Mexico, and the United States (US) as top countries in citrus production (WorldAtlas, 2017). Particularly in Asia, Vietnam produced 9.98 million tons, while Thailand with 11.02 million tons in 2016 (FAO, 2017). However, citrus plants suffer from disease infestation such as greening, citrus Tristeza virus (CTV), anthracnose, and root rot. Among these diseases, researchers and farmers have identified only greening as a destructive diseases. However, root rot disease is more prevalent from the research findings on the field. It is estimated to affect 20 to 80 percent of citrus trees. Diseased plants showed yellowing of leaves, dieback, stunt, and eventually die. The disease is also associated with foot rot, brown-rot, gummosis, or similar gum disease caused by *Phytophthora* spp. The presence of these diseases has been reported widely across countries producing citrus. Older citrus trees are more prevalent with disease occurrence than young citrus trees. The situation indicates that citrus root rot needs much attention as it widely affects citrus trees and often leads to an outbreak (Ploetz, 2003).

Chemical fungicides are widely used in controlling the presence of diseases in plants. However, applying chemical fungicides has increased pathogen resistance and residues in soil water, causing environmental pollution (Levy *et al.*, 1983). Research and development on the application of biological control agents against plant pathogens have been undertaken for several years in both government and

This material is presented for educational use only. Not allowed for commercial use.
Forbidden to modify the content, and cite the document when use.

private sectors, as natural agents are needed to take the place of chemical fungicides (Soytong *et al.*, 2001). At the same time, Kean *et al.* (2010b) reported that *Chaetomium* spp. and *Trichoderma* spp. have been reported to control root rot disease caused by *P. ultimum* of the citrus plant in Cambodia, similar to a chemical fungicide. Moreover, *Chaetomium* and *Trichoderma*'s bioproducts could recover citrus trees within 3-4 months regarding new leaves and root flashes. Nanoparticles derived from *Ch. cochliodes* also resulted in controlling root rot disease in *Citrus reticulata* caused by *Pythium* spp. (Udompongsuk *et al.*, 2017).

1.2 Introduction to durian

Moving on with the second crop covered in the study. Durian (*Durio zibethinus* L.) originated from Borneo and Sumatra of the Indonesian archipelago. Durian is an agricultural commodity of high economic value and is considered as the king of fruits in Thailand, Malaysia, Indonesia, and other Southeast Asian countries (Ketsa, 2018). In terms of production, Malaysia is the world's largest durian fruit producer, followed by Indonesia (Somsri, 2011). Whereas the exportation of durian fruit, Malaysia and Thailand are the two largest exporters globally (Yahia, 2011). However, durian cultivation in Thailand encounters problems associated with *Phytophthora* spp., which causes root rot disease affecting growth stages.

Generally, chemical fungicides are the first consideration in controlling root rot disease in durian plants. However, the use of chemical fungicides has resulted in causing environmental pollution and contamination in soil, water, and agricultural commodities (Shaw, 1998). Whereas among the application of chemical pesticides, which have been used to control plant pathogens, only 0.01 percent of fungicides hit the target pathogen, while the remaining percentage of pesticides are residues in the environment, especially in the soil, air, and water, which affect the ecology and food chain (Matthews *et al.*, 2014). Moreover, chemical control of specific fungicides resulted in plant pathogen resistance (Hahn, 2014). The disadvantages of chemical fungicide prompt the need to reduce and minimize its use in agriculture. It indicates the need to consider biological control agents to control plant pathogens, which have been much safer for human consumption and the environment (Narayanasamy, 2013; Singh *et al.*, 2020).

This material is reserved for educational use only, not allowed for commercial use.
Forbidden to modify the content, and cite the document when use.

Recently, biological technology has played an essential role in controlling disease and can replace the chemical fungicide. It was realized as using antagonists against plant pathogens. The control mechanism produced by *Chaetomium* spp. is promising as microbial antagonists as they can degrade cellulolytic plant debris to increase high organic matter in soil and inhibit several pathogens (Soytong & Quimio, 1989). For example, *C. globosum* and *C. cochlioides* can inhibit the growth of *Fusarium* spp. and *Helminthosporium* spp. (Tveit & Moore, 1954). *Trichoderma harzianum* and *Trichoderma viride* are used to control late blight disease caused by *P.inestans* in potatoes (Soytong & Ratanacherdchai, 2005; Stephan *et al.*, 2005). The antagonism is the control mechanism to inhibit the growth of pathogens and disease incidence. Antagonism is expressed between two organisms: antibiosis, competition, and parasitism (Heydari & Pessarakli, 2010). Biological technology of plant disease control has been successfully demonstrated, either in whole or part, when integrated with other control measures for appropriate disease management. Bio-products play an essential role in antagonism control for plant disease protection and curative effects and promote plant growth (Kasem *et al.*, 2001). There have been numerous reports that the research and development on the application of biological technology to control disease problems using microbial antagonists, e.g., nanoparticles from *Chaetomium brasilience,* reported preventing root rot disease caused by *Phytophthora palmivora* in durian (Tongon *et al.*, 2018). Nanoparticles from *Chaetomium cupreum* controlled *Phytophthora* spp., causing root disease in durian (Thongkham *et al.*, 2017c).

1.3 Objectives

1.3.1 To investigate the disease problem associated with citrus and durian.

1.3.2 To evaluate the antifungal activity of antagonistic fungi against plant pathogens and enhance plant immunity through phytoalexin production.

1.3.3 To identify bio-techniques for organic citrus and durian in the pots experiment

This material is reserved for educational use only, not allowed for commercial use.
Forbidden to modify the content, and cite the document when use.

1.4 Scope of the study

The study included a general disease survey of citrus and durian trees. The collection of disease samples, soil isolation of the pathogen, and pathogenicity test was conducted in the Association of Agricultural Technology in Southeast Asia (AATSEA) organic farm in Phecthabun and Chanthaburi province, Thailand. A disease complex was diagnosed, isolated, and identified. Identification of pathogens using morphological and molecular phylogeny was done to confirm their species and pathogenicity test. Biological active substance tests included an antagonism test of *Ch. lucknowense* CL and *T. hamatum* K01. Screening microbial elicitors derived from *Ch. lucknowense* CL and *T. hamatum* K01 to inhibit plant pathogens of citrus and durian, e.g., *P. palmivora* and *C. gloeosporioides.* Application of natural microbial elicitor from *Ch. lucknowense* CL and *T. hamatum* K01 to induce plant immunity in citrus and durian was conducted. Research findings on bio-techniques for organic agriculture of citrus and durian in pot experiments were done.

This material is reserved for educational use only, not allowed for commercial use.
Forbidden to modify the content, and cite the document when use.

CHAPTER 2

REVIEW LITERATURE

2.1 Citrus and citrus disease problems

Citrus (*Citrus reticulata*) is a small, and evergreen shrub crop belonging to the Rutaceae. This crop grows in tropical and sub-tropical climates and temperate regions (Abobatta, 2019). Citrus fruits are considered economically essential crops due to their valuable component and health-related benefits (e.g., soluble, and insoluble fibers) (Pragasam & Rasool, 2013). Citrus cultivation is also one of the major agricultural livelihoods of small-scale farmers; hence, policies supporting citrus farmers help increase employment opportunities and income (Nguyen *et al.*, 2020). Thailand produced 1.2 million tons of citrus fruits on 0.1 million ha, which was reported by the Food and Agricultural Organization of the United Nations (FAO) (Phung *et al.*, 2015c)

However, disease infestation greatly affects citrus production, particularly by the frequency of incidence of *Phytophthora* rot, which has several secondary microorganisms like *Pythium*, *Fusarium* spp., and *Aspergillus* spp. in the rhizosphere of citrus. Several literatures revealed that diseases such as the Tristeza virus, greening disease, and *Phytophthora* rot significantly affect citrus production. In the case of root rot diseases, it cannot be treated once the plant becomes infected. The diseased plants must be removed and replanted (Molina *et al.*, 1998). *C. gloeosporioides* is a known pathogenic species worldwide causing anthracnose of citrus fruit (Phoulivong *et al.*, 2010). This anthracnose disease shows the dieback of branches and affects the postharvest condition of crops (Figure 2.1) (Wang *et al.*, 2021a). Moreover, it compromises the quality and quantity of citrus fruits, thereby limiting production and negatively impacting fruit export and marketability (Phoulivong *et al.*, 2012)

This material is reserved for educational use only, not allowed for commercial use.
Forbidden to modify the content, and cite the document when use.

Figure 2.1 The disease symptoms of citrus anthracnose caused by *C. gloeosporioides* (Daoud *et al.*, 2019)

2.2 Management of citrus disease

2.2.1 Chemical control of citrus disease problem

Often, chemical fungicides are widely used to control diseases in the citrus orchard, especially root rot caused by *Phytophthora* spp., and *C. gloeosporioides*, one of the known pathogenic species worldwide causing anthracnose of citrus fruit (Phal *et al.*, 2023a; Phoulivong *et al.*, 2010). However, the application of chemical fungicides remains on the surface of plant tissues, fruits of agricultural commodities, and the environment, causing serious health risks for the producers and consumers. At the same time, the application of chemical fungicides contributed more to the problems by its adverse effect of increasing the pathogen's resistance (Levy *et al.*, 1983).

2.2.2 Biological control of citrus disease problem

Several reports revealed that a biological fungicide could control citrus disease problems. For example, *Ch. lucknowense* CL and *Trichoderma viride* have been proven to control *Phytophthora* spp. (O'Brien, 2017; Singh *et al.*, 2020). Soytong *et al.* (2001) found that bio-fungicide formulated from effective isolates of *Chaetomium* spp. are promising in degrading the cellulolytic plant debris to the promoted organic matter in soil isolate, which will enable to control of plant pathogens. *Ch. globosum* and *Ch. cochlioides* inhibit the growth of *Fusarium* spp. and *Helminthosporium* spp. (M & MB, 1954). The *Ch. globosum* produces specific metabolites that can inhibit the growth of *P. ultimum,* which causes damping-off of sugar beet (Di Pietro *et al.*, 1992) and can reduce the pathogen inoculation of *Botrytis cinerea* on dead lily leaves in the field (Kohl *et al.*, 1995). Meanwhile, *Ch.*

This material is reserved for educational use only, not allowed for commercial use.
Forbidden to modify the content, and cite the document when use.

cupreum also reported being able to control soybean plant pathogens, e.g., *Phomopsis* and *Colletotrichum* spp. (Manandhar *et al.*, 1987). Phung *et al.* (2015a) revealed that *Chaetomium* species such as *Ch. globosum, Ch. lucknowense,* and *Ch. cupreum* exhibit antifungal activities against mycelial growth of *P. nicotianae*. It reduced root rot by 66% to 71% and increased plant weight by 72% to 85% compared to the nontreated control treatment. In contrast, the crude extracts of these *Chaetomium* species exhibited antifungal activities against the mycelial growth of *P. nicotianae,* with adequate doses of 2.6 to 101.4 µg/m. The *Ch. cupreum* and *Ch. globosum* result in controlling *Curvularia lunata* causing leaf spot disease of corn, rice blast caused by *Magnaporthe grisea* (*P. oryzae*), and sheath blight of rice caused by *Rhizoctonia oryzae* (Soytong & Quimio, 1992). The study of Kean *et al.* (2010a) stated that *Trichoderma* and *Chaetomuium's* bioproducts significantly controlled citrus disease as the application of chemical fungicide when compared to the non-treat control.

2.3 Durian and durian disease problem

Durian is divided into various varieties or cultivars based on the fruit's characteristics. Whereas cultivated durian is mainly propagated asexually (Brown, 1997). However, the durian plantation faces several problems. The study of Vawdrey *et al.* (2005), found that 13 durian farms were surveyed during the season (July- September). They found that durian dieback has become a severe durian disease in the orchards in northern Queensland. Durian rot caused by *P. palmivora* has been reported to be a very serious disease, in which the disease symptoms are dieback, leave yellowing, twigs-dry, fruit rot, and root rot (Figure 2.2) (Phal *et al.*, 2023b; Tongon & Soytong, 2022). causing yield losses and increasing production costs, estimated at 20-25% (Kongtragoul *et al.*, 2021).

C. gloeosporioides have also been reported to affect durian production, causing anthracnose disease. This pathogen also leads to postharvest losses, affecting the volume and quality of the fruits. Anthracnose disease has been reported to be the most severe disease in stems of durian in Malaysia (Masyahit *et al.*, 2009). Generally, anthracnose disease affects twigs, leaves, fruits, flowers, and stems and shows symptoms such as dieback, sunken spots, water-soaked lesions, and rapid

This material is reserved for educational use only, not allowed for commercial use.
Forbidden to modify the content, and cite the document when use.

expansion to full size, with brownish-red to black spots (Figure 2.3) (Vidyalakshmi & Divya, 2013).

Figure 2.2 The disease symptoms of durian rot caused by *P. palmivora*

This material is reserved for educational use only, not allowed for commercial use.
Forbidden to modify the content, and cite the document when use.

Figure 2.3 The disease symptoms of durian anthracnose caused by *C. gloeosporioides*

2.4 Management of durian disease problem

2.4.1 Chemical control of the durian disease problem

Conventionally, chemical fungicides have been extensively applied to control anthracnose disease of durian. However, the application of chemical fungicides remains on the surface of plant tissues, fruits of agricultural commodities, and the environment, causing serious health risks for the producers and consumers. In addition, excessive chemical fungicide application causes pathogen mutation and allows some pathogens to develop resistance to those chemical fungicides (Brent & Hollomon, 2007). This causes serious economic problems for producers (Ishii & Holloman, 2015; Steffens *et al.*, 1996). Because of this, the effects to control the disease became negligible, resulting in increased amounts required in succeeding use. This causes the production cost to increase as farmers need to apply more amounts of chemical fungicide than before (Kongtragoul *et al.*, 2021).

2.4.2 Biological control of the durian disease problem

To reduce or discontinue the use of chemical fungicides, biological control is being considered as an alternative to combat plant disease with economic and environmental benefits. In recent years, researchers have explored biological control techniques against various plant pathogens that are safe and eco-friendly (Dawson & Hilton, 2011). The control mechanism produced by *Chaetomium* spp. is promising as a microbial antagonist as it can degrade cellulolytic plant debris to increase high organic matter in soil and inhibit several pathogens. On the other hand, it is safe for human consumption that the environment increases organic matter in the soil. The bio-culture tests *Ch. elatum* significantly inhibited the growth of colony *P. palmivora* and spore production of *P. palmivora* by 38.89 and 46.13%, respectively (Thongkham *et al.*, 2018). A similar report by Tathan *et al.* (2012) indicated that *Ch. elatum* significantly inhibited the colony growth of *P. palmivora* and spore production of *P. palmivora* by 32.49 and 26.23%, respectively. The crude extracts from *Ch. elatum* gave significantly the highest inhibited spore production

This material is reserved for educational use only, not allowed for commercial use.
Forbidden to modify the content, and cite the document when use.

of *P. palmivora* at a concentration of 1,000 ppm. Meanwhile, ED_{50} values of Crude-CEE was 175.31 µg/ml. Soytong (2015) found that crude extract from *Ch. elatum* gave significantly the highest inhibited *Fusarium oxysporum* f.sp. *lycopersici* causing wilt disease of tomato at a concentration of 1,000 ppm with the ED_{50} value of 5.94 µg/ml. The nanoparticle derived from *Ch. elatum* significantly inhibited sporangia production of *P. palmivora* at a concentration of 15 ppm. Meanwhile, ED_{50} values of Crude-CEH were 3.49 µg/ml. Song and Soytong (2016) stated that nanoparticles derived from *Ch. elatum* significantly inhibited *P. oryzae,* causing rice blast disease at a concentration of 15 ppm. Tango *et al.* (2018) revealed that nanoparticles from *Ch. brasiliense* significantly affected the colony growth and spore production of *P. palmivora,* in which the ED_{50} values were 1.08 µg/ml and 8.68 µg/ml prospectively. Thongkham *et al.* (2017b) also reported that nano-CCH, nano-CCE, and nano-CCM derived from *Ch. cupreum* significantly inhibited spore production mycelial growth of *Phytophthora* spp., which the ED_{50} values were computed of 3.49, 3.47, and 3.80 µg/ml, respectively.

2.5. Phytoalexine production technology

Plants stimulate the production of phytoalexins as a defense mechanism for responding to microbial infection. *Citrus* spp. accumulated phenolic compound, Xanthoxylin (2-hydroxyl-4,6-dimethoxy acetophenone), after it is infected by *P. citrophthora* and *Hendersonula toruloiddea,* which is the fungi toxic compound was found in the bark of *citrus* spp. (Afek & Sztejnberg, 1988). Terpenoids naphtaldehydes Gossypol is phytoalexin induced by the plants under the Malvaceae family, including durian and cotton (Arruda *et al.*, 2016). Camalexin is the primary substance in Arabidopsis, kauralexin, zealexin in maize, scopoletin, and capsidiol in *N. tabacum* (Ahuja et al., 2012). The possibility of wide-spectrum disease control using plant-specific resistance mechanisms has increased production agents that can imitate natural resistance inducers (Walters *et al.*, 2005). Metabolites of microbial origin, including proteins, polysaccharides, and fatty acids (biotic elicitors), also induce phytoalexin synthesis and plant immunity accumulation (Afek & Sztejnberg, 1988; Paxton, 1988). Investigation on resistance mechanisms has shown that plant immunizes after infection. Infected plants change many biochemical mechanisms occurred in the plant (Hammerschmidt, 1999). Morrissey and Osbourn (1999) cited

This material is reserved for educational use only, not allowed for commercial use.
Forbidden to modify the content, and cite the document when use.

that Phytoalexins are a group of structurally diverse molecules typically lipophilic, non-specific, and not especially active in their antifungal action. The accumulation of phytoalexins represents an array of induced defense mechanism responses associated with resistance to plant disease. Scopoletin, a phenolic coumarin with intense blue fluorescence under UV light originating from the phenylpropanoid pathway (Kai *et al.*, 2006), can be isolated from several species of plant (Murray *et al.*, 1982), and scopoletin is an important phytoalexin that acts as a control mechanism against the pathogen (Gnonlonfin *et al.*, 2012). Citrus (Nagami Kumquat) treated by Pathogen-associated molecular pattern (PAMP) Flg22 (Xflg22) resulted in inducing of several defense genes (EDS, NDR1, PBS1, SGT1, PAL1, NPR2, and NPR3) at early 6 hours up to 72h resistance to canker disease of citrus (Shi, 2015).

Soytong *et al.* (2013) revealed that the microbial elicitor's application as chaetomanone A derived from *Ch. lucknowense* and Chaetoglobosin-C derived from *Ch. globosum.* Trichotoxin A50 derived from *T. harzianum* PC01 was reported to induce immunity in the chili plant against *C. capsici* and the accumulation of capsidot at 5 to 10 days after treatment. Additionally, the microbial elicitor of Chaetoglobosin-C from *Ch. globosum*, chaetomanone A from *Ch. lucknowense,* and Trichotoxin A50 from *T. harzianum* PC01 also reported eliciting α-tomatine in tomato seedling variety Sida as a response against *Fusarium*, the mixture of these three compounds at concentration 50 ug/ml after 10 days were 44.97, 35.18 and 39.43%, respectively. At the same time, prochloraz showed a disease immunity of 29.95%. Trichotoxin A50 derived from *T. harzianum* was also reported to induce immunity against Phytophthora root rot of citrus seedlings compared to the chemical fungicide metalaxyl (Treetong *et al.*, 2000). Nanoparticles (nano-CBH) derived from *Ch. brasiliense* stimulated an immunize against *M. oryzae*, causing rice blast disease. Song *et al.* (2020) reported that the combination of benzene: ethyl acetate (10:1) with the extraction of rice leaves treated with nano-CBH, spots on the TCL plates absorbent under 360 nm UV light with RF value of 0.08 was supposed to be Sakuranertin., At the same time, the R_f value of 0.28 was supposed to be Oryzalexin B.

Chaetomium species act as control mechanisms for antibiotics and reported to induce plant immunity against plant pathogens. Udompongsuk, M. (1017)

This material is reserved for educational use only, not allowed for commercial use.
Forbidden to modify the content, and cite the document when use.

microbial elicitor from *Ch. brasilences* and *Ch. cochliodes* also reported to induce plant immunity against *Pythium* spp., causing root rot disease of tangerine (*citrus reticulata*) with Rf = 0.6. Nono-elicitor from *Ch. elatum, Ch. cupreum,* and *Ch. lucknowense* and metalaxyl resulted in scopoletin synthesis against *P. palmivora,* causing root rot disease in durian with the R_f =0.75 (Tongon & Soytong, 2022). *Trichoderma* species is one of the other choices reported by many researchers to control plant disease and can immunize against pathogens. Antibiotic substances Trichotoxin A50 from *T. harzianum* PC01 and *T. harzianum* PC01 reduced disease incidence on leaves, twigs, and grapefruit fruits. Trichotoxin A50 from *T. harzianum* PC01 also indicated an immunizing capacity against *Phytophthora* spp., causing citrus seedling root rot disease (Treetong *et al.*, 2000).

2.6. Morphology identification of pathogens and antagonists

2.6.1. Morphology identification of pathogens

2.6.1.1. General characteristics of *C. gloeosporioides*

C. gloeosporioides, the anamorphic facultative parasite, is part of the Phyllachoraceae the Ascomycota. The fungus is made of *C. gloeosporioides* as an incomplete or asexual an imperfect state, while *Glomerella cingulata* is perfect stage. *G. cingulata* occurs in various host species that develop asexual acervuli within the host tissue (mitotic). The teleomorph stage is also recognized for its ability to cause serious disease (Cannon *et al.*, 2007). Humid conditions contribute to the uniform and efficient transmission of anthracnose disease (Farr *et al.*, 2006). The fungus is infected with damaged or compromised plant tissue and develops numerous specialized structures during infection. These specialized structures, viz. conidia, acervuli, setae, and appressoria, are formed during the interaction between host and pathogen. *C. gloeosporioides* colonies injure plant tissues and form several acervuline and conidia. Conidia can spread over relatively short distances by rain splash or overhead irrigation and infect other healthy plant tissues. The penetration into host tissues generally relies on the formation of specialized infection structures known as appressoria. These appressoria allow the fungus to penetrate the host cuticle and hyaline. Conidia are hyaline, one-celled, straight, cylindrical, and obtuse at apices. Variation in the dimension of conidiogenous cells is also observed in

This material is reserved for educational use only, not allowed for commercial use.
Forbidden to modify the content, and cite the document when use.

different studies. The fungus produces hyaline, one-celled, ovoid to oblong, slightly curved or dumbbell-shaped conidia, 10-15 µm (average) up to 20 µm in length and 5-7 µm. There is a significant variation in the size and shape of conidia of *C. gloeosporioides* depending upon the host from which the pathogen is isolated and its area of origin. Usually, the conidia may be oblong with obtuse ends (Freeman *et al.*, 1998).

2.6.1.2. General characteristics of *Phytophthora* sp.

Phytophthora belong to Pythiaceae, Peronosporales Oomycota, (Beakes *et al.*, 2012). The Genus of *Phytophthora* has more than 120 species detected and officially described (Park *et al.*, 2008). Furthermore, Oomycetes share many ecologies and life history characteristics with the true fungi such as Basidiomycetes and Ascomycetes. They are clearly distinguished from those fungi by their genetics, cell wall opposition, and biochemical pathways. Oomycetes are diploid, whereas fungi are haploid. Cell walls of Oomycete are composed of β-glucans but not chitin, which is a standard cell wall component of fungi. Unlike fungi, members of Oomycota do not synthesize sterol. Therefore, they are sensitive to fungicides targeting chitin and sterol synthesis. Besides, its oospores are biflagellate, which is not characteristic of fungi (David, 1998). One sexual spore form is called oospore, and up to three diploid asexual spore forms (chlamydospore, sporangium, and zoospore) pass through a dispersal cycle and encasement before germinating. Some species, such as *P. cinnamomic, P. palmivora, P. nicotianae,* also produce sexual chlamydospores from the mycelium. Meanwhile, oospores result from sexual reproduction. All these spore types are potentially infective. Besides, chlamydospores and oospores also have functioned as overwintering or resting structures. All species of Phytophthora have a soil-borne resting stage. Most species are dispersed primarily in the soil via the release of zoospores from infected plant material. However, some species can disperse aerially by producing caducous (deciduous) sporangia, such as *P. Palmivora* and *P. infestans* (Erwin & Ribeiro, 1996).

This material is reserved for educational use only, not allowed for commercial use.
Forbidden to modify the content, and cite the document when use.

2.6.2. Morphology identification of antagonists

2.6.2.1. General characteristics of *Chaetomium* spp.

The genus of *Chaetomium* spp. is one of the largest saprophytic ascomycetes, having more than 300 genera. Gustav Kunze was the first recognized of *Chaetomium* spp. in 1817 (Rodríguez *et al.*, 2002). It belongs to the Chaetomiaceae, Sordariomycetes, and order Sordariales (Prokhorov & Armenskaya, 2001). *Chaetomium* produced an imperfect acremonium–like stage on culture media and was identified by the presence of flask-shaped perithecia superficially surrounded by long, dark, and stiff ascomata hairs. Ascomata hairs are erect, flexuous, or coiled globose (Udagawa *et al.*, 1979), colony character, ovate or obovate ascomata, evanescent asci, slightly fusiform or clavate; limoniform or ovate ascospore with an apical germ pore (Wang *et al.*, 2016).

2.6.2.2. General characteristics of *T. hamatum* K01.

The genus of *T. hamatum* belongs to the Hypocreaceae, Hypocreales. *Trichoderma* occurs globally and is readily isolated from soil, rotting wood, and other plant organic matter sources. Mostly, they are categorized as incomplete fungi in that they have no sexual stage identified. It is distinguished by the rapid growth rate in culture and the development of multiple spores (conidia) with shades of green. Sometimes uncolored, buff, black, amber, or light green are the reverse side of colonies, and many species develop prodigious amounts of thick-walled spore (Gams *et al.*, 2002)

2.7. Molecular identification of pathogens and antagonists

Identification of related species relies strongly on sequence-based identification. Resources are rare for identifying several fungal and oomycete pathogens. *Phytophthora* genus contains some of the most destructive plant pathogens known, such as *P. infestans*, the potato late blight pathogen (Fry, 2008). Method for quick and easy identification of *Phytophthora* spp. Several criteria have been met. This tool should be based on sequence because classical morphology cannot identify many of the currently recognized species. For example*, P. infestans, P. ipomoea, and P. mirabilcannot* are easily differentiated which based on

This material is reserved for educational use only, not allowed for commercial use.
Forbidden to modify the content, and cite the document when use.

morphology alone since these species are similar for sporangia (semi papillate and caducous) and oospore morphology (Cooke *et al.*, 2007; Flier *et al.*, 2001). Traditionally, the molecular detection of *Phytophthora* spp. Polymerase chain reaction (PCR) amplification of the internal transcribed spacer (ITS) region accompanied by either restriction analysis (Drenth et al. 2006) or direct sequence and BLAST search quest GenBank or other databases. However, molecular identification based on the ITS region is not without its pitfalls (Kang *et al.*, 2010)

DNA sequencing offered a big leap forward in knowledge of *Phytophthora* species (Kroon *et al.*, 2012). Sequencing analysis of specific loci is the most accurate molecular method of isolating to a species level. Suppose the sequences for genes or DNA regions are identical or nearly identical. In that case, the isolate supposedly belongs to the same species from nuclear (ITS, lard subunit rRNA, TigA gene fusion, translation elongation factor 1α) and mitochondrial (*cox*l, *and* l*, cox*2*, nad*9*, rps*10*,* and *secY)* were purposed sequence for identification and phylogenic resolution within *Phytophthora* (Grunwald *et al.*, 2011a; Martin *et al.*, 2012). of the loci, the non-coding ITS region consisting of ITS1, the 5.8SrDNA, and ITS2 contain stretches of high homology that have been used to design primers for polymerase chain reaction (PCR) amplification (Grunwald *et al.*, 2011b). For almost all *Phytophthora* species, the same primer can amplify the region. The first extensive phylogenic study of the gene *Phytophthora* based on ITS sequence analysis was described by Cooke *et al.* (2000). It is based on analysis of ITS sequence 234 isolates from 50 distinct *Phytophthora* species to divide the genus into 10 clades currently used to group *Phytophthora* species and replace the Waterhouse classification. Lately, phylogenetic analysis of the genus was based on the combination of sequence data from nuclear loci and mitochondria (Kroon *et al.*, 2012; Martin *et al.*, 2012).

Sequencing the ITS region is usually the first choice to isolate Pathogenic organisms and antagonistic fungi into species level under molecular identification. It is easy to amplify and is diverse enough to distinguish among most species (Grunwald *et al.*, 2011b; Kroon *et al.*, 2012; Martin *et al.*, 2012). ITS sequences are the largest and more ready in the database than sequence data of other loci. When conducting BLAST analyses, it is necessary to use accurate species classification.

This material is reserved for educational use only, not allowed for commercial use.
Forbidden to modify the content, and cite the document when use.

Some good databases can be used for BLAST analyses of *Phytophthora* sequences, including *Phytophthora* databases (Park *et al.*, 2008).

This material is reserved for educational use only, not allowed for commercial use.
Forbidden to modify the content, and cite the document when use.

CHAPTER 3

RESEARCH METHODOLOGY

3.1 General disease survey, isolation, identification of pathogens

3.1.1 General disease survey and samples collection

Initially, the disease incidence of citrus and durian plants were surveyed at the Association of Agricultural Technology in Southeast Asia (AATSEA) organic farm in Phetchabun and Chanthaburi province. Disease samples of citrus and durian leaves, roots, and fruits from different symptoms were separated using tissue transplanting and baiting techniques. All collected samples were brought to the laboratory at the School of Agricultural Technology, King Mongkut's Institute of Technology Ladkrabang (KMITL), Bangkok, Thailand.

3.1.2 Isolation of plant pathogens

The samples of root rot disease were taken from infected trees with yellow leaves and root rot symptoms, collected from Chanthaburi province, and an anthracnose disease sample was collected from an infested plant in Bangkok. Root rot samples and anthracnose samples were washed with running tap water, and then 2 mm pieces of root portion or anthracnose were cut using a sterilized scissor. Tissue pieces were soaked for 5 min in a 10% sodium hypochlorite solution for surface disinfection and washed with sterilized distilled water three times plotted dry with sterilized tissue paper before placing onto water agar (WA) incubated at room temperature condition (27-30^{o}C) for 24-72hrs and Peripheral colonies growth in water agar (WA) were cut and transferred to potato dextrose agar (PDA) to obtained pour culture. All isolates were kept in PDA slants for further experiments.

Baiting techniques were used for isolation of *Phytophthora* sp. Soil samples were collected from root zone infected durian trees that caused root rot pathogen, which expressed early symptoms of yellow leaves dieback of twigs and stems, located at the durian farm in Chanthaburi province. The soil at a 10 to 20 cm depth was collected and packed in a plastic bag. Soil samples weighing 40g were air-dried overnight and ground into fine particles. Fine particles were transferred to a sterilized Petri dish filled with 20 mL sterilized distilled water, and healthy leaf

This material is reserved for educational use only, not allowed for commercial use.
Forbidden to modify the content, and cite the document when use.

pieces of durian 2 cm^2 diameter were floated to bait soil. Culture plates were incubated at room temperature (27-30^oC) for 24-72 hrs. until the mycelial was grown from the baiting leaves of durian, then transferred to water agar (WA). After 1-2 days, the Petri dishes were observed daily in the presence of hyphae under a binocular compound microscope. Peripheral hyphae growth in water agar (WA) was cut and placed in potato dextrose agar (PDA) to get pure culture for further experiments.

3.1.3 Morphological identification of *P. palmivora* and *C. gloeosporioides*

P. palmivora was identified which based on morphology following the method of (Howard *et al.*, 1970); Van der Plaats-Niterink (1981). The pathogens were separately cultured in a potato dextrose agar (PDA) incubated at room temperature (27-30^oC) for seven days. The colony's growth was observed under a binocular compound microscope and scanning electron microscopy (SEM). The hyphal tips of the young colony on PDA were cut and allowed to float in sterilized distilled water for 24-72 hours at room temperature to investigate the sporangia development, colony growth characteristics, sporangiophore, and oospores. All morphologically identified isolates were noted with photos and species descriptions. For morphology identified, *Colletotrichum* sp. was produced on sterilized grass blades and observed under the binocular compound microscope scanning electron microscopy (SEM) to observe conidia production and other structures.

3.1.4 Morphological identification of *T. hamatum* K01 and *Ch. lucknowense* CL

The antagonistic fungi, *T. hamatum* K01 and *Ch. lucknowense* CL were offered by Assoc.Prof. Dr. Kasem Soytong, King Mongkut's Institute of Technology Ladkrabang. These antagonists were morphologically identified to confirm the species level. The antagonistic fungi were separately cultured in PDA media for seven days. The colony growth rate of *T. hamatum* K01 was recorded, and other characteristics, including size and shape hyphal elongations, roughened conidiophores, and Phialides conidia, were measured using scanning electron microscopy (SEM) and light compound microscopy following Younesi *et al.* (2021). Characteristics of *Ch. lucknowense* CL, including the size of ascospores, ascomata

This material is reserved for educational use only, not allowed for commercial use.
Forbidden to modify the content, and cite the document when use.

hairs, asci, and ascomata were observed and measured using SEM and light compound microscope.

3.1.5 Molecular identification

The isolates of the pathogens and antagonistic fungi were molecularly identified to confirm species. The pathogens and antagonist were separated culture in potato dextrose broth (PDB) for seven days at room temperature (27-30ºC). The mycelia were collected, and then the mycelia were freeze-dried. Freeze-dried mycelia were cleaned through centrifugation using 25 mM EDTA (Ethylenediaminetetraacetic acid). Then, ground with liquid nitrogen to get a fine powder. The DNA was extracted using CTAB, which followed the method of Prabha *et al.* (2013). The fungal biomass was lysed in the CTAB buffer, β-mercaptoethanol, and heated at 60ºC in a water bath for 1 hr. The lysates were extracted using chloroform/isoamyl alcohol (24:1) and centrifuged at 14000 rpm for 5 minutes at 4ºC. Then, 2 µL Rnase (20µg/ml) was added to the sequence phase in a sterile tube for 30 minutes at 37ºC before being mixed with 50 µL 10% CTAB. The mixture was centrifuged at 14000 rpm for 5 minutes at 4 ºC. The DNA was precipitated in isopropanol and centrifuged at 4 ºC for 20 minutes at 14000 rpm. The pellet was cleaned two times with 70% and 95% ethanol air-dry and dissolved in a 100 µL TE buffer at 37ºC. PCR mixed were prepared 25 µL in PCR buffer, which contained water NA 14.3 µL, Tag Buffer 2.5 µL, Tag DNA 0.2 µL, dNTP 4 µL, DNA 1 µL, ITS1 1 µL and ITS4 1 µL. DNA regions were amplified by PCR using the universal primers ITS1 (5'-TCCGTAGGT-GAACCTGCGG-3') and ITS4 (5'-TCCTCCGCT-TATTGATATGC-3') for *Chaetomium* sp., *Trichoderma* sp. and *Colletotrichum* sp. (Phung *et al.*, 2015b) and ITS5 (5'-GAAGGTGAAGTCGTAACAAGG-3') and ITS4 (5'-TCCTCCGCTTATTG-ATATGC-3') for identification of *P. palmivora* (U.G, 1990). The PCR program set up the condition with an initial denaturation at 94 ºC for 5 minutes, 94 for 1 minute with 30 cycles, 52ºC for 1 minute, 72ºC for 50(s), and a final extension of 72ºC (Table 3.1). PCR products were monitored by electrophoresis in 1% agarose gel to check the DNA bands. In addition, DNA sequences of related species based on the ITS, including 5.8S gene data retrieved from GenBank and by primary local alignment search tool (BLAST) analysis in the National Centre for Biotechnology Information (NCBI) database (Altschul *et al.*,

This material is reserved for educational use only, not allowed for commercial use.
Forbidden to modify the content, and cite the document when use.

1997). The phylogenetic trees were created with the MEGA-X software using the Tamura-Nei model maximum-likelihood approach, and bootstrap generated 1000 replications using the same software mentioned above (Tamura & Nei, 1993).

Table 3.1 Polymerase chain reaction (PCR) amplification

Primers used for PCR and sequencing		
Primers	Sequence (5′-3′)	
ITS1	TCCGTAGGT-GAACCTGCGG	
ITS4	TCCTCCGCT-TATTGATATGC	
ITS5	GAAGGTGAAGTCGTAACAAGG	
Primer's mix		
Components	Concentrations	
DNA	1 µL	
dNTP	0.5 µL	
Primers	1 µL	
Taq Buffer	2.5 µL	
Taq DNA	0.2 µL	
DI Water	19.8 µL	
PCR program		
Steps	Cycles	Condition
1	1	95°C for 5 minutes
2	35	94°C for 1 minute
3	-	60°C for 2 minutes
4	-	72°C for 3 minutes
5	-	72°C for 5 minutes
-	-	Stored at -20 C until used

3.1.6 Pathogenicity test using detached leaves and root inoculation method

Pathogenicity tests were done to prove pathogenic isolates using the root inoculated method. The pathogenicity test is expected to get the virulent isolates of *P. palmivora*. of durian and citrus. The experiment was done using a completely randomized design (CRD) with four replicates. For root rot disease, the test was conducted in a pot experiment using one year old citrus and durian seedlings. The

This thesis is the property of King Mongkut's Institute of Technology Ladkrabang
Forbidden to modify the content, and cite the document when use.

isolates of *P. palmivora* were sub-cultured and multiplied on PDA and incubated at room temperature (27-30° C) for seven days. The mycelia were collected and filtered using a two-layer cheesecloth to obtain sporangia suspension, which was adjusted to $2x10^6$ sporangia/ml using a hemocytometer. The root-dipped method was used to inoculate P. *palmivora* following the method of Marlatt *et al.* (1996). The seedlings were moved from the plastic pots and cleaned with running tap water. The root tips of seedlings were cut at about 5 mm using sterilized scissors to make a wound and then soaked in sporangial suspension for 15 minutes. Seedlings were transplanted to a 8 cm-diameter plastic pot with soil mixture (loam soil: fine coconut shield: sand = 2:1:1) and sterilized for 30 days at 121°C 15 lbs/inch^2 for 1 hour. The root tips were dipped in sterilized distilled water without the inoculum being served as control. All treatments were kept in a greenhouse at 25-32° C for 30 days after inoculation. The disease severity index (DSI) was recorded. Root systems were evaluated based on the 3 levels of DSI with the following scales: level 0= all roots healthy; level 1= root rot apparent; 3= no healthy root, stem girdled. The percentage of infection was calculated using Equation 1

$$\% \text{ Root rot} = \frac{\text{Total test plants} - \text{infected plants}}{\text{Total test plans}} \; x\, 100 \qquad (1)$$

The pathogens were re-isolated from infected root symptoms, and morphological characteristics were compared with the inoculated isolate. The most pathogenic isolate was selected for further experiment. DSI was analyzed using analysis of variance (ANOVA). Treatment means were compared using Duncan's Multiple Range Test (DMRT) at $p<0.05$.

The detached leaves method was also used to prove the pathogenic isolate of pathogens on citrus leaves and durian following the procedure Soytong (2010). The isolates of the pathogens were sub-cultured in potato dextrose agar at room temperature (27-30°C) for seven days. The experiment was conducted with four replications in a completely randomized design (CRD). Leave samples were collected from healthy citrus and durian trees, and then the surface was disinfected with 75% ethyl alcohol. Detached leaves were wounded 4-5 points using a sterilized needle, and the culture agar plugs of pathogen 0.5 cm^2 diameter were cut and then

This material is reserved for educational use only, not allowed for commercial use.
Forbidden to modify the content, and cite the document when use.

inoculated onto the wounded leaves from each isolate. Non-inoculated ones were treated with agar plugs, served as control, and incubated in a moist chamber at room temperature (27-30°C) for seven days. Disease incidence was classified as follows: 1 = green is usual and non-aggressive, 2 = pale green is low aggressive, 3 = pale brown is medium aggressive, and 4 = dark brown is highly aggressive. The data were collected by measuring the area of test leaves and infected area using Image J software. The percentage for infection was computed using Equation 2

$$\% \text{ Infection} = \frac{\text{Area test leaves} - \text{Area infected leaves}}{\text{Area test leaves}} \text{ x } 100 \qquad (2)$$

3.2 Isolation of secondary metabolites of antagonistic fungi

Secondary metabolites from *T. hamatum* K01 and *Ch. lucknowense* CL were identified using gas chromatography and mass spectrometry (GC/MS). In detail, the compounds were analyzed by an Agillen 6890 N gas chromatograph with an Agilent 5973 mass detector equipped with an HP-5 silica capillary column (30 m 0.25 mm ID, 0.25 µL film thickness). The oven temperature program contained an initial 50 °C for 3 minutes, and the temperature was increased from 10 °C/minute to 200 °C held for 3 minutes. Then, the temperature was increased from 15 °C/minute to 260 °C, held for 20 min. Helium was used as the carrier gas at a 1 mL/ minute flow rate. MS analysis was carried out over a 30–500 amu detection range. The sample was prepared with (1/1) g/mL crude methanol from *T. hamatum* K01, crude ethyl acetate, and nanofiber from *Ch. lucknowense* CL. Samples 0.2 µL were injected with a split ratio 50:1. The injector and detector were kept at 250 °C and 270 °C, respectively. MS identified the specific compound, and their identity was confirmed by comparing the Kovats retention index regarding a homologous series of n-alkanes. Percentage composition based on GC peak area and retention time as calculated by a Shimadzu CR6A data processor.

3.3 Laboratory research

3.3.1 Bi-culture test

Ch. lucknowense CL and *T.* hamatum K01 from the collection of Prof. Dr. Kasem Soytong, Department of Plant Production Technology, School of Agriculture

This material is reserved for educational use only, not allowed for commercial use.
Forbidden to modify the content, and cite the document when use.

Technology, King Mongkut's Institute of Technology Ladkrabang, (KMITL), Ladkrabang, Bangkok, Thailand. These antagonists tested the abilities to control plant pathogens *P. palmivora,* causing root rot disease, and *C. gloeosporioides,* a causal agent of anthracnose disease, by following the method of Soytong and Quimio (1992). The Experiment was carried out using a completely randomized design (CRD) with four replications. *Ch.* lucknowense CL and *T.* hamatum K01 and all isolates of plant pathogens, *P. palmivora* and *C. gloeosporioides* were separately cultured in PDA at room temperature (27-30ºC) for 5 days. 0.5 cm^2 diameter mycelial disc, each isolate of pathogens was cut and placed into the PDA plates (9 cm) on one side, and agar plug of *C.* lucknowense CL or *T.* hamatum K01 was placed on the opposite site. The agar plugs of *P. palmivora* and *C. gloeosporioides,* and *Ch.* lucknowense CL or *T.* hamatum K01 were cultured to PDA plates alone served as controls. All plates were incubated at room temperature (27-30ºC) for 30 days. The colony diameter (cm), spore number, and conidia production of pathogens were measured. The growth inhibition of mycelial and spore production and conidia production of pathogens were computed using Equations 4 and 5. The data was statistically computed through analysis of variance (ANOVA), and treatment means were compared with DMRT at $p<0.05$.

$$\% \text{ Colony growth inhibition} = \frac{\text{Colony growth in conttrol} - \text{Colony growth in biculture}}{\text{Colony growth in control}} x\ 100 \quad (4)$$

$$\% \text{ Sporulation inhibition} = \frac{\text{Sporulation in control} - \text{Sporulation in biculture}}{\text{Sporulation in control}} x\ 100 \quad (5)$$

3.3.2 Screening crude extract from antagonistic fungi against pathogens in *vitro*

3.3.2.1 Extraction method

Antagonism assay of *Ch.* lucknowense CL and *T.* hamatum K02 was done through a biologically active substance test. The antagonistic substances were extracted following the method of Kanokmedhakul *et al.* (2006). The antagonistic fungi *Ch.* lucknowense CL and *T.* hamatum K01 were separately grown in potato dextrose broth (PDB) for 35 days at room temperature (27-30ºC). Fungal biomasses were harvested from the PDB and filtrated through a two-layer cheesecloth to yield fresh weight biomass. Fresh weight of fungal biomass was air-dried for seven days

This material is reserved for educational use only, not allowed for commercial use.
Forbidden to modify the content, and cite the document when use.

to obtain dry biomass. Dry biomasses were ground into fine particles with an electric blender. Each fine particle of fungal biomass was extracted using hexane, ethyl acetate, and methanol (1:1 v/v) in (1000 ml flask). The extraction was done with the following method, as shown in Fig 2. Biomass was soaked with hexane (1:1 v/v), shaken for three days, with ethyl acetate, and finally with methanol, respectively, and filtrated using filter paper (Watman No 4). The solutions from each solvent were evaporated to yield crude extract (Figure 3.1).

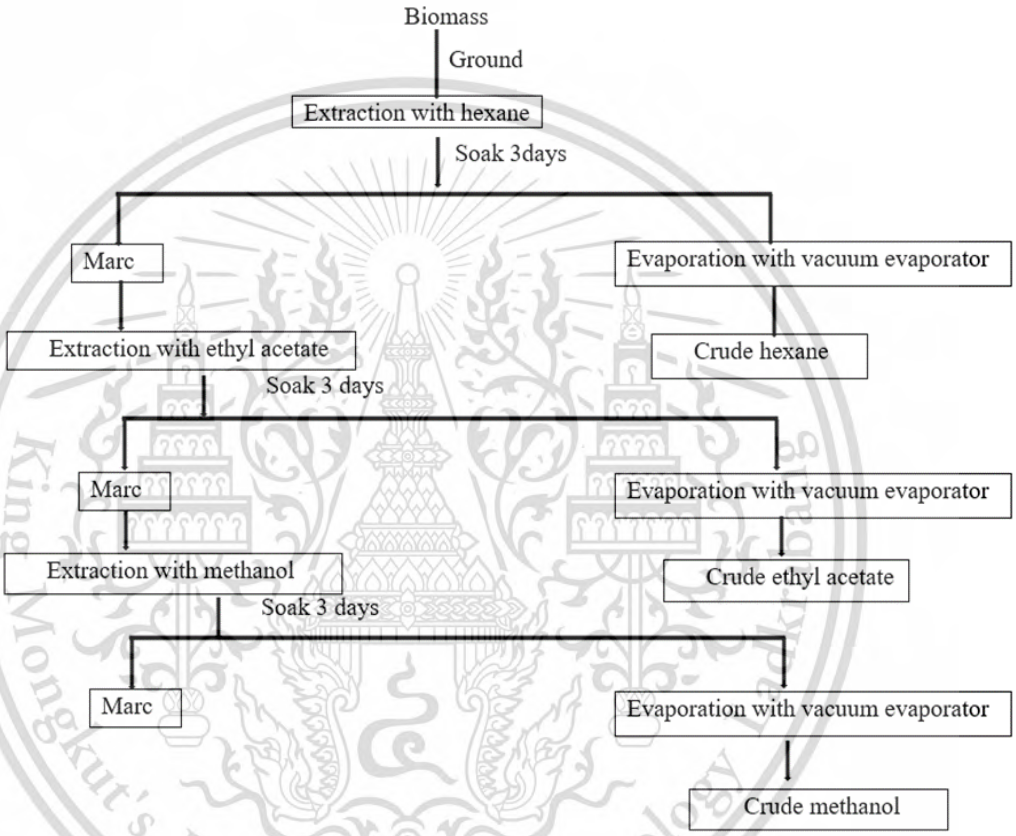

Figure 3.1 The extraction method for crude extract from antagonistic fungi (Kanokmedhakul *et al.*, 2006)

3.2.2.2 Testing crude metabolites against pathogens in *vitro*

Crude metabolites from *Ch. lucknowense* CL, and *T. hamatum* K01 were tested for their abilities to control *P. palmivora* caused root rot pathogen and *C. gloeosporioides* causal agent of anthracnose disease of citrus and durian using the poison food method. The experiment was conducted using a 3x6 factorial in a completely randomized design (CRD) with four replications. Factor A represented crude extracts where A1= hexane, A2= EtOAc, and A3= MeOH. Factors B

This material is reserved for educational use only, not allowed for commercial use.
Forbidden to modify the content, and cite the document when use.

represented concentrations where B1= 0 (control), B2= 10 ppm, B3= 50 ppm, B4= 100 ppm, B5= 500 ppm, B6= 1000 ppm. Each crude extract was weighed in each concentration and dissolved by 2% dimethyl sulfoxide (DMSO), then mixed into PDA before autoclaved at 121ºC 15 lbs/inch2 for 35 minutes. Pathogenic isolates pathogens were separated cultures in PDA for seven days at room temperature. Sterilized cork borer was used to cut 0.5 cm diameter agar plugs and transferred to the center of 5 cm petri dishes of each concentration in PDA and maintained under room temperature conditions (27-30ºC) until the control plates of the pathogen were grown full plates. The data were collected colony diameter, spore, or conidia inhibition of the pathogens. The effective dose (ED_{50}) was computed using Probit analysis. Treatment means were compared using Duncan's Multiple Range Test (DMRT) at $p<0.05$. The growth inhibition was computed using Equations 6 and 7.

3.3.2.3 Natural product nanofibers test

Nanofibers from *T. hamatum* K01 and *Ch. lucknowense* CL were evaluated for their antifungal activity against pathogenic fungi *P. palmivora* and *C. gloeosporioides*. Nanofibers from *T. hamatum* K01 and *Ch. lucknowense* CL were arranged from crude hexane, ethyl acetate, and methanol following the method of Dar and Soytong (2014). Each crude extract was mixed with one drop of dimethyl sulfoxide (DMSO) on the heater, and then it was added to a mixture of 2g of polylactic acid (PLA) with 10 mL of tetrahydrofuran. Nanofibers were conducted by loading the mixture into the electrospinning set-up to yield nanofibers.

The experiment was arranged using a two-factor factorial experiment in CRD with four replicates. Factor A was the microbial nanofibers, while Factor B was the concentrations of 3, 5, 10, and 15 ppm. Each nanofiber was dissolved in 2% dimethyl sulfoxide and mixed to PDA before autoclaving at 121°C,15 lbs/inch^2 for 30 min. The culture of the pathogen was cut at the peripheral colony with a sterilized cork borer (0.5 mm). Agar plugs of the pathogen were transferred to the middle of 5 cm Petri dishes PDA mixed with the concentration of each nanofiber. All plates were incubated at room temperature (27-30°C) until the pathogen in control (0 ppm) grew full plates. The pathogen from each treatment was observed for abnormal spores or conidia production under a light compound microscope.

This material is reserved for educational use only, not allowed for commercial use.
Forbidden to modify the content, and cite the document when use.

3.3.2.4 Data Collection and Statistical Data Analysis

Data collections were measured regarding the colony growth and number of conidia or number of spore production. The data were statistically analyzed. The effective dose (ED_{50}) was calculated by using probit analysis. Treatment means were compared by using Duncan's Multiple Range Test (DMRT) at $p<0.05$. The percentage inhibition was calculated using Equations (6) and (7)

$$\% \text{ Colony inhibition } = \frac{\text{Colony growth in control} - \text{Colony growth in each concentration}}{\text{Colony growth in control}} \times 100 \quad (6)$$

$$\% \text{ Spore suppression } = \frac{\text{Spore produced in control} - \text{Spore produced in treatment}}{\text{Spore produced in control}} \times 100 \quad (7)$$

3.4 Greenhouse experiments

The experiments were conducted in a randomized complete block design (RCBD) for seven treatments with four replications. Treatments were set up as follows:

T1 = Positive control (uninoculated, untreated)

T2 = Inoculated control by chemical metalaxyl

T3 = Inoculated control by *Ch. lucknowense* CL product

T4 = Inoculated control by *T. hamatum* K01 product

T5 = Inoculated control microbial nanofiber from *Ch. lucknowense* CL

T6 = Inoculated control by microbial nanofiber from *T. hamatum* K01

T7 = Negative control (inoculated, untreated)

The one-year-old durian plants var. Monthong and citrus were grown in plastic pots (25x16 cm) in diameter, with a mixture of loam soil: fine coconut shield: sand (2:1:1). The durian plants were inoculated with interaction between *C. gloeosporioides* C02 and *P. palmivora* PYSC01 and citrus plants were inoculated with *C. gloeosporioides* C01 before treatment, excepted T1 positive control. 24 hrs after fungal inoculation, T1 positive control uninoculated, nontreated spayed by water, T2, treatment was applied metalaxyl 1 g/L, T3, was applied *Ch. lucknowense* CL product 1 g/L, T4, was applied by *T. hamatum* K01 product 1g/L, treatment T5 was applied by microbial nanofiber from *Ch. lucknowense* CL 1mL/L, T6 was applied 1 mL/L of microbial nano elicitor from *T. hamatum* K01 and T7 negative

This material is reserved for educational use only, not allowed for commercial use.
Forbidden to modify the content, and cite the document when use.

control, untreated spayed by water. All agricultural inputs were applied every seven days.

3.4.1 Disease reduction

Disease incident (DI) was evaluated on days 30 and 90 after inoculation. Fifteen leaves of durian and citrus plants counted from the top were selected, and disease symptoms, such as yellow leaves, died back from the tip, and leaves dropped in control and treatment. The percentage of infection was computed using Equation (8), described by Mergawy *et al.* (2023)

$$\text{DI}\ (\%) = \frac{\text{Number of infected leaves}}{\text{Total of test leaves}} * 100 \quad (8)$$

The grade of disease incident was classified into five grades following the method described by El-Sharkawy *et al.* (2023) as follows: level 0=0%, no disease symptom, level 1=1–25% disease symptom coverage, level 2=26–50% disease symptom coverage, level 3=51- 75% disease symptom coverage, level 4=76–100% disease symptom coverage. The disease severity (DS) was calculated using Equation (9) following the method of Masoud *et al.* (2023).

$$\text{DS}\ (\%) = \frac{\text{Number of infected leaves} * \text{level of disease}}{\text{number of tests leave} * \text{the highest level of disease}} * 100 \ (9)$$

Data was statistically analyzed using analysis of variance (ANOVA). Treatment means were compared using Duncan's Multiple Range Test (DMRT) at $p<0.05$. Disease reduction (DR) was computed using Equation (10).

$$\text{DR}\ (\%) = \frac{\text{Disease severity in control} - \text{disease severity in treatments}}{\text{disease severity control}} * 100 \quad (10)$$

3.4.2 Phytoalexin production

Pot experiments of either citrus or durian were examined for phytoalexin production**.** The determination of citrus and durian phytoalexin was investigated through thin-layer chromatography (TLC) following the method illustrated by Tongon and Soytong (2022). The samples of citrus and durian leaves were collected from all the treatments. Each fresh leaf sample was weighed 1 g and washed with methanol, then cut into small pieces, ground with a pestle, soaked in 10 mL

This material is reserved for educational use only, not allowed for commercial use.
Forbidden to modify the content, and cite the document when use.

methanol, put in a water bath at 50 °C for 60 minutes, and filtrated through filter paper. The solution was evaporated using a rotary vacuum evaporator to yield crude extract. The crude extract was dissolved with sterilized water and spotted on TLC plates, and standard compounds were also spotted on TLC plates for comparison. The TLC plate was soaked in a tank containing 20 mL of 12% acetic acid as a developing solvent. The developed chromatograms were dried until spots appeared and examined under UV illumination. The absorbance was read at 254 nm. The retention factor (R_f) was computed using Equation (11). Xanthoxylin (2-hydroxyl-4,6-dimethoxyacetophenone) is a target compound induced by citrus and scopoletin induced by durian.

$$Rf = \frac{\text{distance traveled by the compound}}{\text{distance traveled by the solvent front}} \quad (9)$$

Where: R_f – retention factor

3.4.3 Assessment of growth parameter

The greenhouse experiment examined bio-products' effect as agricultural inputs and chemical fungicides compared to positive and negative control. Plant growth parameters regarding durian and citrus plant height were assessed before and on days 30, 60, 90, and 120 after treatment. Using Duncan's Multiple Range Test (DMRT), the treatment means were compared at $p<0.05$.

3.4.4 Plant physiological parameters

The photosynthetic pigments of citrus and durian, including total chlorophyll and carotenoid contents, were assessed 60 days after treatment following the method described by Phal *et al.* (2023b). Fresh leaf samples of citrus and durian were collected from each treatment. Samples 0.1 g were weighed and ground in mortar and pestle, extracted with 10 mL 80% of acetone, then centrifuged for 20 min at 10000 rpm. The chlorophyll a, b, and carotenoid absorbance were read at 663nm, 647nm, and 470nm, respectively. The amount of pigment was calculated using Lichtenthal's Equation below:

$C_a\ (\mu g/g) = 12.25A_{663} - 2.79A_{647}$

$C_b\ (\mu g/g) = 21.50A_{647} - 5.10A_{663}$

This material is reserved for educational use only, not allowed for commercial use.
Forbidden to modify the content, and cite the document when use.

C_{x+c} (μg/g) = $(100A_{470} – 1.82C_a – 85.02C_b)/198$

C_a=chlorophyll a, C_b=chlorophyll b, C_{x+c}= carotenoid, and A= wavelength of sunlight absorbance. Treatment means were compared using Duncan's Multiple Range Test (DMRT) at $p<0.05$.

This material is reserved for educational use only, not allowed for commercial use.
Forbidden to modify the content, and cite the document when use.

CHAPTER 4

RESULTS

4.1 Isolation and identification of pathogens

4.1.1 Isolation and morphological identification of *C. gloeosporioides* from citrus and durian

Disease samples were collected from anthracnose lesions on the citrus plant leaves for the pathogenic fungus. A tissue transplanting technique was used to isolate *Colletotrichum* spp. Characterization results showed that isolate C01 grew full in PDA plates at seven days by about 9 cm. Colonies on PDA were cottony white at the beginning and turned to dark gray from the center. They also have a purple color when observed upside down. The fungus produced conidiophores and dark brown setae of about 52-131 µm with an average of 98.5 µm in length and 4.2-7.9 µm with an average of 6.4 µm in width. One-cell conidium was also observed as ovoid and slightly carved of about 8-17 µm with an average of 12.5 µm in length and 5.5-7 with an average of 6.25 µm in width, which was identified as *C. gloeosporioides* as shown in Table 4.1 and Figure 4.1.

This material is reserved for educational use only, not allowed for commercial use.
Forbidden to modify the content, and cite the document when use.

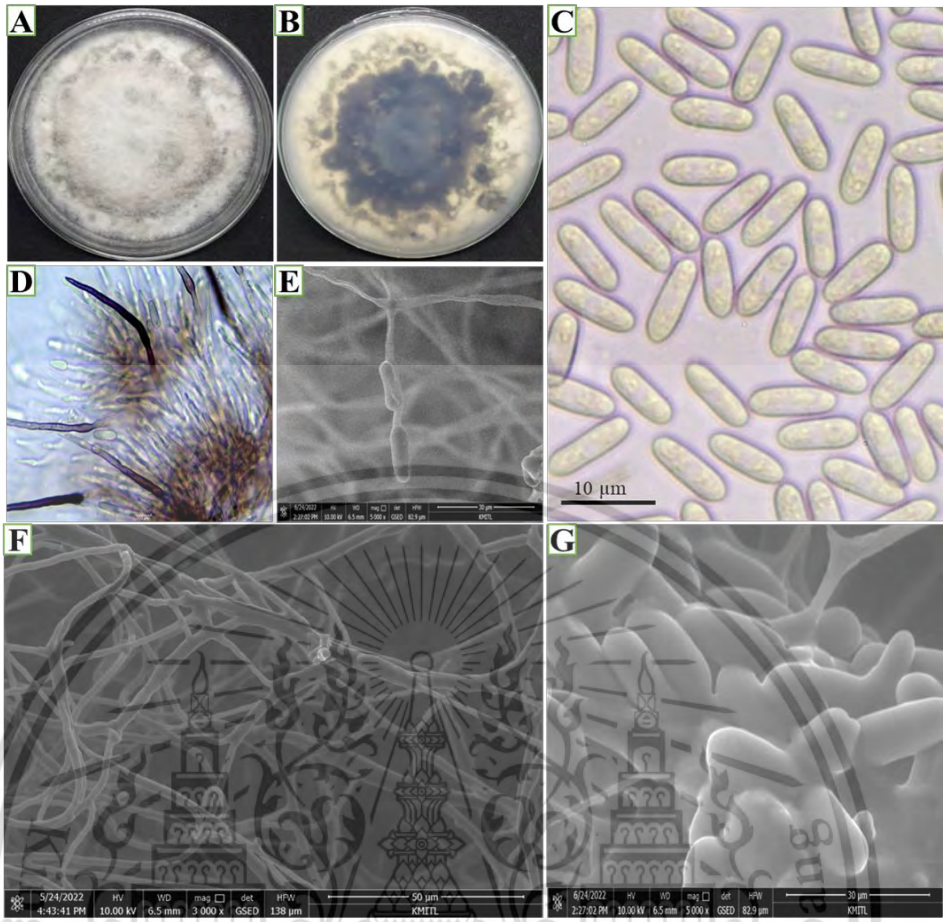

Figure 4.1 Colony growth patterns and the general characteristic of *C. gloeosporioides* C01.A, colony pattern on PDA; B, colony pattern on PDA upside down; C, G, conidia; D, E setae conidiophores, and F, hyphae. E, F, and G were observed using SEM.

C. gloeosporioides C02 was isolated from anthracnose symptoms of durian leave. Results showed that the mycelia grew about 9 cm in diameter in PDA Petri dishes within seven days. The colony characteristic was cottony white to gray for a more extended period. The colony pattern was purple when observed from upside to down. Under a binocular compound microscope, the fungus produced a dark brown setae conidiophore of about 25.2-107.3 µm length. Hyaline, one-cell conidium, ovoid, and dumbbell-shaped conidiophores were also observed to form conidia of about 6-19.5 µm in length and 5.1-7.6 µm in width (Table 4.1., Figure 4.2).

This material is reserved for educational use only, not allowed for commercial use.
Forbidden to modify the content, and cite the document when use.

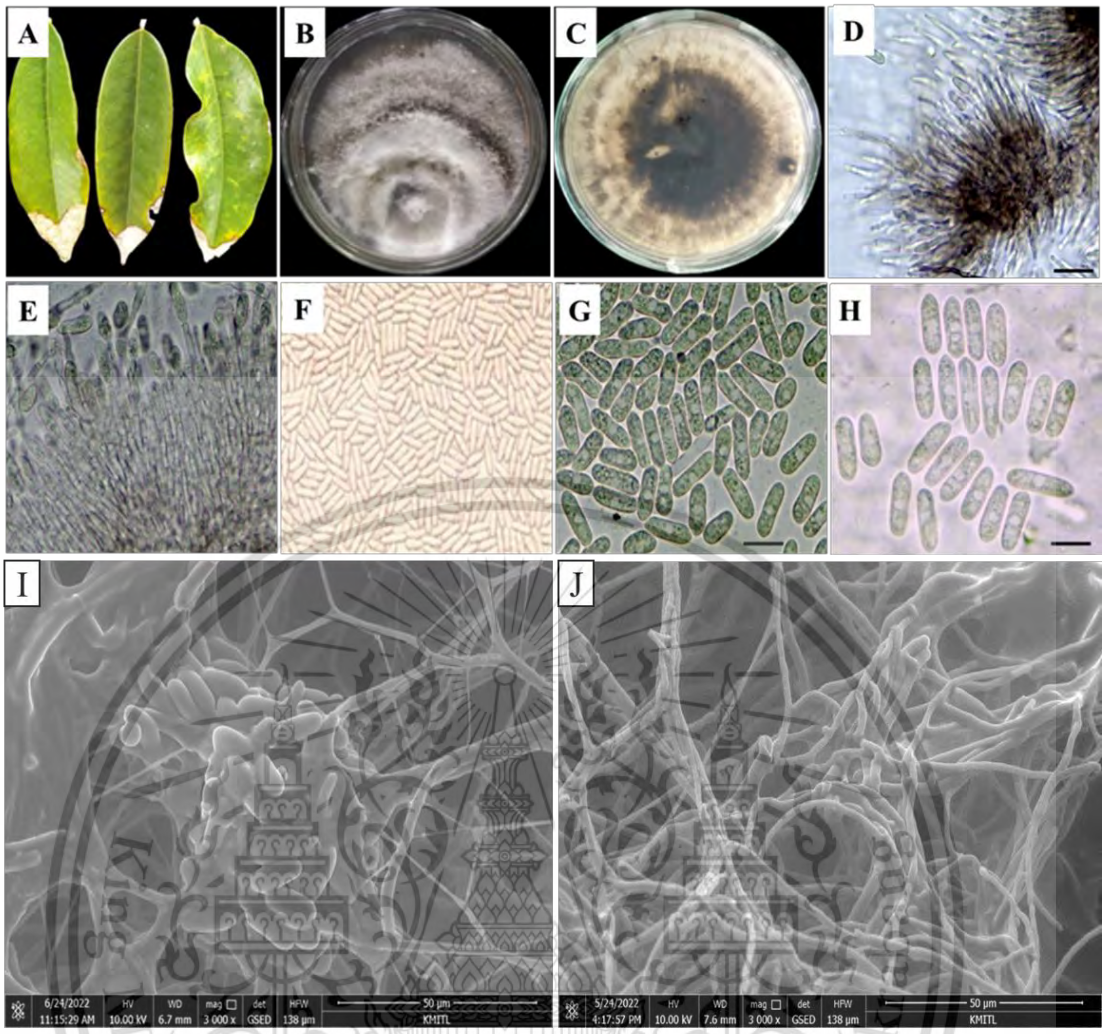

Figure 4.2 Morphological characterized of *C. gloeosporioides* C02 isolated from infected durian leaves; A, disease samples from durian leaves; B, colony growth of *C. gloeosporioides* C02 in PDA media; C, colony growth upside down; D, E, setae conidiophores and F, G, H, I, conidia and J, Hyphae. D-H were observed under a light compound microscope, and I; J were observed using SEM.

4.1.2 Isolation and morphological identification of *P. palmivora*

The *P. palmivora* PYSC01 was obtained directly from the root rot of durian using the baiting technique and identified based on morphological characteristics. The result showed that *P. palmivora* PYSC01 was grown fully in 9 cm diameter PDA petri dish within eight days. The colony's characteristics presented stellate mycelium of cotton white, uniformly grown, and slightly diffuse. Under a light compound microscope, hyphae were non-septate, hyaline, undulating, and lumpy

This material is reserved for educational use only, not allowed for commercial use.
Forbidden to modify the content, and cite the document when use.

branching, 3.5-4.9 µm in diameter in width. Sporangia are produced by inflation from the tips of the branch of sporangiophore, with different shapes, elongate ellipsoid, lemon shapes and ovoid 24.7-41 µm with the means size of 28.5 µm diameter in length and 11.4-30 µm with means size of 18.3 µm diameter in width, the papilla is a conic protuberance or small rounded size 2.8-4.2 µm with means size 3.5 µm diameter in width, generally translucent, break open of the sporangia wall and role as the exit point of the zoospore. Sporangia were directly released zoospores when flooded in sterilized distilled water for 12 to 48 hrs. It has a smooth wall oogonium 24.2 x 34.5 µm diameter in size with spherical, short cylindrical mono antheridium. Sporangiophores are thin and globose or sub-globose shapes of chlamydospore 15.1-34.5 µm diameter length with means size 23.5 µm and 15.6-24.6 µm diameter with mean size 19.7 µm diameter in width which was identified as *P. palmivora* based on morphological identification (Table 4.1, Figure 4.3).

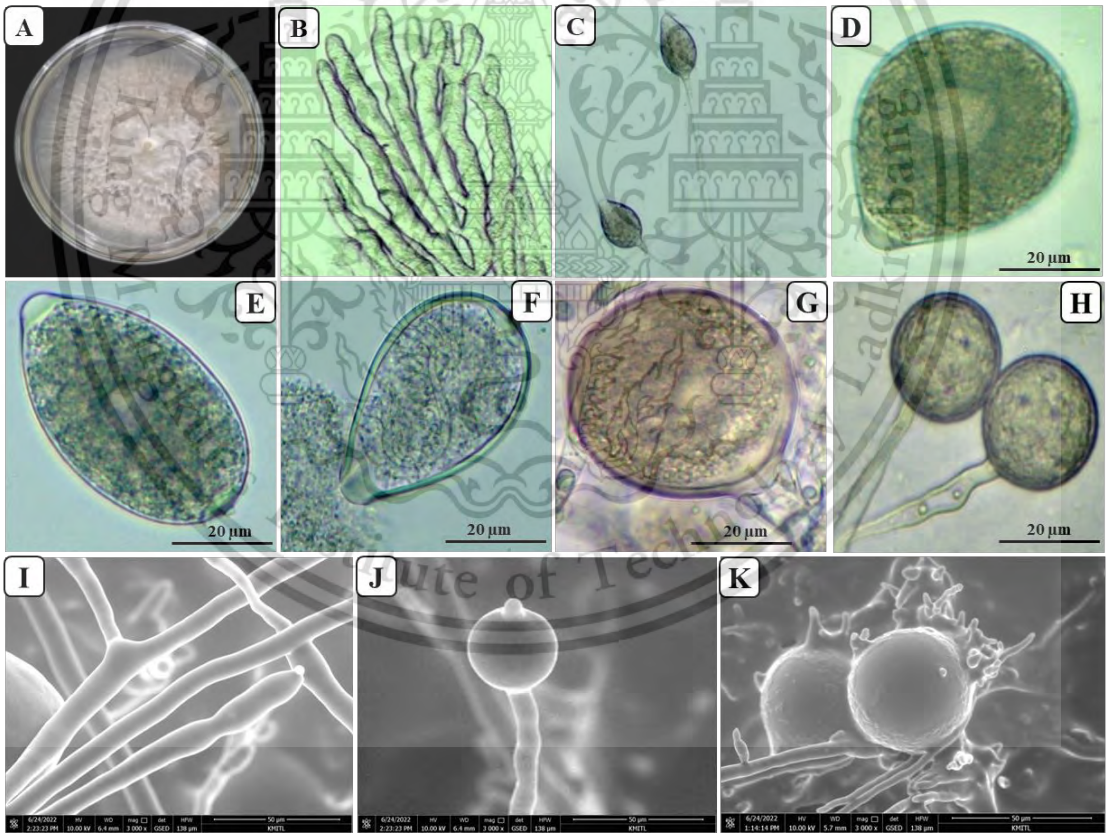

Figure 4.3 Morphologically characterized *P. palmivora* PYSC01. A; colony growth in PDA at ten days old; B, I, lumpy branding mycelial; C, J, occurrence of sporangia on sympodium; D, E, F, sporangia with different shapes; F, zoosporangia released from sporangia; G, one antheridium with one

This material is reserved for educational use only, not allowed for commercial use.
Forbidden to modify the content, and cite the document when use.

oogonium and H, K, chlamydospore. B-H were observed under a light compound microscope, and I-K were observed using SEM.

4.2 Morphological identification of antagonistic fungi

4.2.1 Morphological identification of *T. hamatum* K01

T. hamatum K01 was also identified under morphological characteristics. The identification results showed that *T. hamatum* K01's colony pattern was thin, white on the surface and brown when it was older, and yellow pigment on the reverse side. It was pure yellow when observed upside down. Observation under a light compound microscope showed that the culture was smooth-walled whip-like, with hyphal elongations of 2.8 to 5.7 µm with an average of 4.4 µm diameter. It constructs apices roughened conidiophores 3.2 to 18.3 µm with an average of 11.3 µm diameter with granules. It produces Phialides conidia 2.7 to 4.1 µm with an average of 3.27 µm in width, 3.8 to 5.7 µm with an average of 4.63 µm in length, and germination of chlamydospore (Table 4.1., Figure 4.4).

This material is reserved for educational use only, not allowed for commercial use.
Forbidden to modify the content, and cite the document when use.

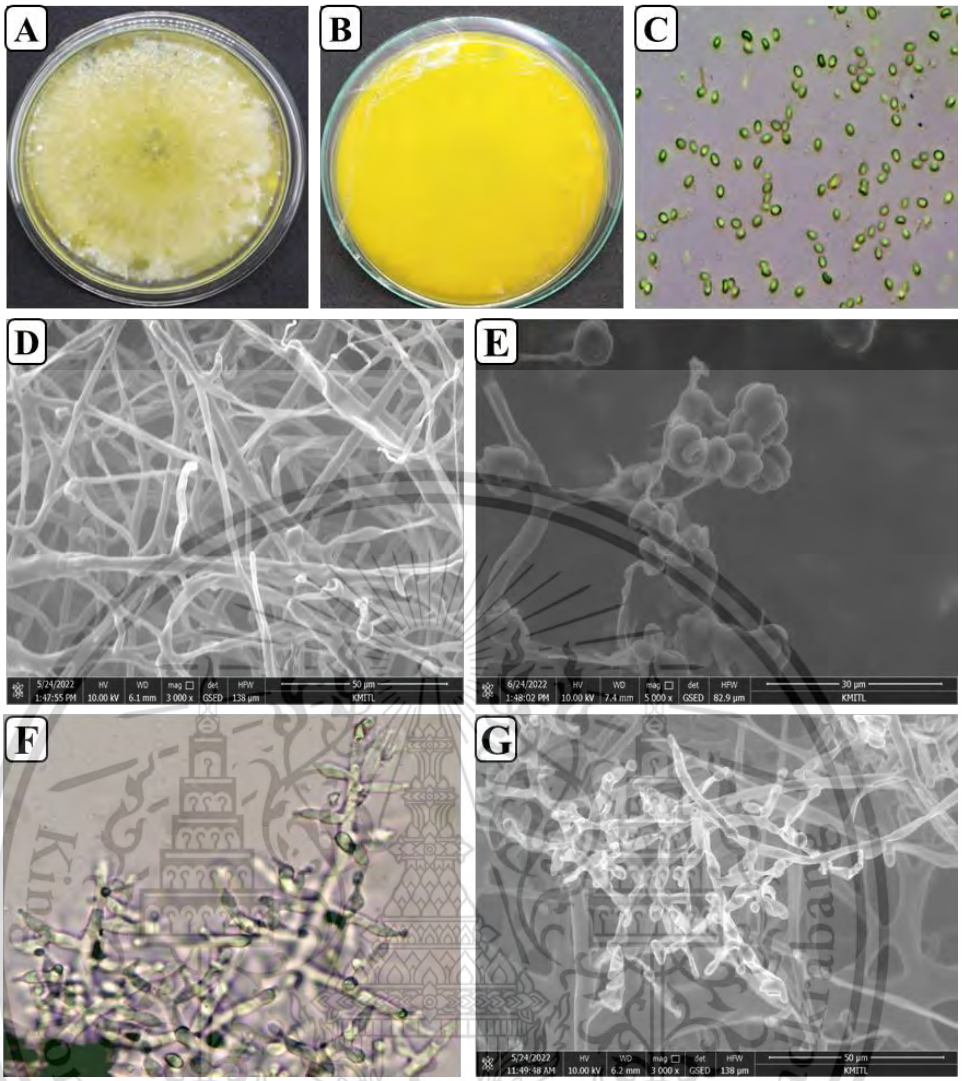

Figure 4.4 Morphological identification of *T. hamatum* K01; A, colony pattern growing in PDA at 7 days; B, colony pattern growing in PDA observed upside down; C, E conidia production; D, hyphae; F, G, apices roughened conidiophore. C and F were observed under a light compound microscope, and D, E, and G were observed using SEM.

4.2.2 Morphological identification of *Ch. lucknowense* CL

The identification result showed that *Ch. lucknowense* CL had grown to a full 9 cm diameter PDA plate in 7-8 days at room temperature (27-30°C). When observed upside down, the colony pattern was observed from green to brown, turning grey as it grew older and pure brown. Furthermore, ascomata were dark-brown, superficial, spherical, and ovate 146-195 x 107-157.2 µm in size. Ascomata hairs are numerous and flexuous. The asci are clavate in shape and have a short stalk

This material is reserved for educational use only, not allowed for commercial use.
Forbidden to modify the content, and cite the document when use.

of 60.41-99.8 µm in size. Each ascus contains eight ascospores. Ascospores are flattened lemon-shaped, olivaceous brown with 6.3-10.6x4.7-7.8 µm in size and have a single apical germ spore (Table 4.1., Figure 4.5).

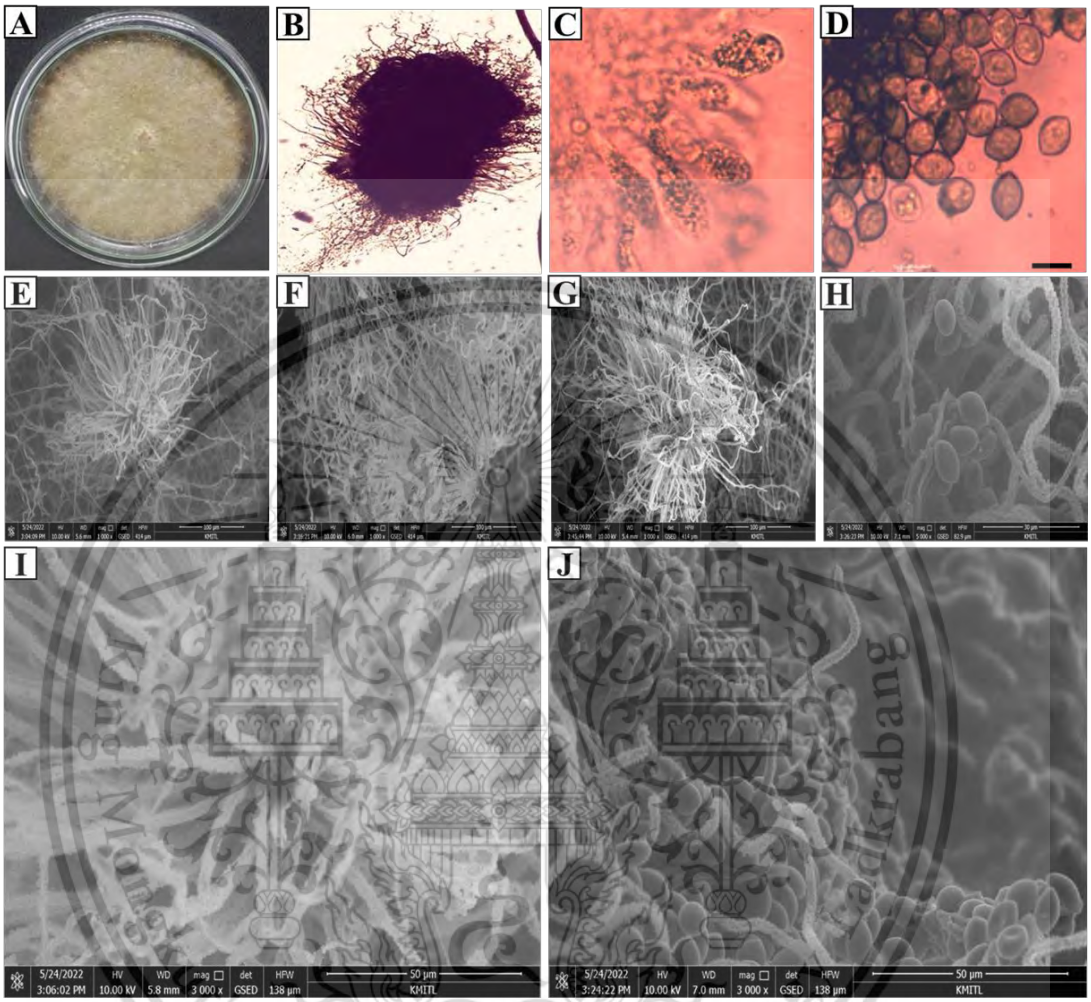

Figure 4.5 Characteristics of *Ch. lucknowense* CL; A, colony pattern at ten days old on PDA media; B, colony pattern upside to down; C, ascomata; D, ascomata hair; E and F, asci; G and H, ascospores. E-J was observed using SEM

This material is reserved for educational use only, not allowed for commercial use.
Forbidden to modify the content, and cite the document when use.

Table 4.1 Measurements of the general characteristics of the pathogens and antagonistic fungi

Fungi	Sources	Structure (µm)	Max	Min	Mean
P. palmivora PYSC01	Root rot of durian	Sporangium[a] (length)	41.0	24.7	28.5
		Sporangium[a] (width)	30.0	11.4	18.3
		Papilla[b] (length)	4.2	2.8	3.5
		Pedicel[b] (diameter)	3.7	2.1	2.9
		Chlamydospore[b] (length)	34.5	15.1	23.5
		Chlamydospore[b] (width)	24.6	15.6	19.7
		Hyphae diameter[b]	4.9	3.5	4.2
C. gloeosporioides C01	Anthracnose lesion of citrus	Setaea (length)	195.1	52	98.53
		Setaea (width)	7.9	4.2	6.4
		Conidiab (length)	17	8	12.5
		Conidiab (width)	7	5.5	6.25
C. gloeosporioides C02	Anthracnose lesion of durian	Conidiophores (length)	107	25.2	54.2
		Conidiab (length)	19.5	6	12.4
		Conidiab (width)	7.6	5.1	5.8
		Hyphaea (diameter)	5.8	2.7	4.4
T. hamatum K01	Offered from Dr. Kasem Soytong	Phialides conidia[a] (length)	5.7	3.8	4.63
		Phialides conidia[a] (width)	4.1	2.7	3.27
		Chlamydospore[b] (diameter)	18.3	3.2	11.3
		Hyphae[b] (diameter)	5.7	2.8	4.4
Ch. lucknowense CL	Offered from Dr. Kasem Soytong	Ascomata[b] (length)	195	146	170.5
		Ascomata[b] (width)	157.2	107	132.1
		Ascospore[a] (length)	10.6	6.3	8.45
		Ascospore[a] (width)	7.8	4.7	6.4
		Asci[b] (diameter)	99.8	60.41	80.1

[a]Data was collected from 50 separate of each structure.

[b]Data was collected from 30 separate of each structure.

4.3 Molecular identification of the pathogens

The molecular identification of isolates C01 and C02 was done to confirm the species level. The phylogenetic tree showed *Colletotrichum gloeosporioides* C01-ITS1. This isolate was in the same clade with KM519999 *C. gloeosporioides*

This material is reserved for educational use only, not allowed for commercial use.
Forbidden to modify the content, and cite the document when use.

isolate LL5, KY033215 *C. gloeosporioides* isolate p1-1, MT993622 *C. gloeosporioides* isolate s12, HQ264182 *C. gloeosporioides* isolate Cg-224, MT919170 *C. gloeosporioides* isolate ESP15, and KY930619. KY930619 with *Sordaria fimicola* compared as the outgroup (Figure 4.6). Moreover, the rDNA sequence analysis showed seven complicated nucleotide sequences. It demonstrates that the isolate C02-ITS1 was the same clade of KJ777830 *Colletotrichum gloeosporioides* CgloTIN20, MT729939 *Colletotrichum gloeosporioides* Y14, KJ777825 *Colletotrichum gloeosporioides* CgloTIN26, KF697685 *Colletotrichum gloeosporioides* C3345, MZ021314 *Colletotrichum gloeosporioides* SQYJCG-1, CBS 112999 *Colletotrichum gloeosporioides* Apn2, and HQ264183 *Colletotrichum gloeosporioides* Cg-246 with LC684558 *Phytophthora palmivora* DCHU1304 being compared as the outgroup (Figure 4.7). *Phytophthora palmivora* isolate PYSC01 ITS5-4 was the same clade as HQ237479 *Phytophthora palmivora*, MH219857 *Phytophthora palmivora*, LC684558 *Phytophthora palmivora*, MH219852 *Phytophthora palmivora*, LC684540 *Phytophthora palmivora,* GU111683 *Phytophthora arecae* and KP050545 *Phytophthora taxon banihhashemiana*. EF025942 *Colletotrichum gloeosporioides* were compared as an outgroup (Figure 4.8).

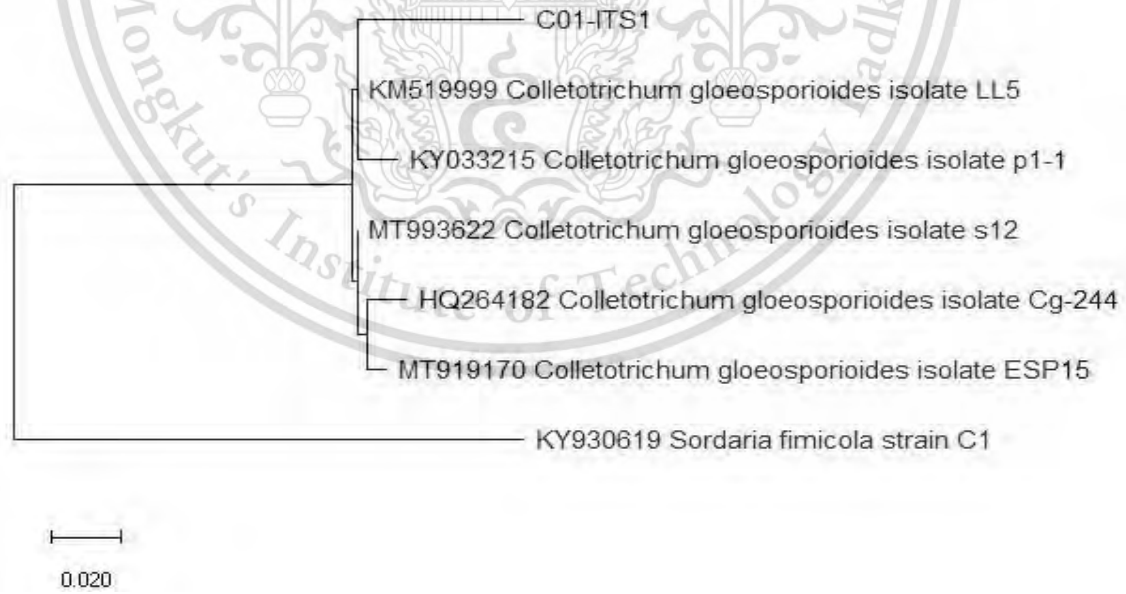

Figure 4.6 Phylogenetic tree of *C. gloeosporioides* C01 from GenBank with 99.54% bootstrap value constructed after the distance-based analysis of the rDNA's universal primer ITS1, ITS4, and 5.8S region

This material is reserved for educational use only, not allowed for commercial use.
Forbidden to modify the content, and cite the document when use.

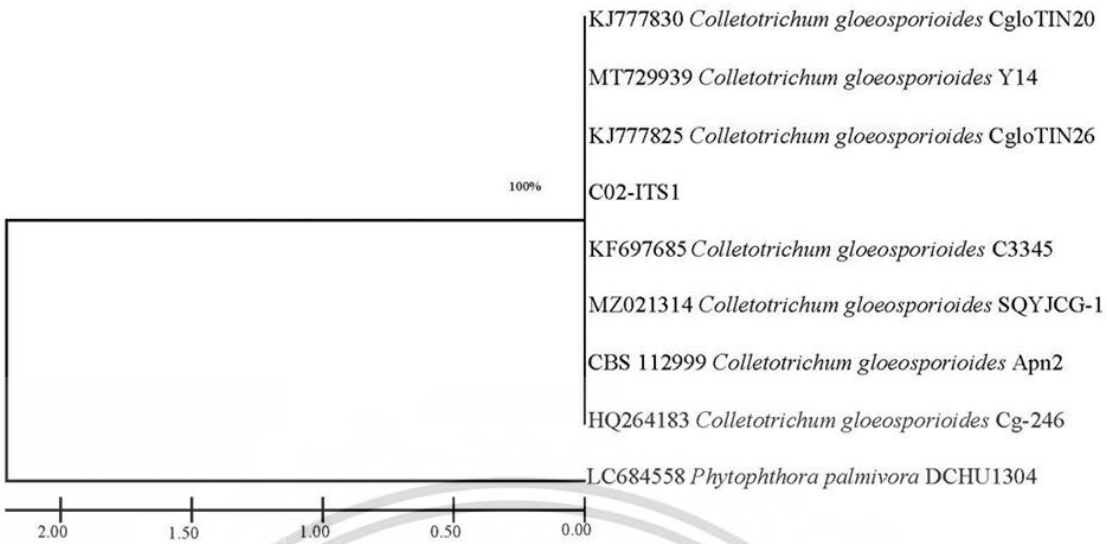

Figure 4.7 Phylogenetic tree of *C. gloeosporioides* isolate C02 retrieved from GenBank with 100% bootstrap value made after the distance-based analysis of the universal primer ITS1, ITS4, and 5.8S region of the rDNA. Twelve nucleotide sequences were analyzed, and a bootstrap consensus tree was inferred from 1000 replicates

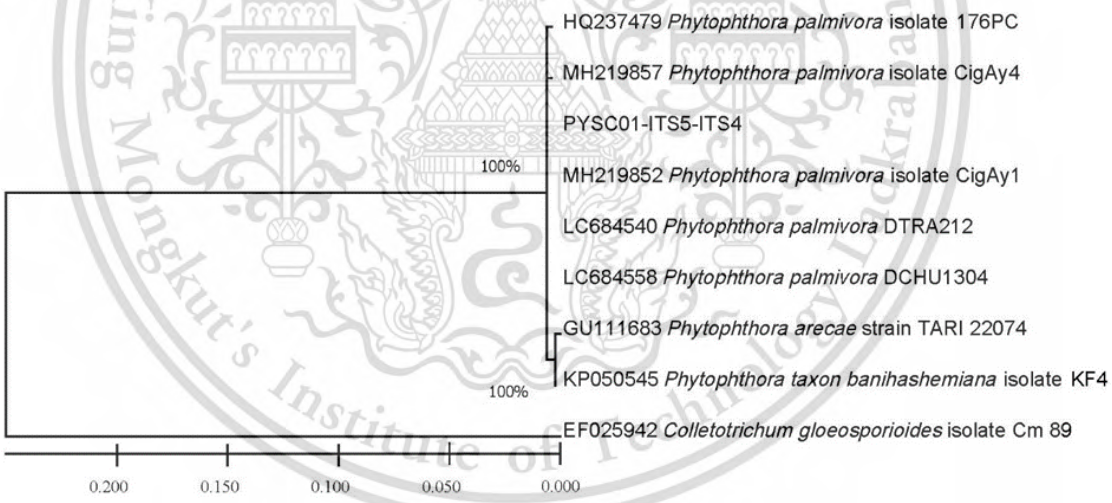

Figure 4.8 The phylogenetic tree of *P. palmivora* PYSC01 from GenBank with 100% bootstrap value was constructed after the distance-based analysis of the universal primer ITS5, ITS4, and 5.8S region of the rDNA. Nine nucleotide sequences were analyzed, and the bootstrap consensus tree was inferred from 1000 replicates

This material is reserved for educational use only, not allowed for commercial use.
Forbidden to modify the content, and cite the document when use.

4.4 Molecular identification of antagonistic fungi

To characterize organisms to strain and sub-species level of antagonistic fungi. *T. hamatum* K01 and *Ch. lucknowense* CL have confirmed the species level based on molecular identification. *Trichoderma hamatum* K01-ITS1 is the same clade with *Trichoderma hamatum* AB737864 isolate FKI-6011, *Trichoderma hamatum* MW750434 isolate GL19, *Trichoderma hamatum* OL439486 strain Th23, Trichoderma hamatum MW763159 isolate TISC-3, *Trichoderma hamatum* MN880214 strain JAHLH2, and *Trichoderma hamatum* KX424842 isolate NGL1, with *Colletotrichum gloeosporioides* EF025942 Cm 89 compared as an outgroup (Figure 4.9). It demonstrates that *Chaetomium lucknowense* CL-ITS1 was the same clade as MH877835 *Chaetomium lucknowense* CBS 243.84, MH860360 *Chaetomium lucknowense* CBS 796.71, MH860312 *Chaetomium lucknowense* CBS 727.71 and MT186188 *Chaetomium lucknowense* GSM-14. MZ799225 *Colletotrichum gloeosporioides* Apn2 was being compared as an outgroup (Figure 4.10).

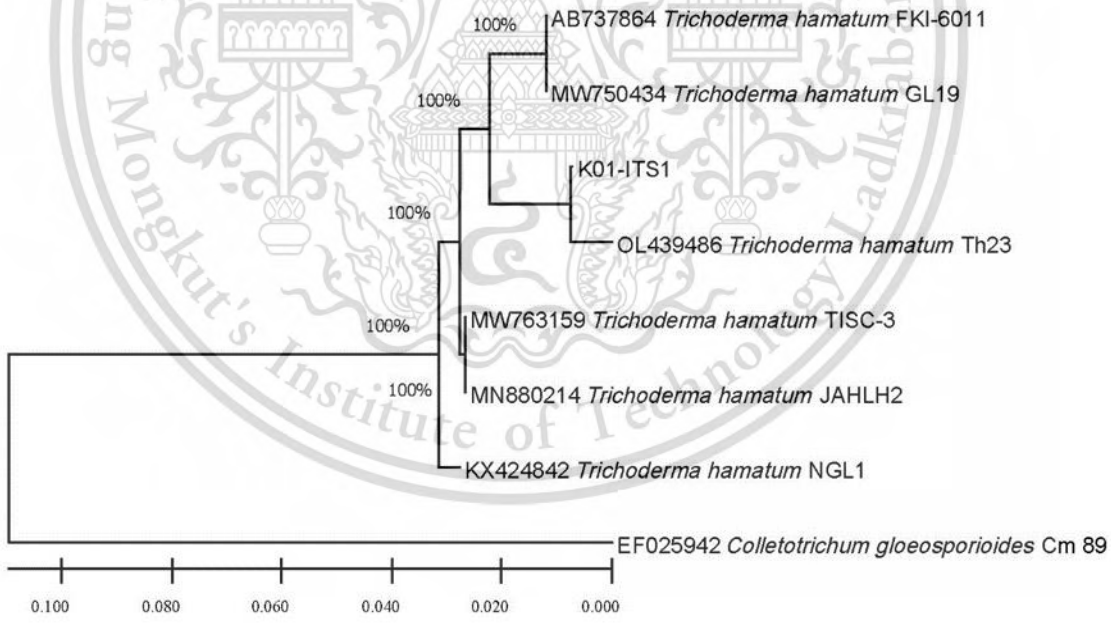

Figure 4.9 The phylogenetic tree of *T. hamatum* K01 from GenBank with 100% bootstrap value was constructed after the distance-based analysis of the universal primer IT, S1, ITS4, and 5.8S region of the rDNA. Nucleotide nine sequences were analyzed, and a bootstrap consensus tree was inferred from 1000 replicates

This material is reserved for educational use only, not allowed for commercial use.
Forbidden to modify the content, and cite the document when use.

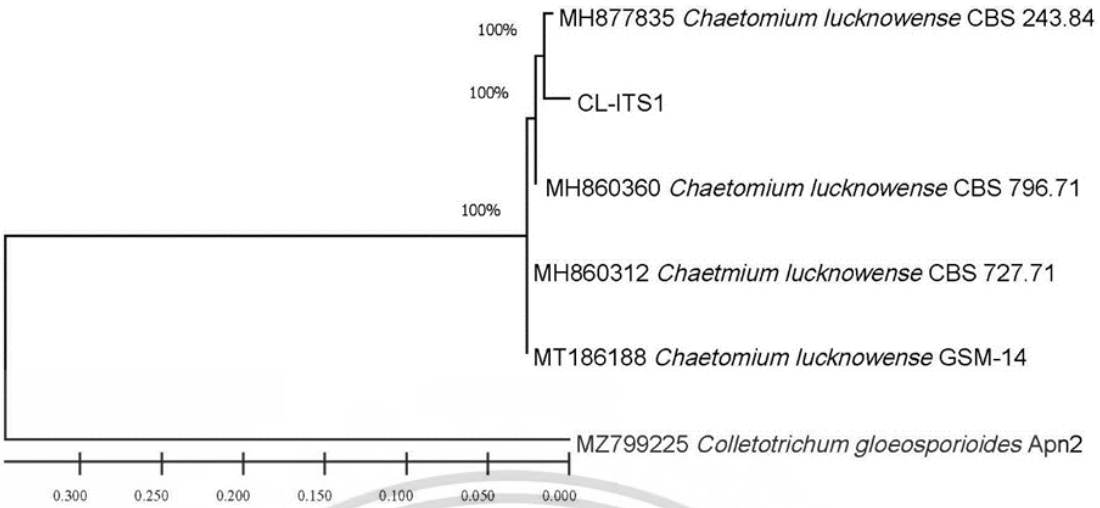

Figure 4.10 The phylogenetic tree of *Ch. lucknowense* CL K01 from GenBank with 100% bootstrap value was constructed after the distance-based analysis of the universal primer ITS1, ITS4, and 5.8S region of the rDNA. Nucleotide sequences of six were analyzed, and a bootstrap consensus tree was inferred from 1000 replications

4.4 Pathogenicity test

4.4.1 Pathogenicity test of *C. gloeosporioides* C01

C. gloeosporioides C01 was proven to be the pathogenic isolate on citrus leaves using the detached leaves technique in a moist chamber. The results showed that *C. gloeosporioides* C01 caused anthracnose disease on citrus leaves after the sixth day of inoculation with 24.46% using ImageJ software. The detached leaves' symptoms changed to dark brown lesions around agar plugs from 1.5 to 2.75 cm in

This material is reserved for educational use only, not allowed for commercial use.
Forbidden to modify the content, and cite the document when use.

diameter and expanded larger lesions to all the detached leaves. In addition, it was seen that *C. gloeosporioides* C01 infected citrus leaves at a medium aggressive level compared to non-inoculated control with no symptoms and remained healthy (Table 4.2., Figure 4.11).

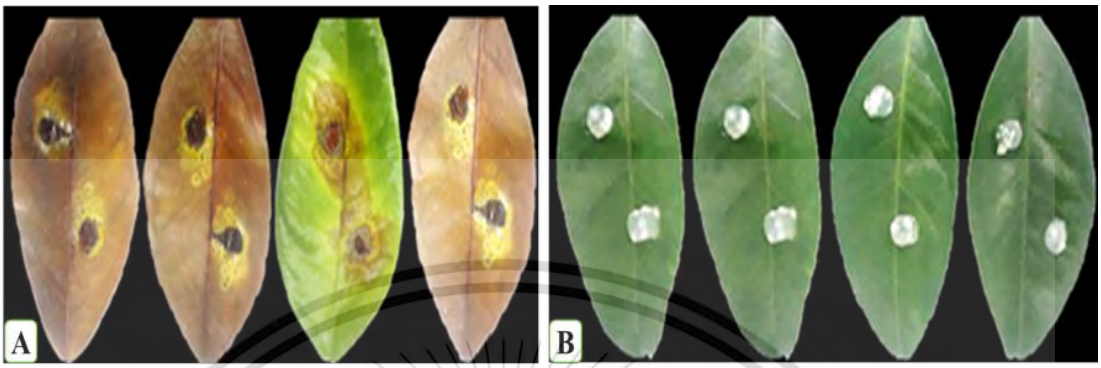

Figure 4.11 Pathogenicity of *C. gloeosporioides* C01 on citrus leaves using the detached method. A, the detached citrus leaves inoculated by *C. gloeosporioides* C01, B, non-inoculated control.

Table 4.2 Measurement of leaf damage using ImageJ software

Reps.	Area of test leaves (cm^2)	Areas of infection (cm^2)	% Infection
1	53.02	8.83	16.65%
2	53.37	8.95	16.77%
3	45.36	13.77	30.35%
4	45.2	15.4	34.07%
Percentage of damage of all test leaves			24.46%

4.4.2 Pathogenicity test of *C. gloeosporioides* C02

A pathogenicity test of *C. gloeosporioides* C02 was done with the durian leaves to prove the pathogenic isolate. The findings confirmed that inoculated durian leaves with the pathogen showed anthracnose disease, with symptoms starting to appear within three days after inoculation. The disease lesions measured on the sixth day showed a 2-3.5 cm diameter surrounding the inoculation agar with 9.63% using ImageJ software. The lesions expanded larger to the whole leaves for an extended period. A clear presence of lesions was observed when the inoculated

This material is reserved for educational use only, not allowed for commercial use.
Forbidden to modify the content, and cite the document when use.

leaves were removed from the moist chamber and air-dried overnight. Meanwhile, the non-inoculated control showed no disease symptoms and remained healthy, as shown in Table 4.3., Figure 4.12.

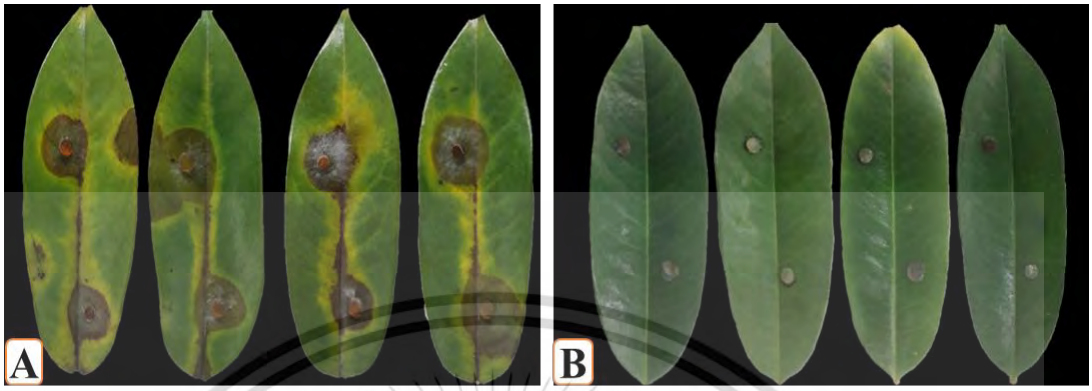

Figure 4.12 The pathogenicity test of *C. gloeosporioides* C02 on durian leaves using the detached leaves method; A, the durian leaves inoculated by *C. gloeosporioides* C02 and B, non-inoculated control

Table 4.3 Measurement of damage leaves of durian leaves using ImageJ software

Reps.	Area of tested leaves cm^2	Areas of infected cm^2	% Infection
1	64.23	6.39	9.94%
2	53.18	6.76	12.71%
3	60.53	5.82	9.61%
4	63.48	3.97	6.26%
Percentage of damage of all test leaves			9.63%

4.4.3 Pathogenicity test of *P. palmivora* PYSC01

4.4.3.1 Pathogenicity test using detached leaves method.

The detached leaves assay was done to prove the pathogenic fungus *P. palmivora* PYSC01 to the durian leaves var. Montong. The result indicated that the inoculation of *P. palmivora* PYSC01 was infected with the durian leaves within three days. The detached leaves presented water-soaked dark brown around the pathogen's agar plugs. On the fifth day, the lesions were measured with a disease lesion of 2.5-3 cm diameter with 16.29 % using ImageJ software (Table 4.4), and

This material is reserved for educational use only, not allowed for commercial use.
Forbidden to modify the content, and cite the document when use.

the lesions expanded larger to the whole test leaves with the long inoculation period. While the non-inoculated controls showed no disease symptoms, they remained healthy. Therefore, it was seen that *P. palmivora* PYSC01 causing rot disease, which was highly virulent to the durian leaves var Montong (Figure 4.13).

Table 4.4 Measurement of test leaves of durian using ImageJ software

Reps.	Areas of test leaves (cm^2)	damaged areas (cm^2)	% damaged
1	45.18	12.68	28.07%
2	58.40	5.84	10.00%
3	50.55	6.66	13.17%
4	48.78	6.78	13.90%
The average of four replications of damaged			16.29%

Figure 4.13 Pathogenicity test of *P. palmivora* PYSC01 on durian using detached leaves method. A, the durian leaves inoculated by *P. palmivora* PYSC01, and B, non-inoculated control

4.4.3.2 Pathogenicity test using root inoculated method

P. palmivora isolate PYSC01 was done to prove the pathogenic isolate to the durian root using Koch's postulate method. The result revealed that the inoculation of *P. palmivora* PYSC01 caused root rot disease of the durian. The disease symptoms on the root system presented root rot with an average of 75%, with DI rated as level 3. The root cortex turned soft and sloughed to leave. There was no new root produced, while the symptoms on leaves and stems of durian seedlings were changed to wilt and dry, it was observed at the sixth week of inoculation, which

This material is reserved for educational use only, not allowed for commercial use.
Forbidden to modify the content, and cite the document when use.

was similar to the disease symptom that infected the durian plants in Chanthaburi province where the disease samples have been collected. While the non-inoculate controls showed no root rot symptoms, all root systems above the durian plant remained healthy. Moreover, durian seedlings in control produced numerous new root systems (Figure 4.14).

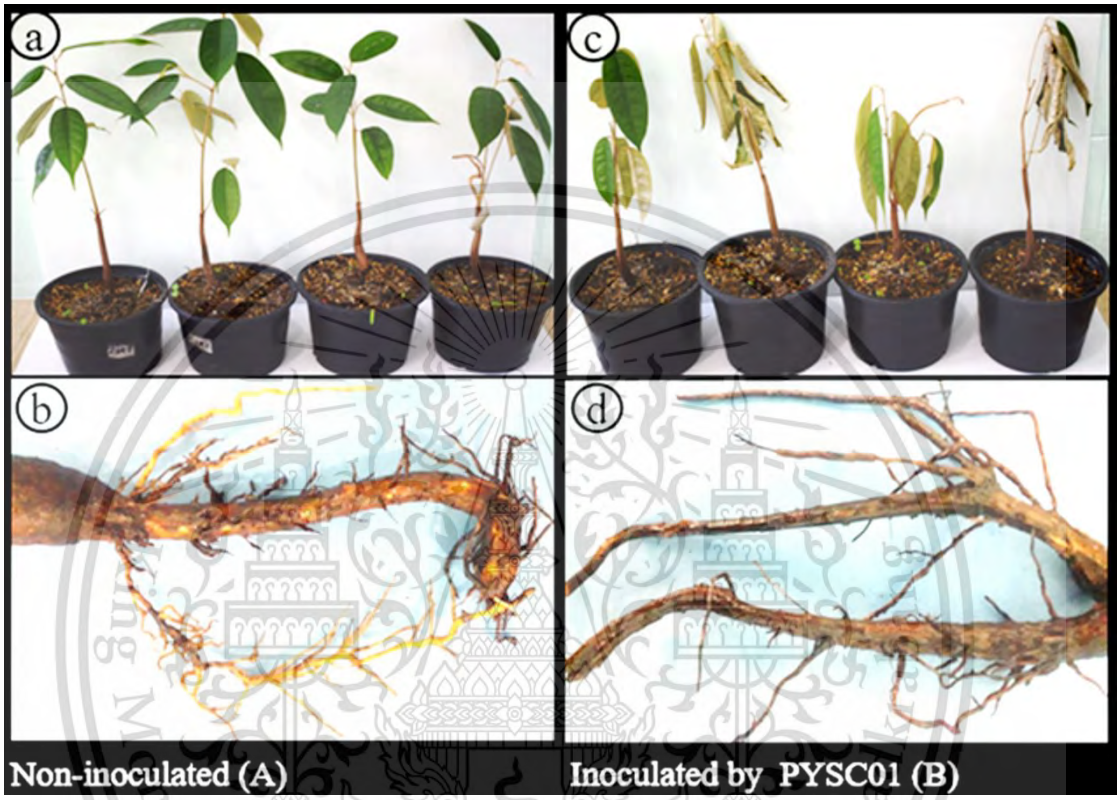

Figure 4.14 Pathogenicity test of *P. palmivora* PYSC01 to durian. A; non-inoculated; a, healthy durian plant in non-inoculated; b, New roots produced in non-inoculated; B, durian inoculated with *P. palmivora* PYSC01; c, durian plant showing the disease symptom and d, the root of durian inoculated by *P. palmivora* PYSC01

4.5 Analysis of secondary metabolites of antagonistic fungi

4.5.1 Analysis of secondary metabolites from *T. hamatum* K01

The secondary metabolite constituents from *T. hamatum* K01 were identified using GC-MS analysis. The constituent analysis showed 34 compounds, which accounted for 97.37% of the total crude MeOH. It was found to contain main antifungal metabolites such as pyrone metabolite (6-pentyl-2H-Pyran-2-one), fatty acid and sorbicillin as shown in (Table 4.5., Figures 4.15 and 4.16).

This material is reserved for educational use only, not allowed for commercial use.
Forbidden to modify the content, and cite the document when use.

Table 4.5 Constituents detected from *T. hamatum* K01 using (GC/MS) analysis.

No	Constituents	%	RT*	M* (g/mol)
1	Glycerin	17.83	7.261	92.11
2	1,2,3-Propannetriol	2.35	8.502	92.09
3	Mannitol	0.17	18.56	182.17
4	Oxirane	0.77	9.619	58.07
5	Benzoic acid	0.31	10.833	112.12
6	Phenol	0.13	14.254	94.11
7	2-Methyl-1-(m-methoxybenzyl)-1-pyrrolinium	0.30	14.637	289.71
8	Hexadecane	0.33	15.268	226.44
10	1,2-Azaborolidine, 1-(1,1-dimethylethyl)	0.68	16.498	127.18
11	6-pentyl-2H-Pyran-2-one	1.14	16.612	166.22
12	Tetracosane	0.22	17.507	338.65
13	Benzene	4.10	10.892	78.11
14	5,5-diphenyl-2-cyclohexenone	0.34	23.113	248.3
15	Exo-(5,6-Dihydro 3,8-phenanthrolino)	1.01	24.608	210.18
16	Benzene acetamide	3.36	12.862	59.07
17	2H-Pyran-2-one, tetrahydro-4-hydroxy-6-pentyl-	1.29	13.903	186.25
18	4-Methyl-2,6-di-tert butylphenol	0.34	14.319	220.35
19	Tetradecanoic acid	0.27	16.682	228.37
20	Palmitic acid	0.57	17.820	256.42
21	12-methyl-Tetradecanoic acid	0.41	18.236	242.40
22	Pentadecanoic acid	15.50	19.849	242.39
23	Hexadecenoic acid, ethyl ester	12.33	20.389	284.47
24	Hexadecenoic acid, 14-methyl-, ethyl ester	0.22	20.890	284.47
25	9,12-Octadecadienoic acid (z, z)-, methyl ester	6.26	21.797	294.47
26	9- Octadecadienoic acid (z)- methyl ester	4.55	21.867	296.48
27	Octadecadienoic acid	3.06	22.148	280.44
28	Linoleic acid	4.51	22.239	280.45
29	9- Octadecadienoic acid, (E)-trans-delta	8.25	22.299	282.46
30	Linoleic acid ethyl ester	3.65	22.531	308.49
31	Ethyl Oleate	1.37	22.590	310.51

This material is reserved for educational use only, not allowed for commercial use.
Forbidden to modify the content, and cite the document when use.

32	Octadecadienoic acid, ethyl ester	0.57	22.838	308.49
33	Sorbicillin	0.99	20.890	232.27
34	naphtho[2,1-b] furan	0.19	21.506	184.19

RT* retention of time, M* molecular weight

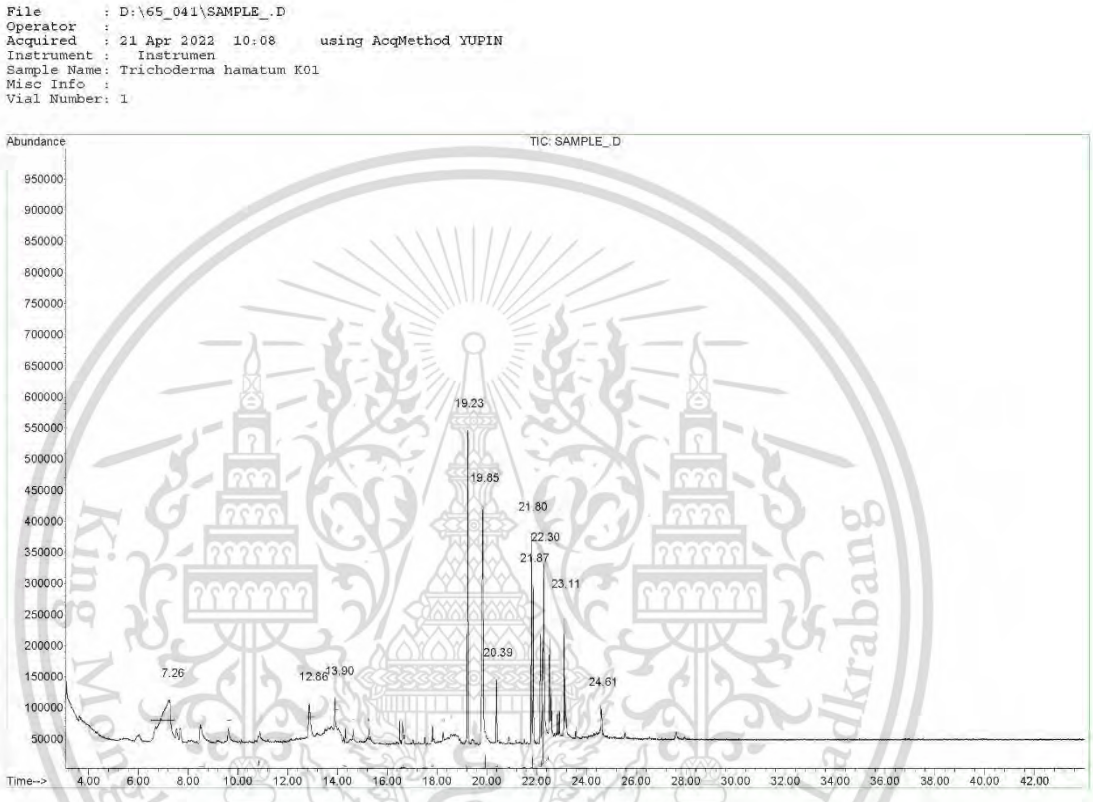

Figure 4.15 Chromatography GC-MS analysis of secondary metabolites from *T. hamatum* K01

This material is reserved for educational use only, not allowed for commercial use.
Forbidden to modify the content, and cite the document when use.

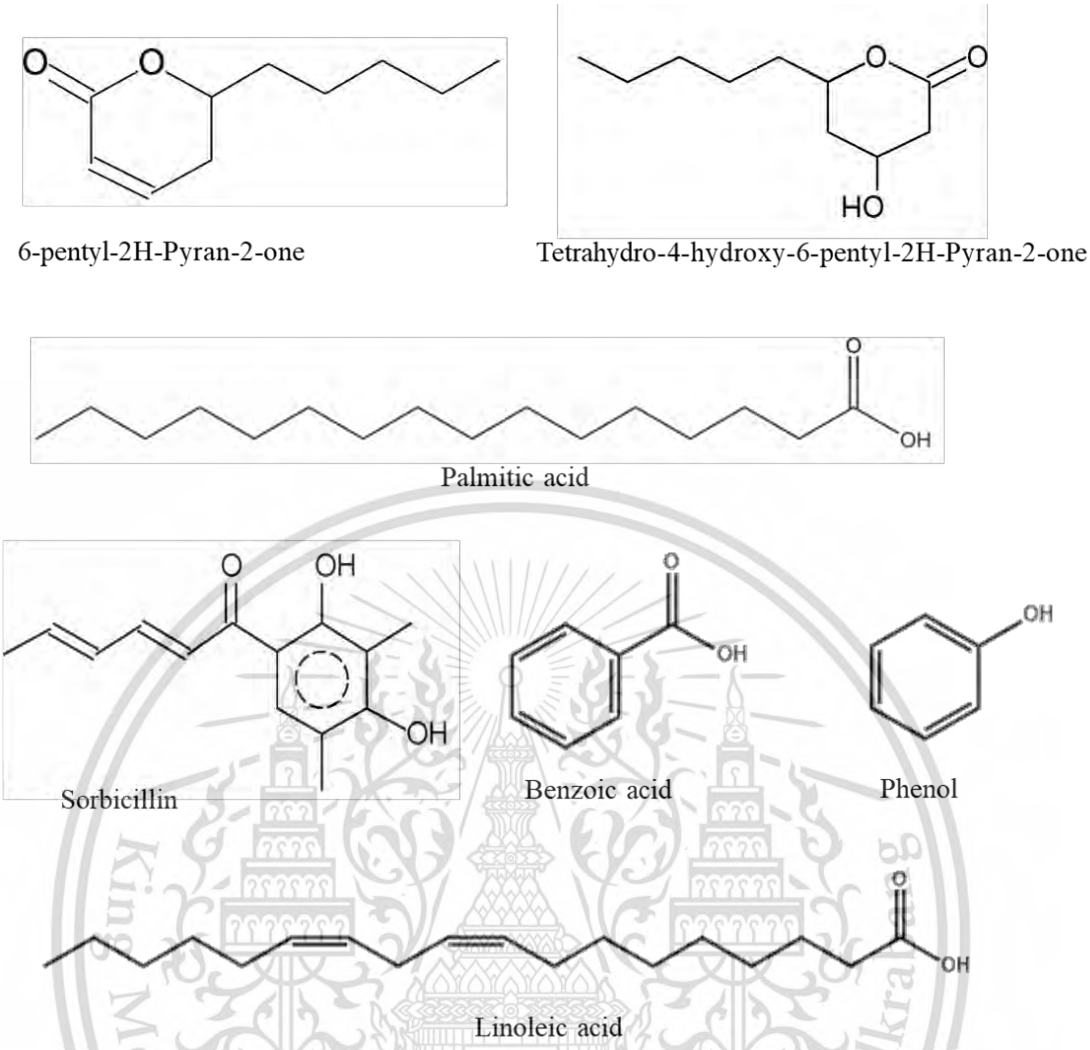

Figure 4.16 The structure of the secondary metabolites derived from *T. hamatum* K01, which were identified using GC-MS analysis

4.5.2 Analysis of secondary metabolites from *Ch. lucknowense* CL

4.5.2.1 Secondary metabolites from crude ethyl acetate

Secondary metabolites from crude ethyl acetate extract derived from *Ch. lucknowense* CL were identified using GC-MS. The result revealed that a total of eight compounds were identified as shown in (Table 4.6). Among these, Hexadecanoic acid, 9, 12-Octadecadienoic acid (Z), and Octadecanoic acid, have been reported as antibiotic substaces to control plant pathogens (Figure 4.17, 4.18).

This material is reserved for educational use only, not allowed for commercial use.
Forbidden to modify the content, and cite the document when use.

Table 4.6. Constituents detected from crude ethyl acetate extract from *Ch. lucknowense* CL using (GC/MS) analysis.

No	Constituents	%	RT*	M* (g/mol)
1	Toluene	9.25	3.204	92.14
2	Hexadecanoic acid	37.51	20.637	256.43
3	Hexadecanoic acid, ethyl ester	8.05	21.214	284.48
4	9, 12-Octadecadienoic acid (Z)	3.88	24.176	280.44
5	Oleic acid	7.87	24.290	282.46
6	Octadecanoic acid	13.54	24.732	284.48
7	Ethyl Oleate	4.99	24.840	310.51
8	Octadecanoic acid, ethyl ester	6.51	25.288	312.53

RT* retention of time, M* molecular weight

Figure 4.17 Chromatography GC-MS analysis of secondary metabolites from crude ethyl extract of *Ch. lucknowense* CL

This material is reserved for educational use only, not allowed for commercial use.
Forbidden to modify the content, and cite the document when use.

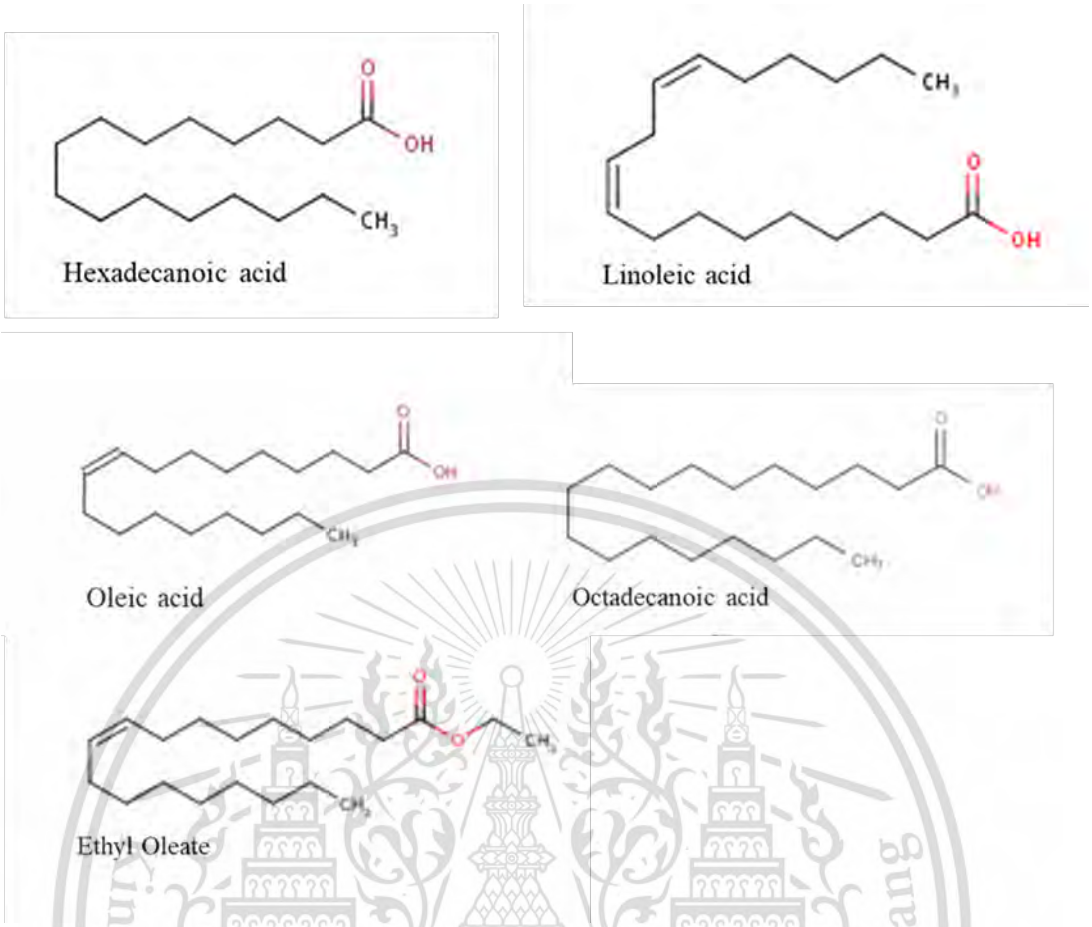

Figure 4.18 The structure of the secondary metabolites from crude ethyl acetate extract derived from *Ch. lucknowense* CL, which was identified using GC-MS analysis

4.5.2.2 Secondary metabolites from nano-CLE from *Ch. lucknowense* CL

Nano-CLE from *Ch. lucknowense* CL was subjected to GC-MS analysis to isolate the bioactive compounds. A total of 23 components were detected, with the main components including acetic acid, butyl ester, hexadecanoic acid, methyl ester, and 9-octadecenamide (Z), which were found to possess antimicrobial properties (Table 4.7., Figure 4.19, 4.20).

This material is reserved for educational use only, not allowed for commercial use.
Forbidden to modify the content, and cite the document when use.

Table 4.7 Constituents detected from nano-CLE from *Ch. lucknowense* CL using (GC/MS) analysis.

No	Constituents	%	RT*(min)	M* (g/mol)
1	Acetic acid, butyl ester	0.45	3.765	116.16
2	Methane, sulfinylbis	85.63	4.143	78.14
3	1,2,4-trimethyl, Benzene	0.17	6.706	120.19
4	Indane	0.32	7.191	118.17
5	1,3-diethyl-Benzene	0.06	7.418	134.22
6	1-methyl-3-propyl-Benzene	0.08	7.628	134.22
7	1,2-Diethylbenzene	0.13	7.655	106.16
8	2-ethyl-1,4-dimethyl-Benzene	0.12	7.731	134.21
9	4-Ethyl-O-xylene	0.08	7.774	134.22
10	P-Cymene	0.76	7.914	134.21
11	2-Methyl-2-Phenylpropane	0.18	8.076	118.18
12	2-ethyl-1,4-dimethyl-Benzene	0.38	8.206	134.21
13	Prehnite	0.03	8.319	395.38
14	1-Methyl-3-isopropylbenzene	0.08	8.551	134.21
15	1,4-Dioxane-2,5-dione	0.26	8.697	116.07
16	Naphthalene	0.39	8.767	128.17
17	4-Methyl-2,6-di-tert-butylphenol	0.16	9.274	424.7
18	Hexadecanoic acid, methyl ester	1.47	9.517	270.45
19	Hexadecanoic acid, ethyl ester	0.14	9.776	284.47
20	Hexadecanamide	0.78	14.20	255.44
21	Stearic acid ethyl ester	1.29	22.574	312.53
22	9-Octadecenamide, (Z)	4.64	24.166	281.47
23	Octadecanamide	0.27	24.354	283.49

RT* retention of time, M* molecular weight

This material is reserved for educational use only, not allowed for commercial use.
Forbidden to modify the content, and cite the document when use.

Figure 4.19 Chromatography GC-MS analysis of secondary metabolites from nano-CLE derived from *Ch. lucknowense* CL

This material is reserved for educational use only, not allowed for commercial use.
Forbidden to modify the content, and cite the document when use.

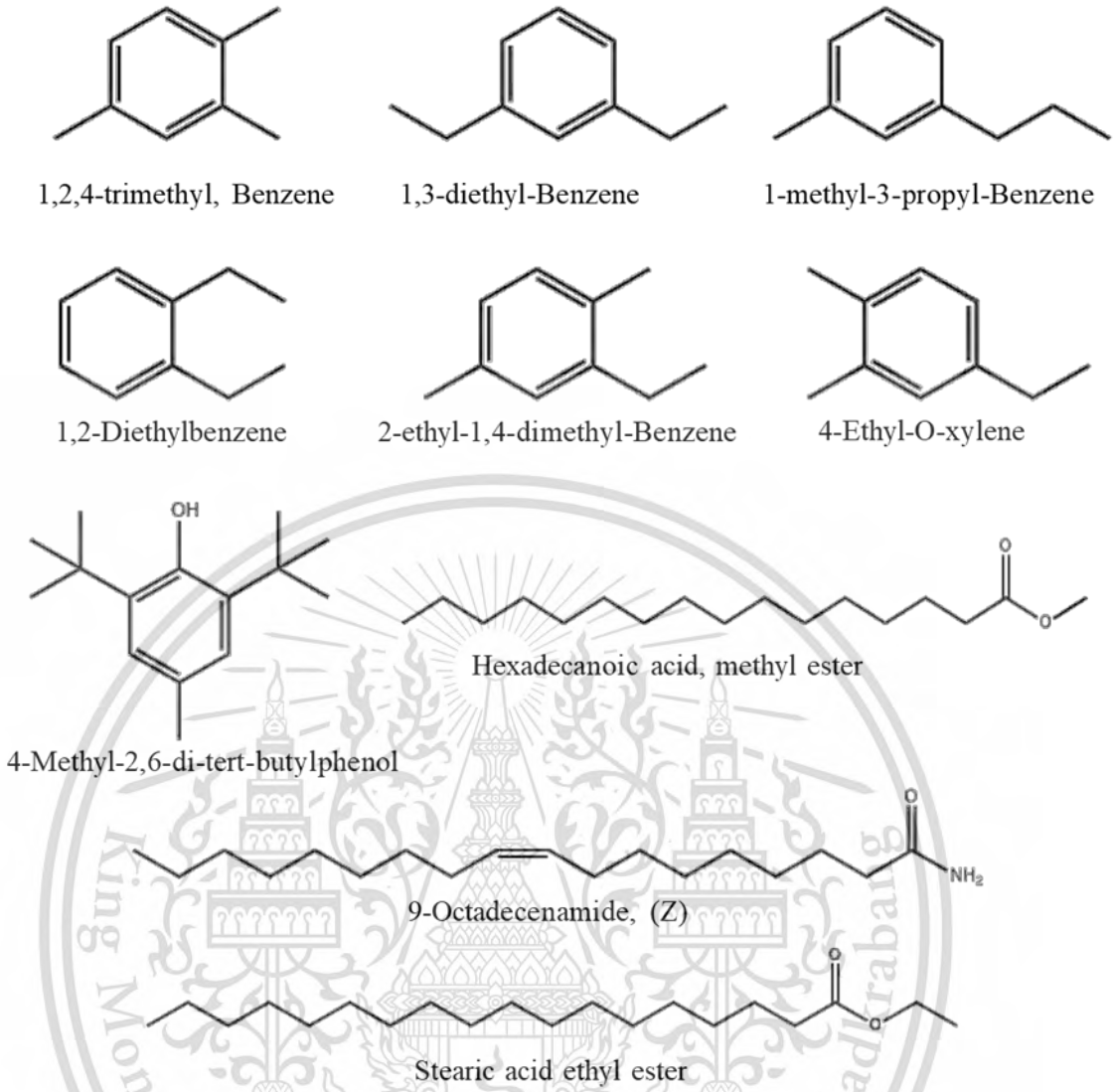

Figure 4.20 Structure of the secondary metabolites from nano-CLE derived *Ch. lucknowense* CL, which were identified using CG-MS

This material is reserved for educational use only, not allowed for commercial use.
Forbidden to modify the content, and cite the document when use.

4.6 Evaluation of antagonistic fungi against plant pathogens

4.6.1 Bi-culture test

4.6.1.1 Bi-culture test of *T. hamatum* K01 against *C. gloeosporioides* C01

T. hamatum K01 was used as a biological control agent against *C. gloeosporioides*, a causal agent of citrus anthracnose. An active-growing edge of mycelia of *C. gloeosporioides* (0.5 cm^2) was paired on the individual 9 cm diameter PDA medium plates with antagonistic fungus *T. hamatum* K01 at 1.5 cm apart. The result indicated that *T. hamatum* K01 expressed control mechanisms by reducing colony growth and conidia production of *C. gloeosporioides* by 70.55% and 79.07%, respectively, at only seven days (Table 4.8). Furthermore, it was observed that the growth of *T. hamatum* K01 almost covered the pathogen colony and caused abnormal conidia, as shown in Figure 4.21. It was demonstrated that *T. hamatum* K01 significantly inhibited *C. gloeosporioides* in the bi-culture test.

Table 4.8 The effect of antagonistic fungus *T. hamatum* K01 against *C. gloeosporioides* C01 using a bi-culture test

Treatments	Colony diameter (cm)	Colony inhibition (%)	Number of conidia (x 10^6)	Conidia inhibition (%)
Control	9.00[a]	0.00	58.55[a]	0.00
Bi-culture	2.65[b]	70.55	12.25[b]	79.07
CV%	2.64	-	27.13	-

Treatment means were averaged of four replications. Mean followed by common letters are not the same letters. It was not significantly different by DMRT at $p < 0.05$.

This material is reserved for educational use only, not allowed for commercial use.
Forbidden to modify the content, and cite the document when use.

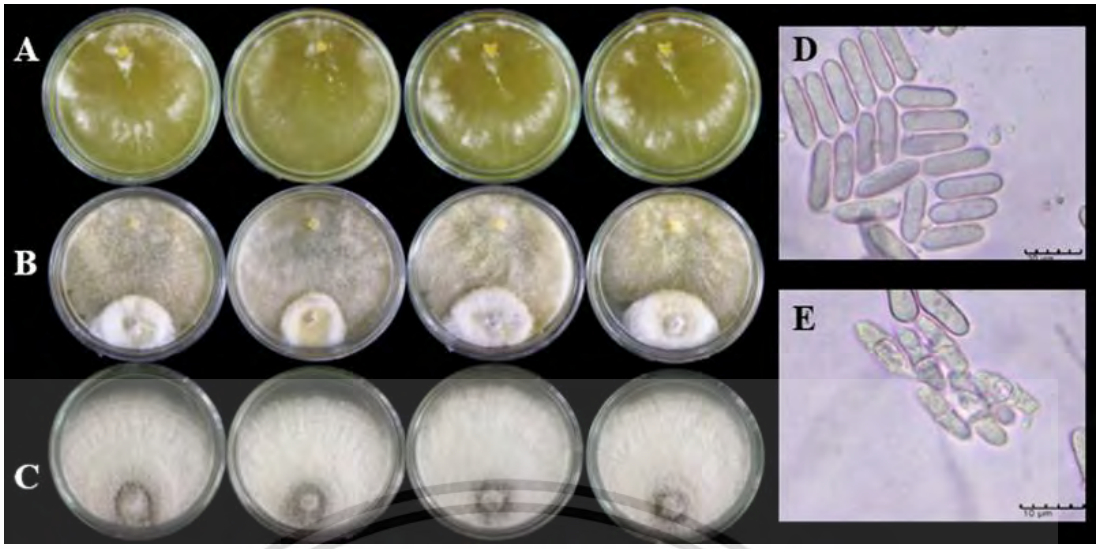

Figure 4.21 A bi-culture test of *T. hamatum* K01 against *C. gloeosporioides* C01. A, *T. hamatum* K01; B, bi-culture plates of *T. hamatum* K01 versus *C. gloeosporioides* C01; C, *C. gloeosporioides* C01; D, normal conidia produced; and E, abnormal conidia produced of *C. gloeosporioides* C01 causing by *T. hamatum* K01

4.6.1.2 Bi-culture test of *Ch. lucknowense* Cl against *C. gloeosporioides* C02

A bi-culture test was conducted to determine the ability of *Ch. lucknowense* CL to control *C. gloeosporioides* C02 causing durian anthracnose. Results showed that *Ch. lucknowense* CL inhibited mycelia growth and conidia production of *C. gloeosporioides* C02. The percentage of inhibition on conidia production was reduced by 64.25%, while the colony growth was inhibited by only 48.66%, compared to the control (Table 4.9., Figure 4.22.). Furthermore, it was observed that the inoculation of *C. gloeosporioides* C02 resulted in growth over the colony of antagonistic fungus *Ch. lucknowense* CL within seven days. Even after the next seven days, the antagonistic fungus still grew over the pathogen and inhibited the colony growth. Moreover, *Ch. lucknowense* CL caused lysis of conidia, resulting in abnormal conidia appearance of *C. gloeosporioides* C02. This finding demonstrates that *Ch. lucknowense* CL could be a promising biocontrol agent against the pathogen within a more extended period, as indicated by its effect on the colony growth and conidia production of *C. gloeosporioides* C02, a causal agent of durian anthracnose.

This material is reserved for educational use only, not allowed for commercial use.
Forbidden to modify the content, and cite the document when use.

Table 4.9 A bi-culture test of *Ch. lucknowense* CL against *C. gloeosporioides* C02 caused anthracnose of durian.

Treatment	Colony diameter (cm)	Colony inhibition (%)	Number of conidia (x 10^6)	Conidia inhibition (%)
Control	9.00[a]	-	83.78[a]	-
Bi-culture	4.62[b]	48.66	29.95[b]	64.25
CV%	2.59	-	10.28	-

Means of four replications. Means followed by common letters are not significantly different by Duncan's multiple range test (DMRT) at $p < 0.05$.

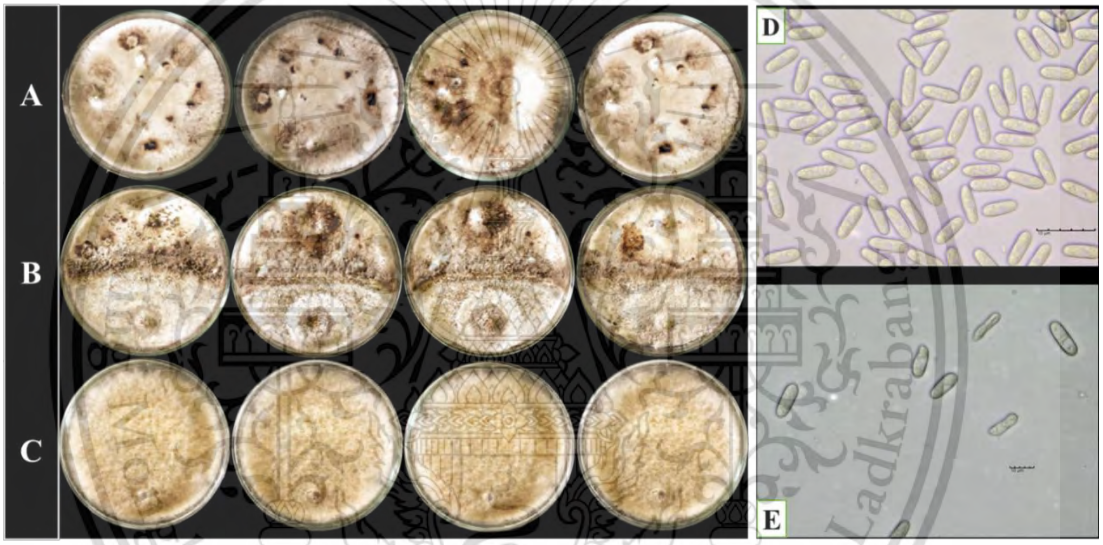

Figure 4.22 Bi-culture test of *Ch. lucknowense* CL against *C. gloeosporioides* C02 in a bi-culture test. A, *C. gloeosporioides* C02; B, bi-culture plates of *Ch. lucknowense* CL and *C. gloeosporioides* C02; C, *Ch. lucknowense* CL; D, normal conidia production; E, abnormal conidia production of *C. gloeosporioides* C02 caused by *Ch. lucknowense* CL

4.6.1.3 Bi-culture test of *T. hamatum* K01 against *P. palmivora* PYSC01

A bi-culture assay was conducted to prove the antagonistic fungi *T. hamatum* K01 for its mycoparasitism against *P. palmivora* PYSC01, causing root rot disease of durian. Inhibition of a broad range of colony growth and sporangia formation of *P. palmivora* PYSC01 were measured, and percentages for inhibition were computed. The finding demonstrated that *T. hamatum* K01 exhibited antifungal activities toward *P. palmivora* PYSC01. *T. hamatum* K01 may release cell wall

Forbidden to modify the content, and cite the document when use.

degrading enzyme into PDA media to inhibit colony growth and sporangia formation of *P. palmivora* PYSC01. *T. hamatum* K01' colony grew over the colony growth of *P. palmivora* PYSC01 for an extended period, resulting in discoloration, which was changed from cottony white to yellow and degraded colony growth and sporangia formation by 58.11% and 92.72%, respectively. (Table 4.10., Figure 4.23).

Table 4.10 Bi-culture assay of *T. hamatum* K01 against *P. palmivora* causing root rot of durian.

Treatments	Colony diameter (cm)	Colony inhibition (%)	Number of sporangia (10^5)	Sporangia inhibition (%)
Bi-culture	3.77[c]	58.11	1.40[b]	92.72
Control	9.00[a]	-	19.25[a]	-
CV%	3.55		13.67	-

The average of four replications means in a column followed by a joint letter, do not differ statically by Duncan's multiple range test (DMRT) at $p<0.05$.

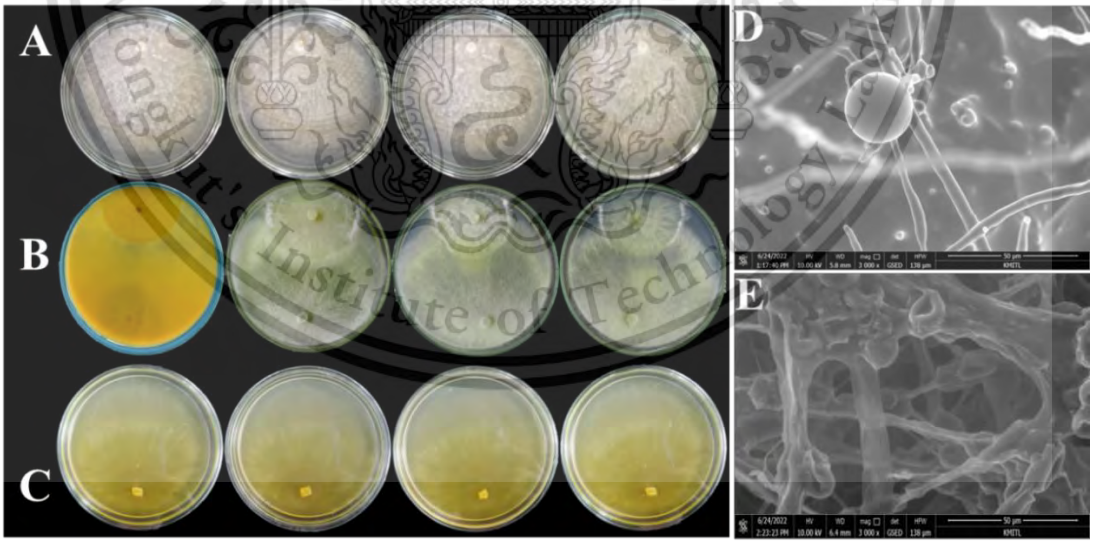

Figure 4.23 Bi-culture test of *T. hamatum* K01 against *P. palmivora* PYSC01; A, *P. palmivora* PYSC01; B, bi-culture plates of *T. hamatum* K01 versus *P. palmivora* PYSC01; C, *T. hamatum* K0, D; normal sporulation of *P. palmivora* and E; abnormal sporulation of *P. palmivora* caused by *T. hamatum* K01

This material is reserved for educational use only, not allowed for commercial use.
Forbidden to modify the content, and cite the document when use.

4.6.1.4 Bi-culture test of *Ch. lucknowense* CL against *P. palmivora* PYSC01

Ch. lucknowense CL was evaluated in a bi-culture test for its ability to suppress *P. palmivora* PYSC01, a causal agent of durian rot. The results indicated that *Ch. lucknowense* CL inhibited the colony growth and spore production of *P. palmivora* PYSC01. The percentage of inhibition on conidia production was reduced by 94.65%, while the colony growth was inhibited by only 52.22%, compared to the control (Table 4.11). It was observed that *Ch. lucknowense* CL's colony grew to inhibit the colony growth of *P. palmivora* PYSC01 on day ten after paring. Moreover, *Ch. lucknowense* CL also caused abnormal spore production by *P. palmivora*, as shown in Figure 4.24.

Table 4.11 Bi-culture test of *Ch. lucknowense* CL against *P. palmivora* PYSC01

Treatments	Colony diameter (cm)	Colony inhibition (%)	Number of sporangia (x 10^5)	Sporangia inhibition (%)
Bi-culture	4.30[b]	52.22	0.65[b]	94.65
Control	9.00[a]	-	19.25[a]	-
CV%	3.55		13.67	-

The average of four replications, mean in a column followed by a joint letter, do not differ statically by Duncan's multiple range test (DMRT) at $p<0.05$.

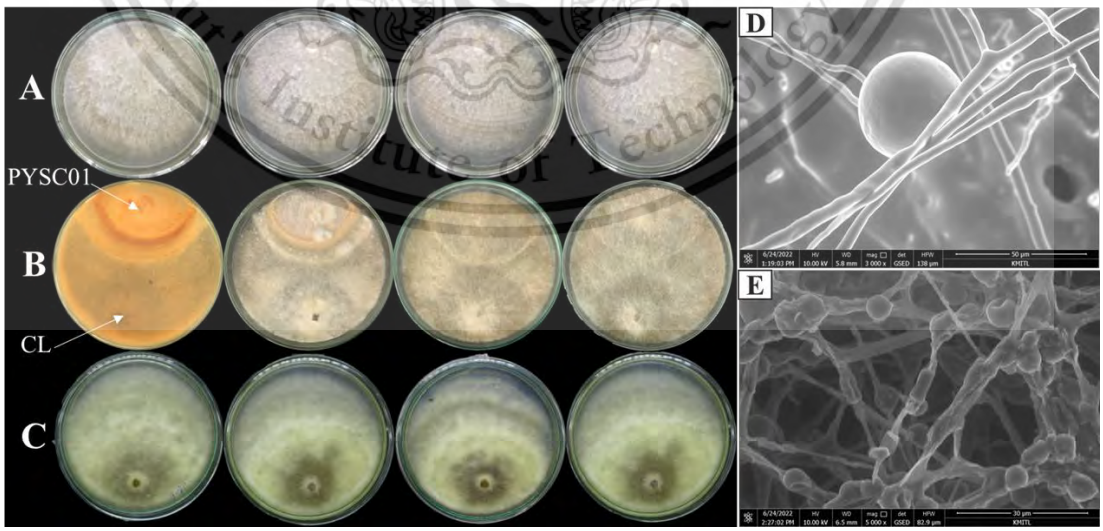

Figure 4.24 Bi-culture test of *Ch. lucknowense CL* to control *P. palmivora* PYSC01; A, *P. palmivora* PYSC01; B, bi-culture plates of *Ch. lucknowense* CL versus *P. palmivora* PYSC01; C, *Ch. lucknowense* CL, D; normal

This material is reserved for educational use only, not allowed for commercial use.
Forbidden to modify the content, and cite the document when use.

sporulation of *P. palmivora* and E; abnormal spore production of *P. palmivora* caused by *Ch. lucknowense* CL

4.6.2 Testing crude extract from antagonistic fungi against pathogens

T. hamatum K01 and *Ch. lucknowense* CL were separated culture in PDB 350 plates for e, approximately 30 ml per plate for 35 days. The fresh weight of fungal biomass yielded 950 g from *T. hamatum* K01 and 1200g from *Ch. lucknowense* CL. They were air-dried for seven days to get dry biomass of 65 g from *T. hamatum* K01 and 65.4 g from *Ch. lucknowense* CL. Dry biomass was separately soaked 1/1(v/v) in hexane, ethyl acetate, and methanol as solvents for three days. Each solution was evaporated in a vacuole to yield crude hexane (TK01-Hexane) of 0.65g, ethyl acetate (TK01-EtOAc) of 1.38g, and methanol (TK01-MeOH) of 2.13g from *T. hamatum* K01 respectively, and crude hexane (CL-hexane) of 0.3g, ethyl acetate (CL-EtOAc) of 2 g, and methanol (CL-MeOH) of 1.7 g derived from *Ch. Lucknowense* CL, respectively, as shown in Figure 4.25.

Figure 4.25 Metabolite crude extracts from *T. hamatum* K01 and *Ch. lucknowense* CL. A; crude TK01-Hexane, B; crude TK01-EtOAc and C; crude TK01-MeOH, E; crude CL-Hexane, F; crude CL-EtOAc, G; crude CL-MeOH from *T. hamatum* K01 and crude CL-Hexane, CL-EtOAc and CL-MeOH from *Ch. lucknowense* CL

This material is for educational use only, not allowed for commercial use.
Forbidden to modify the content, and cite the document when use.

4.6.2.1 Crude extract test from *T. hamatum* K01 against *C. gloeosporioides* C01

Metabolite crude extracts from *T. hamatum* K01 were tested for their bioactivity at different concentration levels (10 ppm to 1000 ppm) in DMSO and PDA to suppress *C. gloeosporioides*. Results indicated that crude TK01-Hexane inhibited the colony growth of *C. gloeosporioides* by 7% to 37% and conidia production by 12.34% to 45.96% (Table 4.12). Crude TK01-EtOAc also expressed fungal activity against *C. gloeosporioides* C01, inhibiting colony growth and conidia production by 6.6% to 44.6% and 7.84% to 63.32%, respectively. Meanwhile, crude TK01-MeOH exhibited inhibitory effect against *C. gloeosporioides* pathogen by significantly inhibiting colony growth by 9.6% to 78.6% and conidia production by 15% to 73.18%.

As for ED_{50} values, crude TK01-EtOAc's effective dose was computed at 607.43 ppm to inhibit conidia production. Moreover, crude TK01-MeOH effective doses for colony growth inhibition and conidia production were computed at 273.38 ppm and 355.28 ppm, respectively. It can be demonstrated that metabolite crude extract TK01-MeOH from *T. hamatum* K01 gave the most effective inhibitory activities against *C. gloeosporioides*'s colony growth and conidia production. It caused abnormal conidia production of *C. gloeosporioides,* as shown in Figures 4.26 and 4.27.

Table 4.12 Crude extracts from *T. hamatum* K01 against *C. gloeosporioides* C01

Crude extract	Concs ppm	Colony diameter (cm)	Growth inhibition (%)	ED_{50} (ppm)	Conidia production (10^6)	Inhibition (%)	ED_{50} (ppm)
TK01-Hexane	0	5.00[a]	-	-	86.75[a]	-	-
	10	4.65[b]	7.00		76.00[a]	12.34	
	50	4.32[c]	13.60		62.45[b]	27.97	
	100	3.82[d]	23.60		60.15[b]	30.62	
	500	3.35[e]	33.00		52.20[bc]	38.63	
	1000	3.12[e]	37.60		46.85[c]	45.96	
TK01-EtOAc	0	5.00[a]	-	-	86.75[a]	-	607.43
	10	4.67[b]	6.60		79.90[ab]	7.84	
	50	3.82[c]	23.60		76.15[ab]	12.16	
	100	3.62[c]	27.60		67.65[b]	21.97	

This material is reserved for educational use only, not allowed for commercial use.
Forbidden to modify the content, and cite the document when use.

	500	3.00[d]	40.00		49.00[c]	43.48	
	1000	2.77[e]	44.60		31.80[d]	63.32	
TK01-MeOH	0	5.00[a]	-	273.38	86.70[a]	-	355.2
	10	4.52[b]	9.60		73.60[ab]	15.10	
	50	4.22[c]	15.60		71.25[b]	17.82	
	100	3.37[d]	32.60		64.20[b]	25.95	
	500	2.17[e]	56.60		42.85[c]	50.57	
	1000	1.07[f]	78.60		23.25[d]	73.21	
C.V. (%)		4.69			14.67		

The average of four replications, the mean followed by the common letters are not significantly different by Duncan's multiple range test (DMRT) at $p<0.05$

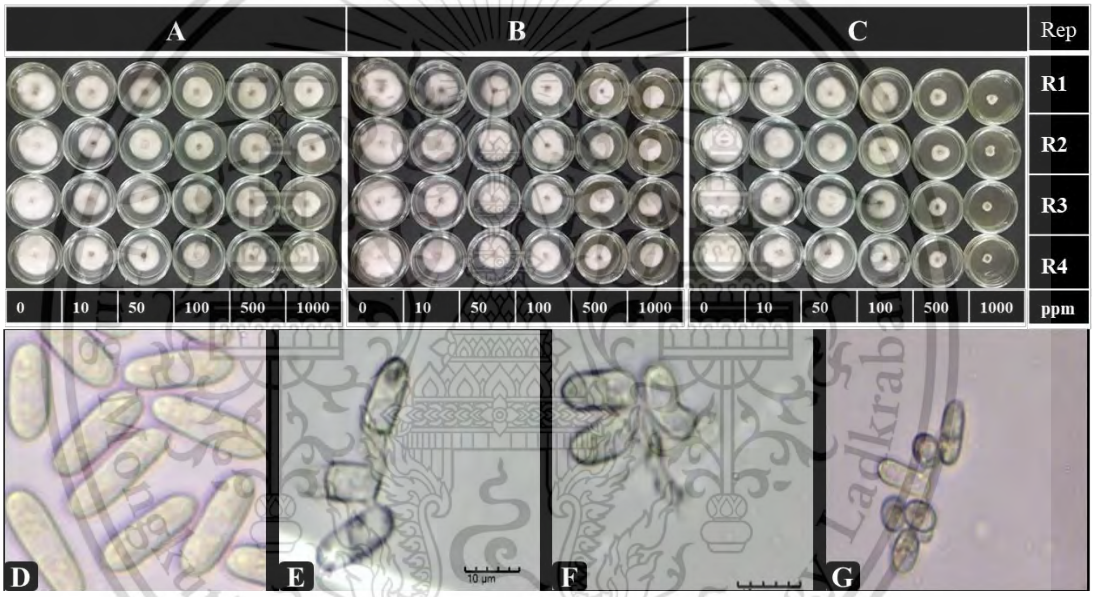

Figure 4.26 Crude extracts derived from *T. hamatum* K01 against *C. gloeosporioides* C01. A, crude TK01-Hexane; B, crude TK01-EtOAc; C, crude TK01-MeOH and the effect of crude extracts derived from *T. hamatum* K01 on conidia production of *C. gloeosporioides* C01; D, normal conidia formation produced by *C. gloeosporioides* C01 in control (0 ppm); E, abnormal conidia caused by crude TK01-Hexane; F, abnormal conidia caused by crude TK01-EtOAc; G, abnormal conidia caused by Crude TK01-MeOH

This material is reserved for educational use only, not allowed for commercial use.
Forbidden to modify the content, and cite the document when use.

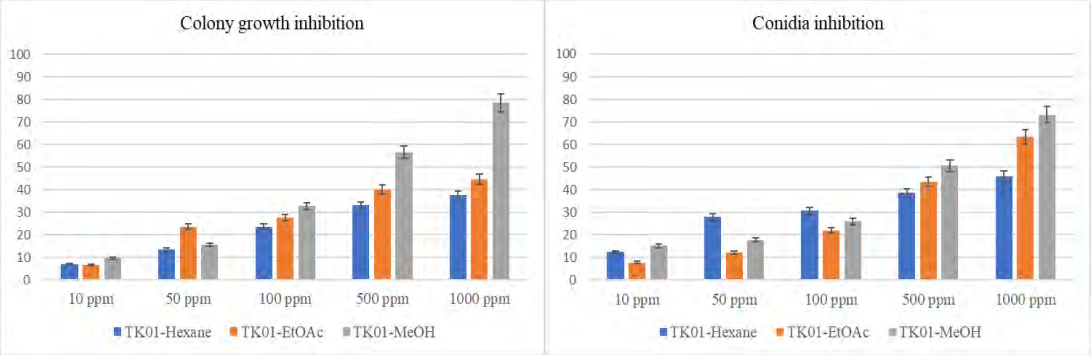

Figure 4.27 The effect of crude extracts from *T. hamatum* K01 to inhibit *C. gloeosporioides* causing citrus anthracnose

4.6.2.2 Crude extract test from *Ch. lucknowense* CL against *C. gloeosporioides* C02

The antibiotic production and biological activity of *Ch. lucknowense* CL were tested to control *C. gloeosporioides* C02 causing anthracnose disease of durian. Results revealed varying ranges of colony growth and conidia inhibition at 10 to 1,000 ppm concentrations in DMSO and PDA, as shown in Table 4.13 and Figures 4.28 and 4.29. As for crude CL-EtOAc, colony growth inhibition ranged from 25% to 61%, and conidia production was inhibited by 31% to 86%. The ED_{50} values of colony growth and conidia inhibition by crude CL-EtOAc were computed at 197.21 ppm and 37.49 ppm, respectively. Crude CL-MeOH also showed a broad spectrum of action against *C. gloeosporioides* C02. The colony growth was suppressed at a range from 5.6% to 54%, while a range of 11% inhibited conidia production to 61.72%. The ED_{50} values of colony growth and conidia inhibition by crude CL-MeOH were computed at 681.73 ppm and 370.06 ppm, respectively. Moreover, crude CL-Hexane expressed antifungal activity against *C. gloeosporioides* C02. Colony growth and conidia production were inhibited, ranging from 1.6% to 59.88%. Crude CL-Hexane inhibited conidia production at ED_{50} value of 451.76 ppm. Moreover, *Ch. lucknowense* CL produced aliphatic, volatile compounds. These bio-compounds also strongly inhibited colony growth and conidia production of *C. gloeosporioides*. It expressed control mechanisms as it caused abnormal conidia production of *C. gloeosporioides* C02.

This material is reserved for educational use only, not allowed for commercial use.
Forbidden to modify the content, and cite the document when use.

Table 4.13 Crude extracts derived from *Ch. lucknowense* CL against *C. gloeosporioides* C02

Crude extracts	Concs (ppm)	Colony diameter (cm)	Growth inhibition (%)	ED_{50} (ppm)	Conidia (10^6)	Inhibition (%)	ED_{50} (ppm)
CL-Hexane	0	5.00^{a}	-	-	75.90^{a}	-	451.76
	10	4.92^{a}	1.60		72.70^{a}	4.26	
	50	4.50^{b}	10.00		58.85^{b}	22.46	
	100	3.92^{c}	21.60		44.60^{def}	41.23	
	500	3.65^{cde}	27.00		41.70^{efg}	45.05	
	1000	2.95^{f}	41.00		30.45^{hi}	59.88	
CL-EtOAc	0	5.00^{a}	-	197.2	75.90^{a}	-	37.49
	10	3.75^{cd}	25.00		52.15^{bcd}	31.29	
	50	3.27^{ef}	34.60		34.90^{gh}	54.01	
	100	2.30^{g}	54.00		24.25^{ij}	68.05	
	500	2.20^{g}	56.00		19.70^{j}	74.04	
	1000	1.95^{g}	61.00		10.65^{k}	85.96	
CL-MeOH	0	5.00^{a}	-	681.73	75.90^{a}	-	370.06
	10	4.72^{ab}	5.60		67.55^{b}	11.00	
	50	3.94^{c}	21.20		56.90^{bc}	25.03	
	100	3.37^{de}	32.60		48.55^{cde}	36.03	
	500	2.90^{f}	42.00		37.15^{fgh}	51.05	
	1000	2.30^{g}	54.00		29.05^{hi}	61.72	
C.V. (%)		6.27	-		10.05	-	

Treatment means an average of four replications. The mean followed by common letters are not significantly different by (DMRT) at $p<0.05$.

This material is reserved for educational use only, not allowed for commercial use.
Forbidden to modify the content, and cite the document when use.

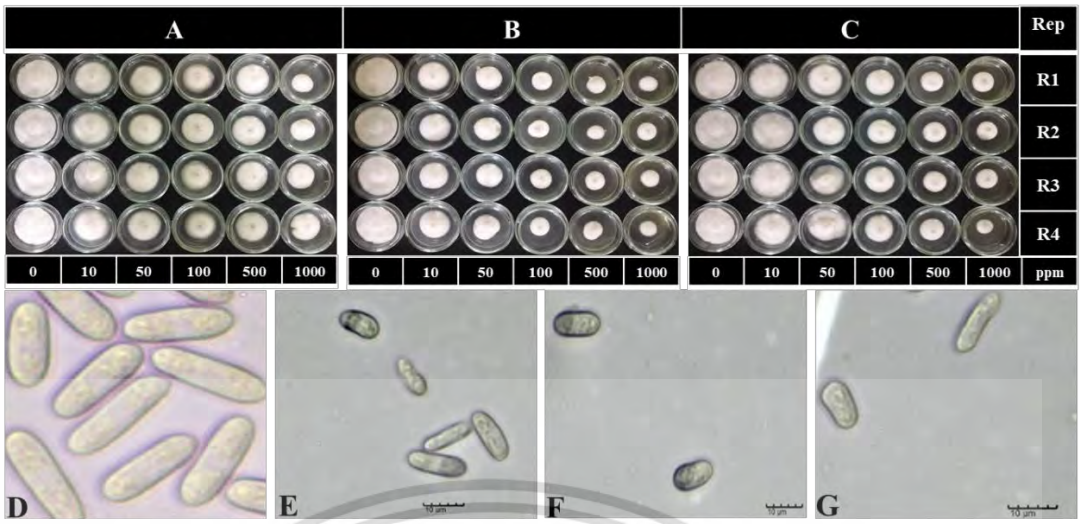

Figure 4.28 Crude extracts from *Ch. lucknowense* CL against *C. gloeosporioides* C02 in each concentration; A, crude CL-Hexane; B, crude CL-EtOAc; C, crude CL-MeOH; D, normal conidia production produced by *C. gloeosporioides* C02 in control (0 ppm); E, F, and G abnormal conidia production caused by crude CL-Hexane; CL-EtOAc and crude CL-MeOH at concentration 1000 ppm

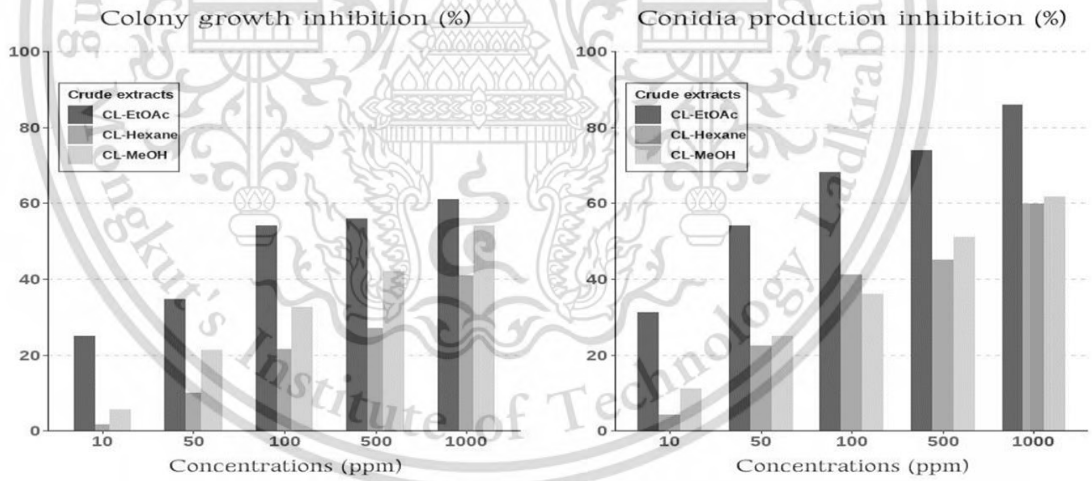

Figure 4.29 Crude extracts derived from *Ch. lucknowense* CL against *C. gloeosporioides* C02 causing durian anthracnose disease

4.6.2.3 Crude extract from *T. hamatum* K01 against *P. palmivora* PYSC01

Metabolite crude extracts from *T. hamatum* K01 were evaluated for their abilities to suppress the colony growth and sporangia formation of *P. palmivora* PYSC01, causing root rot of durian. The result revealed that crude TK01-MeOH from *T. hamatum* K01 gave the highest inhibitory effect against *P. palmivora*

This material is reserved for educational use only, not allowed for commercial use.
Forbidden to modify the content, and cite the document when use.

PYSC01, in which colony growth and sporangia formation were inhibited by 61.62% and 81.65%, respectively, followed by crude TK01-EtOAc suppressed colony growth by 52.53%. Sporangia formation was reduced by 76.45%, while crude TK01-Hexane showed less effectiveness for inhibition of colony growth and sporangia formation by 38.38% and 47.09% at 1000 ppm concentration, respectively. The effective dose (ED_{50}) values on colony growth and sporangia formation of *P. palmivora* PYSC01 and crude TK01-MeOH were required by 288.66 and 118.92 ppm concentrations. Crude TK01-EtOAc required the ED_{50} values by 185 ppm concentration on sporangia inhibition. Crude TK01-Hexane gave the highest effective dose (ED_{50}) with more than 1000 ppm on colony growth and sporangia formation (Table 4.14., Figures 4.30, and 4.31).

Table 4.14 Metabolite crude extract from *T. hamatum* K01 against *P. palmivora* causing root rot of durian

Crude extracts	Concs (ppm)	Colony growth (cm)	Growth inhibition (%)	ED_{50} (ppm)	Spore production (10^4)	Inhibition (%)	ED_{50} (ppm)
TK01-Hexane	0	4.95^{a}	-	-	81.75^{a}	-	-
	10	4.90^{a}	1.01		79.50^{a}	2.75	
	50	4.72^{ab}	4.65		68.50^{b}	16.21	
	100	4.30^{bc}	13.13		66.60^{b}	18.53	
	500	3.32^{d}	32.93		61.75^{b}	24.46	
	1000	3.05^{d}	38.38		43.25^{c}	47.09	
TK01-EtOAc	0	4.95^{a}	-	-	81.75^{a}	-	185.00
	10	4.50^{a}	9.09		79.00^{a}	3.36	
	50	4.10^{d}	17.17		62.00^{b}	24.16	
	100	3.27^{ef}	33.94		42.00^{c}	48.62	
	500	2.97^{ef}	40.00		26.00^{d}	68.20	
	1000	2.35^{g}	52.53		19.25^{de}	76.45	
TK01-MeOH	0	4.95^{a}	-	288.66	81.75^{a}	-	118.92
	10	4.12^{d}	16.77		72.50^{ab}	11.31	
	50	3.15^{ef}	36.36		49.75^{c}	39.14	
	100	2.92^{f}	41.01		40.00^{c}	51.07	
	500	2.40^{g}	51.52		25.00^{de}	69.42	

This material is reserved for educational use only, not allowed for commercial use.
Forbidden to modify the content, and cite the document when use.

	1000	1.90[h]	61.62		15.00[e]	81.65	
C.V. (%)		6.28			12.58	-	

The average of four replications, the means followed by the common letters are not significantly different by Duncan's multiple range test (DMRT) at $p<0.05$

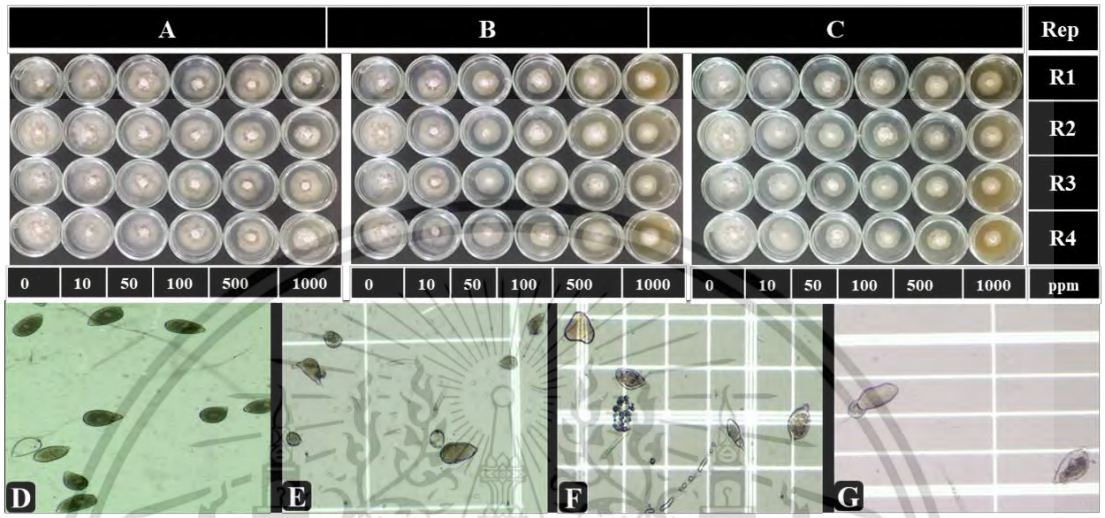

Figure 4.30 Metabolite crude extract from *T. hamatum* K01 against *P. palmivora* PYSC01 causing root rot of durian. A; crude TK01-hexane, B; crude TK01-EtOAc, C; crude TK01-MeOH, D; normal sporangia formation produced by *P. palmivora* PYSC01 in control (0 ppm), E, F, and G abnormal sporangia formation caused by crude TK01-hexane, TK01-EtOAc and, crude TK01-MeOH

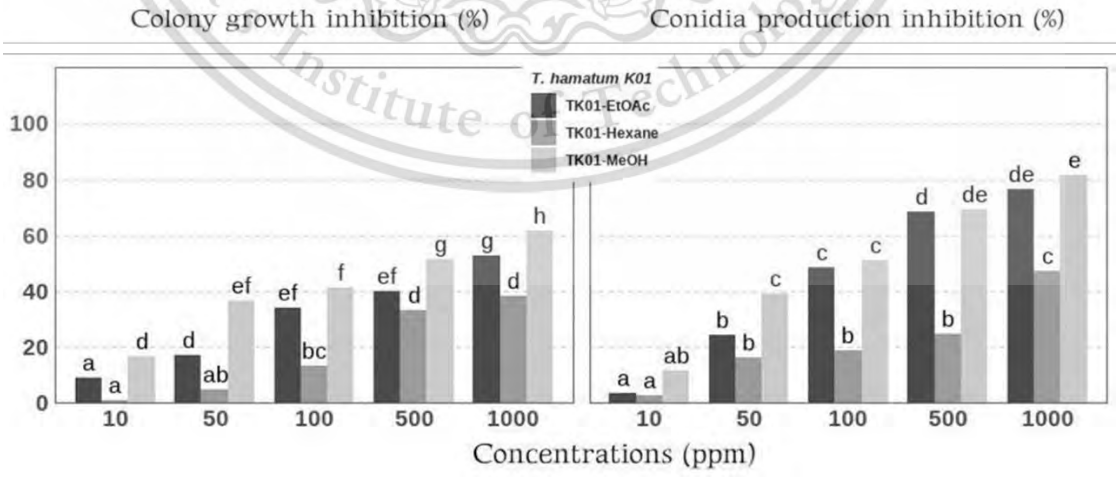

Figure 4.31 Metabolite crude extract from *T. hamatum* K01 against *P. palmivora* PYSC01, caused durian rot

This material is reserved for educational use only, not allowed for commercial use.
Forbidden to modify the content, and cite the document when use.

4.6.2.4 Crude extract from *Ch. lucknowense* CL against *P. palmivora* PYSC01

Metabolite crude extracts from *Ch. lucknowense* CL were evaluated for their fungal abilities to suppress the colony growth and sporangia formation of *P. palmivora* PYSC01, causing root rot of durian. The results indicated that three of these crude extracts exhibited a broad spectrum of action against *P. palmivora* isolate PYSC01 at 10-1000 ppm concentrations. Among these crude extracts, crude CL-EtOAc from *Ch. lucknowense* CL exhibited the highest inhibitory effect against colony growth and sporangia formation at the ED_{50} values of 95.16 and 13.33 ppm, respectively, and in both colony and sporangia did not grow at 500 ppm concentration, followed by crude CL-Hexane gave the better effect against *P. palmivora* PYSC01 which the colony growth and sporangia formation was inhibited by 84.76% and 98.28 % respectively, at 1000 ppm concentration with the ED_{50} values was computed at 341.05 and 68.40 ppm, while, crude CL-MeOH gave the least effective on colony growth by 41.67%. Sporangia formation was reduced by 94.83% at 1000 ppm concentration with an ED_{50} value required of 126.93 ppm (Table 4.15., Figures 4.33 and 4.33).

Table 4.15 Metabolite crude extract from *Ch. lucknowense* CL against *P. palmivora* PYSC01 causing root rot of durian

Crude extracts	Concs (ppm)	Colony growth (cm)	Growth inhibition (%)	ED_{50} (ppm)	Spore production (10^5)	Inhibition (%)	ED_{50} (ppm)
CL-Hexane	0	4.92[a]	-	341.5	14.50[a]	-	68.40
	10	4.30[b]	12.60		11.75[ab]	18.97	
	50	4.12[b]	16.26		10.15[bc]	29.31	
	100	3.40[cd]	30.89		5.50[def]	62.07	
	500	2.65[f]	46.14		2.00[fg]	86.21	
	1000	0.75[h]	84.76		0.25[g]	98.28	
CL-EtOAc	0	4.92[a]	-	95.16	14.50[a]	-	13.33
	10	3.22[cde]	34.55		7.00[cde]	51.72	
	50	2.97[ef]	39.63		5.75[def]	60.34	
	100	1.32[g]	73.17		0.75[g]	94.83	
	500	0.00[i]	100		0.00[g]	100	

This material is reserved for educational use only, not allowed for commercial use.
Forbidden to modify the content, and cite the document when use.

	1000	0.00^{i}	100		0.00^{g}	100	
CL-MeOH	0	4.92^{a}	-	-	14.50^{a}	-	126.93
	10	4.80^{a}	2.44		13.00^{ab}	10.34	
	50	4.40^{a}	10.57		12.50^{ab}	13.79	
	100	3.55^{c}	27.85		7.25^{cd}	50.00	
	500	3.10^{de}	36.99		3.25^{efg}	77.59	
	1000	2.87^{ef}	41.67		0.75^{g}	94.83	
C.V. (%)		6.44		-	36.30	-	

The average of four replications, the means followed by the common letters are not significantly different by Duncan's multiple range test (DMRT) at $p<0.05$

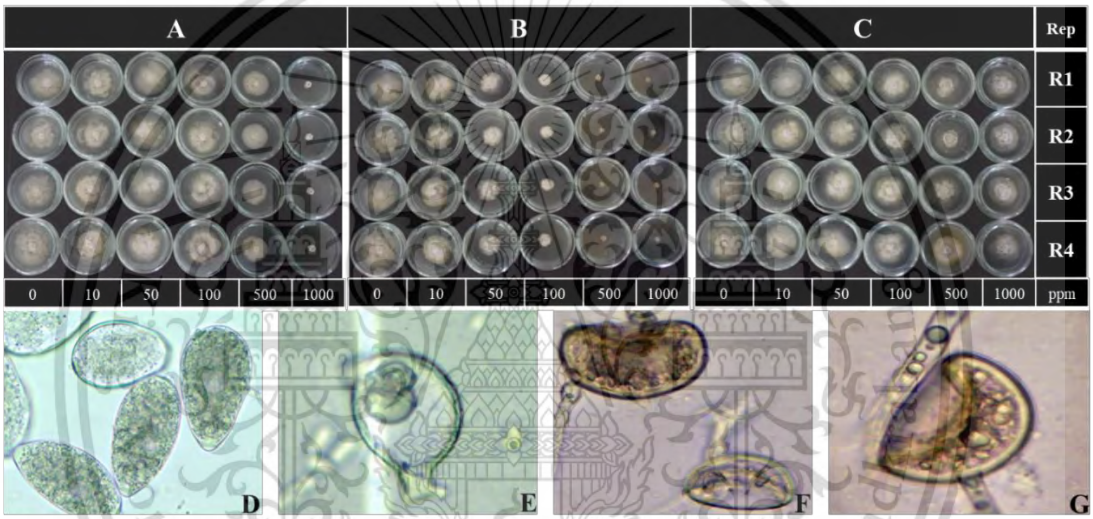

Figure 4.32 Metabolite crude extract from *Ch. lucknowense* CL against *P. palmivora* PYSC01 causing durian rot. A; crude CL-hexane, B; crude CL-EtOAc, C; crude CL-MeOH, D; normal sporangia formation produced by *P. palmivora* PYSC01 in control (0 ppm), E, F, and G abnormal sporangia formation caused by crude CL-Hexane, CL-EtOAc and, crude CL-MeOH, respectively

This material is reserved for educational use only, not allowed for commercial use.
Forbidden to modify the content, and cite the document when use.

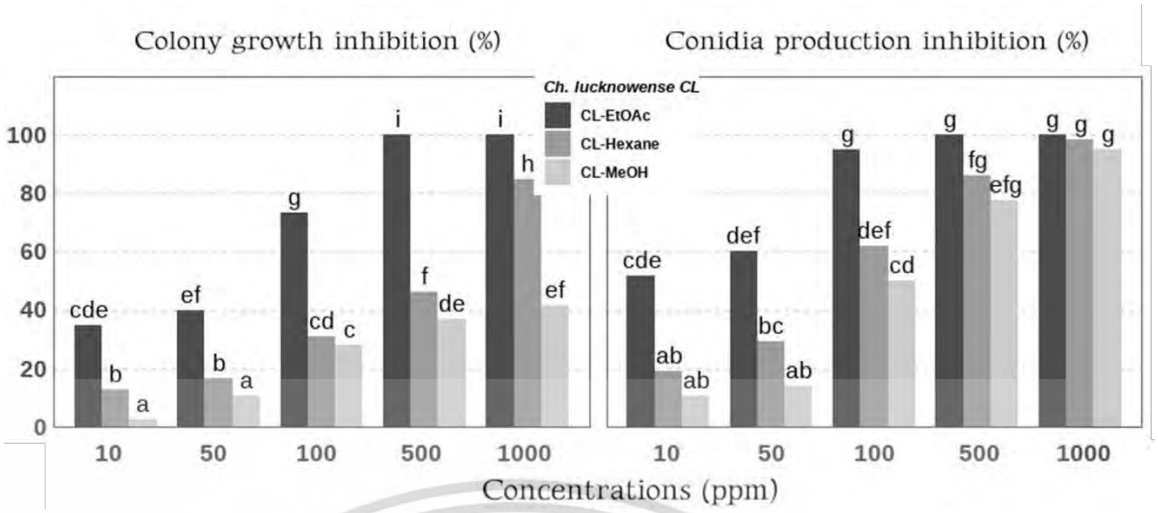

Figure 4.33 Metabolite crude extract from *Ch. lucknowense* CL against *P. palmivora*

4.6.3 Testing nanofibers against plant pathogens

Nanofibers from *T. hamatum* K01 named nano-TK01H, nano-TK01E, and nano-TK01M were loaded by crude TK01-hexane, TK01-EtOAc and crude TK01-MeOH. Each nanofiber was characterized and measured in size at the average of 122.30, 187.23, and 136.87 nm, respectively, using a scanning electron microscope (SEM), as shown in (Table 4.16., Figure 4.34).

Natural product nanofiber derived from *Ch. lucknowense* CL named nano-CLH, nano-CLE, and nano-CLM were loaded by crude CL-hexane, CL-EtOAc, and CL-MeOH, and they were measured the size (diameter) at average of 155.62, 207.91 and 156.87 nm, respectively using SEM (Table 4.16., Figure 4.35).

Table 4.16 Measurement of the size (diameters) of nanofibers

Nanofibers derived from *T. hamatum* K01			
Nanofibers	Mean (nm)	Maximum (nm)	Minimum (nm)
Nano-TK01H	122.34	168.9	75.97
Nano-TK01E	187.24	242.5	57.36
Nano-TK01M	136.87	256.4	90.65
Nanofibers derived from *Ch. lucknowense* CL			
Nano-CLH	155.62	203.5	139.4

This material is reserved for educational use only, not allowed for commercial use.
Forbidden to modify the content, and cite the document when use.

Nano-CLE	207.91	280.4	159.8
Nano-CLM	156.87	244.7	90.17

Dara was collected from 20 samples by measuring each nanofiber's size (diameter) using SEM.

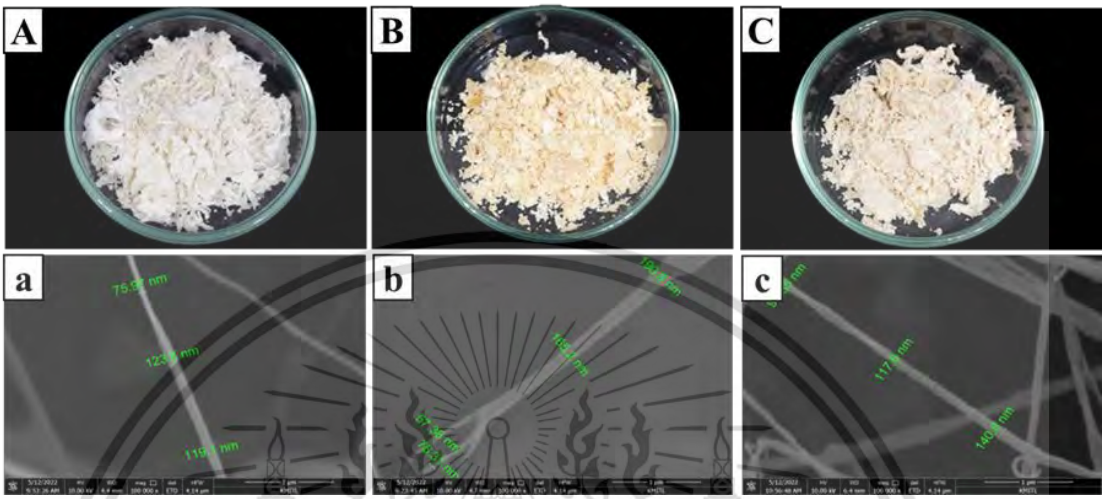

Figure 4.34 Characteristics of nanofibers from *T. hamatum* K01; A, a; B, b; and C c; nano-TK01H, nano-TK01E, and nano-TK01M, respectively. A, B, and C were taken pictures using a camera, and a, b, and c were measured and taken pictures using SEM

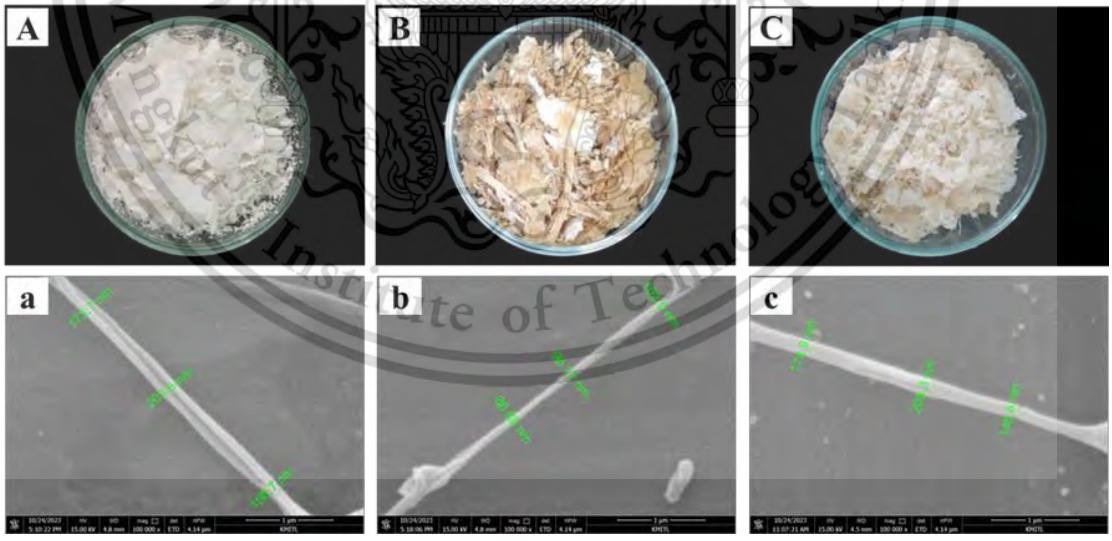

Figure 4.35 Characteristics of nanofibers from *Ch. lucknowense* CL; A, a; B, b; and C c; nano-CLH, nano-CLE, and nano-CLM, respectively. A, B, and C were taken pictures using a camera, and a, b, and c were measured and taken pictures using SEM

This material is reserved for educational use only, not allowed for commercial use.
Forbidden to modify the content, and cite the document when use.

4.6.3.1 Testing nanofibers from *T. hamatum* K01 against *P. palmivora* PYSC01

These nanofibers were evaluated for their antifungal activity at 3 to 15 ppm concentrations in DMSO and PDA toward *P. palmivora* PYSC01, a durian root rot causal agent. The result indicated that nano-TK01M significantly suppressed colony growth of *P. palmivora* PYSC01 ranging from 40.25 to 62.26 % and gave significance to the highest sporangia inhibition at the rate of 46.30 to 100%. The ED_{50} values were computed at 11.06 ppm and 3.13 ppm in colony growth and sporangia inhibition, respectively. However, nano-TK01E gave better control on the colony growth and sporangia formation at the rate of 24.11-49.69% and 24.07-99.07%, respectively, with the ED_{50} values required at 16.66 and 5.48 ppm on colony growth and sporangia inhibition respectively. While nono-TK01E gave the most negligible effect on both colony growth and sporangia formation, ranging from 22.43 to 44.03 and 3.70 to 79.63 %, respectively, with the ED_{50} values computed at 19.96 and 9.83 ppm, respectively, on colony growth and sporangia inhibition (Table 4.17., Figures 4.36 and 4.37).

This material is reserved for educational use only, not allowed for commercial use.
Forbidden to modify the content, and cite the document when use.

Table 4.17 Testing nanofibers from *T. hamatum* K01 against *P. palmivora* PYSC01

Nanofibers	Concs (ppm)	Colony growth (cm)	Growth inhibition (%)	ED_{50} (ppm)	Spore production (10^4)	Inhibition (%)	ED_{50} (ppm)
Nano-TK01H	0	4.77^{a}	-	19.96	27.00^{a}	-	9.83
	3	3.70^{b}	22.43^{f}		26.00^{ab}	3.70^{e}	
	5	3.52^{b}	26.21^{f}		22.50^{ab}	16.67^{e}	
	10	3.02^{c}	36.69^{de}		10.00^{cd}	62.96^{bc}	
	15	2.67^{cde}	44.03^{bcd}		5.50^{de}	79.63^{ab}	
Nano-TK01E	0	4.77^{a}	-	16.66	27.00^{a}	-	5.48
	3	3.62^{b}	24.11^{f}		20.50^{b}	24.07^{d}	
	5	3.40^{bc}	28.72^{ef}		13.75^{c}	49.07^{cd}	
	10	3.02^{cd}	36.69^{de}		3.75^{e}	86.11^{ab}	
	15	2.40^{e}	49.69^{bc}		0.25^{e}	99.07^{a}	
Nano-TK01M	0	4.77^{a}	-	11.06	27.00^{a}	-	3.13
	3	2.85^{cd}	40.25^{cd}		14.50^{c}	46.30^{cd}	
	5	2.47^{de}	48.22^{bc}		4.75^{de}	82.41^{ab}	
	10	2.35^{e}	50.73^{b}		1.50^{e}	94.44^{a}	
	15	1.80^{f}	62.26^{a}		0.00^{e}	100.00^{a}	
CV%		7.89	17.72		29.28	32.87	

The average of four replications, the mean followed by the common letters are not significantly different by Duncan's multiple range test (DMRT) at $p<0.05$

This material is reserved for educational use only, not allowed for commercial use.
Forbidden to modify the content, and cite the document when use.

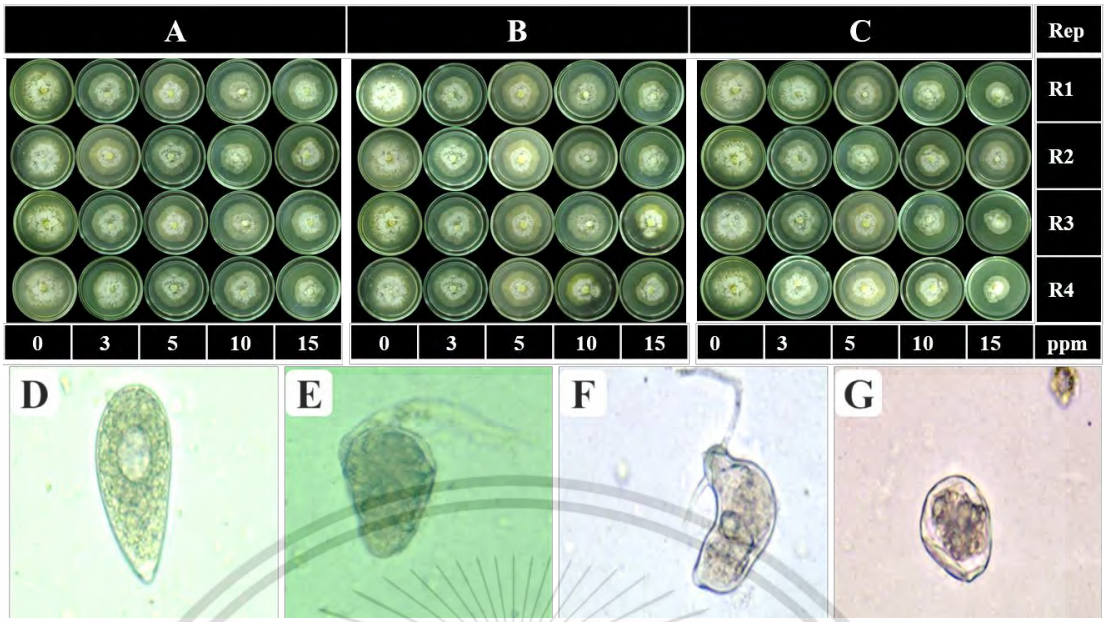

Figure 4.36 Nanofibers from *T. hamatum* K01 tested to inhibit colony growth and sporangia formation of *P. palmivora* PYSC01; A, nano-TK01H; B, nano-TK01E; C, nano-TK01M of each concentration; D, normal sporangia formation produced by *P. palmivora* PYSC01 in control (0 ppm), E, F, and G abnormal sporangia formation caused by nano-TK01H, nano-TK01E and nano-TK01M, respectively

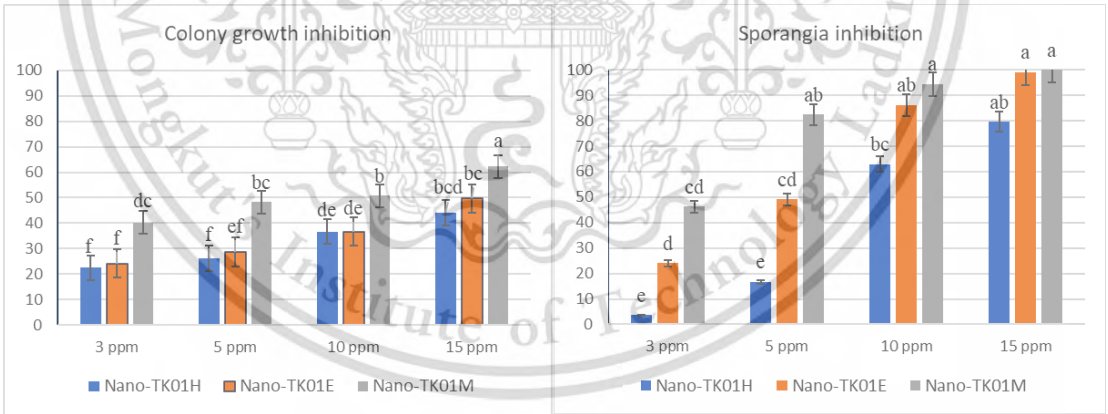

Figure 4.37 Nanofibers from *T. hamatum* K01 against *P. palmivora* PYSC01

4.5.3.2 Testing nanofibers from *T. hamatum* K01 against *C. gloeosporioides* C01

Nanofibers from *T. hamatum* K01 were also tested for their abilities to control *C. gloeosporioides* C01, a causal agent of citrus anthracnose. The results revealed that the nanoparticles from *T. hamatum* K01 exhibited antifungal activity against *C. gloeosporioides* C01. Nano-TK01M demonstrated the highest antifungal

This material is reserved for educational use only, not allowed for commercial use.
Forbidden to modify the content, and cite the document when use.

activity against *C. gloeosporioides* C01. It inhibited colony growth and conidia production by approximately 38.81% to 59.37% and 37.20% to 100%, respectively, at concentrations ranging from 3 to 15 ppm. Notably, at a concentration of 10 ppm, Nano-TK01M completely inhibited conidia production. Nano-TK01 showed better results in inhibiting colony growth and conidia production, with ED_{50} values of 28 and 9 ppm, respectively. Nano-TK01H had a lesser effect, with colony growth and conidia production suppression computed at ED_{50} values of 33 and 15 ppm, respectively (Table 4.18., Figures 4.38 and 4.39).

Table 4.18 Testing nanofibers from *T. hamatum* K01 against *C. gloeosporioides* C01 causing anthracnose disease of citrus

Nanofibers	Concs ppm	Colony growth (cm)	Growth inhibition (%)	ED_{50} (ppm)	Conidia production (10^6)	Inhibition (%)	ED_{50} (ppm)
Nano-TK01H	0	4.90^{a}	-	33.84	216.25^{a}	-	15.04
	3	4.06^{b}	17.04^{f}		162.75^{ab}	19.93^{d}	
	5	3.82^{bc}	21.89^{f}		153.50^{ab}	24.74^{de}	
	10	3.70^{cd}	24.49^{ef}		141.00^{ab}	31.35^{cd}	
	15	3.38^{de}	30.76^{de}		84.24^{bc}	58.59^{bc}	
Nano-TK01E	0	4.90^{a}	-	28.55	216.25a	-	9.92
	3	3.81^{bc}	22.16^{f}		154.00^{ab}	23.91^{d}	
	5	3.41^{de}	30.29^{de}		125^{bc}	36.06^{cd}	
	10	3.32^{ef}	32.10^{cde}		81.75^{bc}	56.72^{bc}	
	15	3.05^{fgh}	37.72^{bcd}		53.50cd	74.21^{bc}	
Nano-TK01M	0	4.90^{a}	-	13.95	216.25^{a}	-	3.88
	3	3.28^{efg}	32.81^{cd}		137.25^{ab}	37.20^{c}	
	5	2.98^{gh}	39.00^{bc}		49.50^{cd}	75.45^{ab}	
	10	2.82^{h}	42.33^{b}		0.00^{d}	100^{a}	
	15	1.98^{i}	59.37^{a}		0.00^{d}	100^{a}	
CV%		4.46	14.49		31.91	40.39	

The average of four replications, the mean followed by the common letters are not significantly different by Duncan's multiple range test (DMRT) at $p<0.05$

This material is reserved for educational use only, not allowed for commercial use.
Forbidden to modify the content, and cite the document when use.

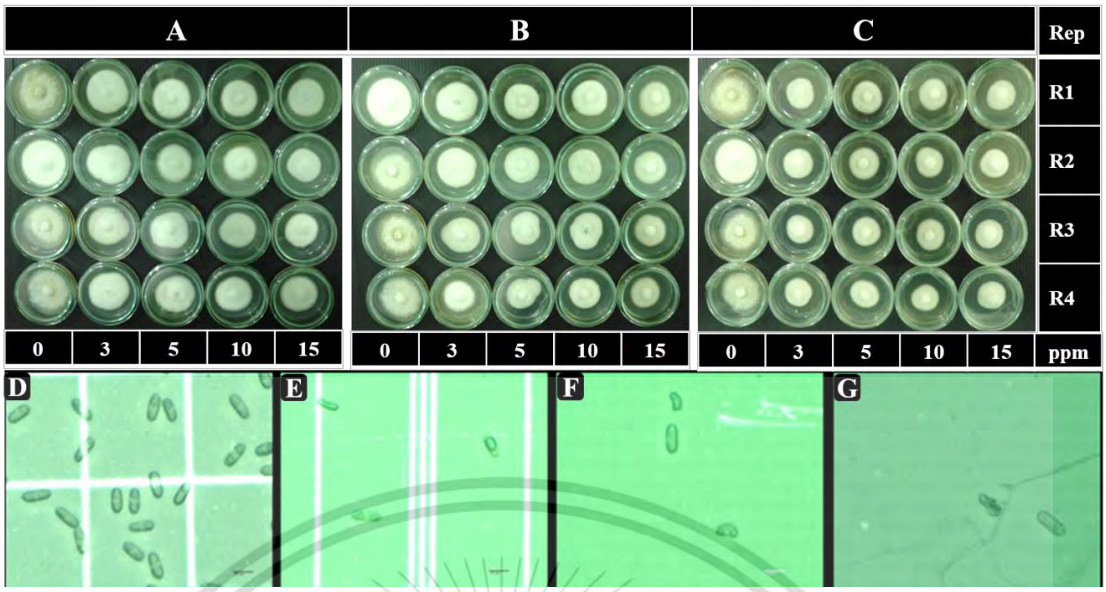

Figure 4.38 Nanofibers from *T. hamatum* K01 tested to inhibit colony growth and conidia production of *C. gloeosporioides* C01; A, nano-TK01H; B, nano-TK01E; C, nano-TK01M for each concentration; D, normal conidia production of *C. gloeosporioides* C01 non-treated control (0 ppm); E, F and G abnormal conidia production caused by nano-TK01H, nano-TK01E and nano-TK01M, respectively

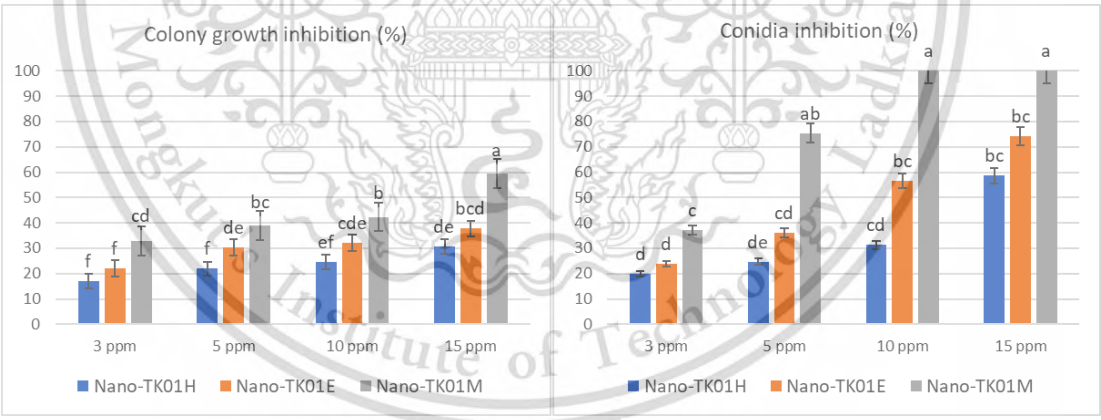

Figure 4.39 Nanofibers from *T. hamatum* K01 against *C. gloeosporioides* C01

4.4.3.3 Nanofibers from *T. hamatum* K01 against *C. gloeosporioides* C02

Nanofibers from *T. hamatum* K01 demonstrated antifungal activity against *C. gloeosporioides* C02, a causal agent of durian anthracnose, at concentrations ranging from 3 to 15 ppm. The results revealed that nano-TK01M at 15 ppm exhibited the highest antifungal activity against *C. gloeosporioides* C02, inhibiting colony growth by 59.37% and sporulation by 100%. The ED_{50} values for nano-

This material is reserved for educational use only, not allowed for commercial use.
Forbidden to modify the content, and cite the document when use.

TK01M to inhibit colony growth and sporulation were computed at 13 and 3 ppm, respectively. For nano-TK01E, the ED_{50} values were 28 ppm for colony growth inhibition and 9 ppm for sporulating inhibition. Nano-TK01H had ED_{50} values of 33 ppm for colony growth inhibition and 15 ppm for sporulating inhibition (Table 4.19., Figures 4.40 and 4.41). Furthermore, the nanofibers resulted to cause abnormal conidia formation, as shown in Figure 4.40.

Table 4.19 Testing nanofibers from *T. hamatum* K01 against *C. gloeosporioides* C02 causing anthracnose disease of durian

Nanofibers	Concs ppm	Colony Growth (cm)	Growth inhibition (%)	ED_{50} ppm	Conidia production (10^7)	growth Inhibition (%)	ED_{50} ppm
Nano-TK01H	0	4.82^{a}	-	40.36	29.37^{a}	-	10.39
	3	4.25^{b}	11.72^{g}		20.47^{ab}	8.37^{de}	
	5	4.02^{bc}	16.44^{gh}		15.47^{abc}	22.67^{cde}	
	10	3.85^{cd}	20.04^{fg}		8.87^{bc}	45.34^{bcde}	
	15	3.71^{de}	22.95^{def}		2.95^{c}	87.07^{ab}	
Nano-TK01E	0	4.82^{a}	-	36.20	29.37^{a}	-	7.76
	3	3.97^{c}	17.74^{fgh}		14.72^{abc}	16.71^{d}	
	5	3.82^{cd}	20.56^{efg}		9.67^{bc}	49.93^{abcd}	
	10	3.53^{ef}	26.56^{cde}		4.60^{bc}	69.75^{abc}	
	15	3.42^{fg}	28.94^{cd}		0.84^{c}	96.91^{ab}	
Nano-TK01M	0	4.82^{a}	-	14.53	29.37^{a}	-	2.68
	3	$3.5e^{fg}$	27.32^{cd}		7.52^{bc}	59.84^{abcd}	
	5	3.26^{g}	32.34^{bc}		5.20^{bc}	71.85^{abc}	
	10	2.98^{h}	37.96^{b}		0.90^{c}	96.07^{ab}	
	15	1.97^{i}	59.02^{a}		0.02^{c}	99.76^{a}	
CV%		4.29	19.08		84.32	67.02	

The average of four replications was analyzed using Duncan's multiple range test (DMRT). The mean values followed by the same letters are not significantly different at $p<0.05$

This material is reserved for educational use only, not allowed for commercial use.
Forbidden to modify the content, and cite the document when use.

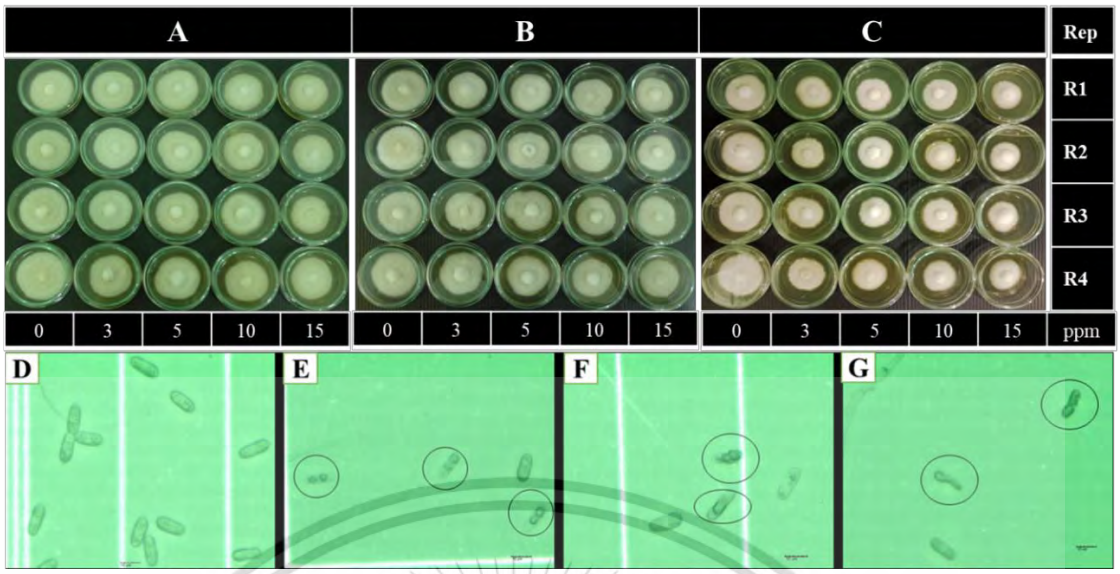

Figure 4.40 Nanofibers from *T. hamatum* K01 tested to inhibit colony growth and conidia production of *C. gloeosporioides* C02; A, nano-TK01H; B, nano-TK01E; C, nano-TK01M for one replication of each concentration; D, normal conidia formation, E, F and G, abnormal conidia formation caused by nano-TK01, nano-TK01E, and nano-TK01M, respectively

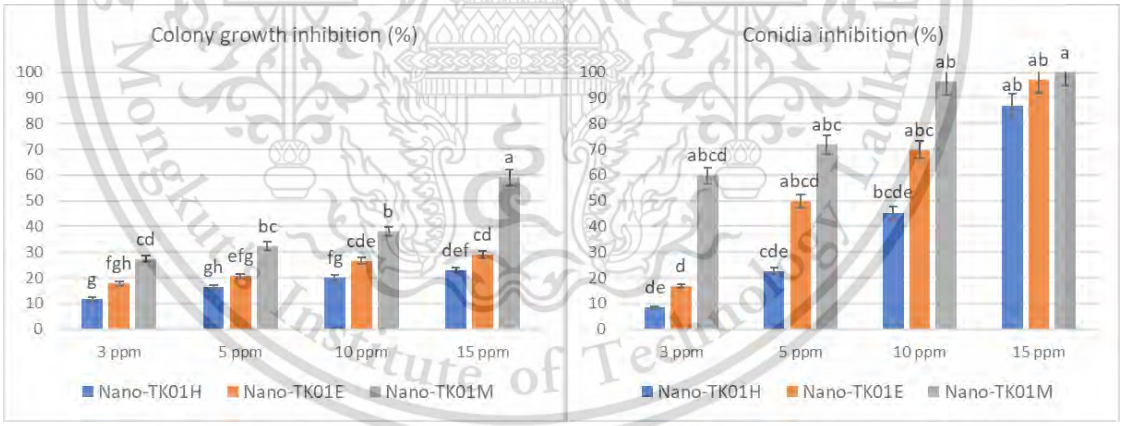

Figure 4.41 Nanofibers from *T. hamatum* K01 against *C. gloeosporioides* C02

4.6.4 Testing nanofibers from *Ch. lucknowense* CL against plant pathogens

Nanofibers derived from *Ch. lucknowense,* namely nano-CLH, nano-CLE, and nano-CLM, were evaluated for their antibiosis activity to inhibit *C. gloeosporioides* a causal agent of citrus and durian anthracnose, and durian rot caused by *P. palmivora* at 3, 5, 10, and 15 ppm of concentrations.

This material is reserved for educational use only, not allowed for commercial use.
Forbidden to modify the content, and cite the document when use.

4.6.4.1 Testing nanofibers from *Ch. lucknowense* CL against *C. gloeosporioides* C01 causing citrus anthracnose.

Nanofibers from *Ch. lucknowense* CL tested their bioactive compounds against *C. gloeosporioides* C01, which caused citrus anthracnose disease. The result indicated that all the nanofibers tested significantly inhibited colony growth and conidia formation of *C. gloeosporioides* C01, in which neither colony growth nor conidia grew at 15 ppm of concentration. However, nano-CLE showed the highest inhibitory effect on colony growth and conidia production at ED_{50} of 2.2 and 0.22 ppm, respectively. (Table 4.20., Figures 4.42 and 4.43).

Table 4.20 Nanofibers derived *Ch. lucknowense* against *C. gloeosporioides* C01 causing citrus anthracnose

Nanofibres	Concentrations ppm	Colony growth (cm)	Growth inhibition (%)	ED_{50} ppm	Conidia production (10^6)	Inhibition (%)	ED_{50} ppm
Nano-CLH	0	4.95^{a}	-	2.61	209.75^{a}	-	0.37
	3	2.07^{b}	58.04^{f}		48.50^{b}	68.21^{b}	
	5	1.25^{d}	74.75^{d}		15.50^{b}	87.30^{a}	
	10	0.00^{g}	100^{a}		1.00^{d}	99.05^{a}	
	15	0.00^{g}	100^{a}		0.00^{d}	100^{a}	
Nano-CLE	0	4.95^{a}	-	2.2	209.75^{a}	-	0.22
	3	1.87^{c}	62.08^{e}		11.75^{c}	92.98^{a}	
	5	0.90^{f}	81.77^{b}		0.00^{b}	100^{a}	
	10	0.00^{g}	100^{a}		0.00^{b}	100^{a}	
	15	0.00^{g}	100^{a}		0.00^{b}	100^{a}	
Nano-CLM	0	4.95^{a}	-	2.37	209.75^{a}	-	1.59
	3	1.95^{bc}	60.58^{ef}		55.00^{b}	63.37^{b}	
	5	1.07^{f}	78.27^{c}		13.00^{b}	91.92^{a}	
	10	0.00^{g}	100^{a}		0.00^{b}	100^{a}	

This material is reserved for educational use only, not allowed for commercial use.
Forbidden to modify the content, and cite the document when use.

	15	0.00^{g}	100^{a}		0.00^{b}	100^{a}
CV%		6.13	2.89		121.25	17.57

The average of four replications, the means followed by the common letters are not significantly different by Duncan's multiple range test (DMRT) at $p<0.05$

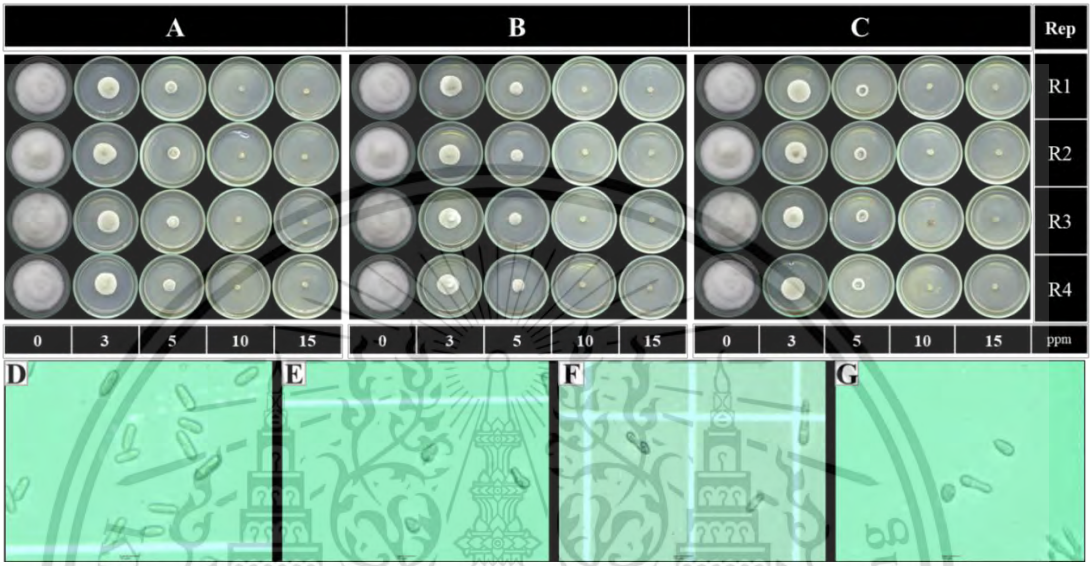

Figure 4.42 The effect of nanofibers from *Ch. lucknowense* CL against *C. gloeosporioides* C01, A, B, and C the effect of nano-CLH, nano-CLE, and nano-CLM respectively, D; normal conidia produced by *C. gloeosporioides* C01, E, F, and G abnormal conidia formation caused by nano-CLH, nano-CLE, and nano-CLM, respectively

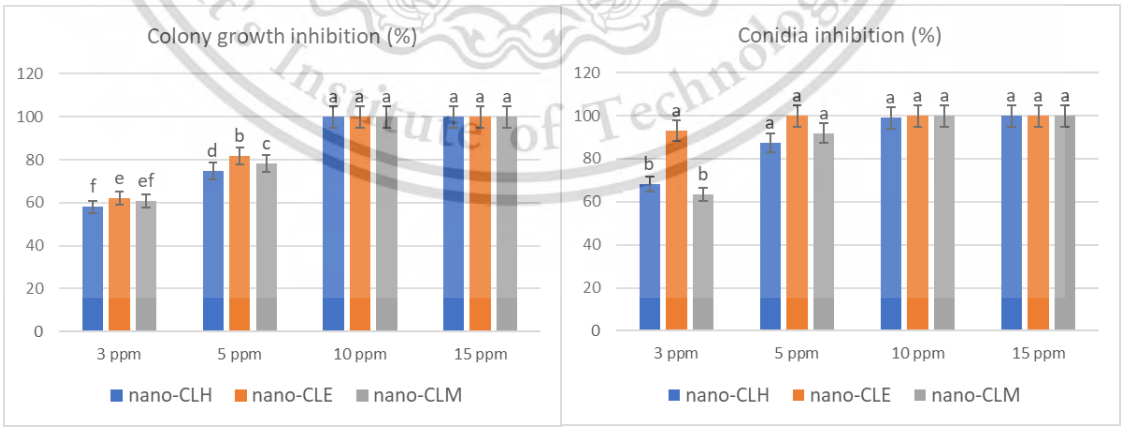

Figure 4.43 The effect of nanofibers from *Ch. lucknowense* CL against *C. gloeosporioides* C01

This material is reserved for educational use only, not allowed for commercial use.
Forbidden to modify the content, and cite the document when use.

4.6.4.2 Testing nanofibers from *Ch. lucknowense* CL against C. *gloeosporioides* C02 causing durian anthracnose.

The antimicrobial properties of microbial nanofibers derived from *Ch. lucknowense* CL were evaluated to suppress *C. gloeosporioides* C02, which caused durian anthracnose disease at 3 to 15 ppm concentrations. The results demonstrated that antimicrobial nano-CLE exhibited high effectiveness in inhibiting mycelial growth and conidia production, achieving 100% inhibition at a concentration of 5 ppm. The ED_{50} values for mycelial growth and conidia production were determined to be only 2 and 1 ppm, respectively. In comparison, Nano-CLM demonstrated superior control of mycelial growth and conidia production, with ED_{50} values of 2.45 and 1.12 ppm, respectively, compared to Nano-CLH, which required an ED_{50} of 2.59 and 1.2 ppm, respectively (Table 4.21., Figures 4.44 and 4.45).

Table 4.21 Testing nanofibers from *Ch. lucknowense* CL against *C. gloeosporioides* C02

Nanofibers	Concs ppm	Mycelia growth (cm)	Growth inhibition (%)	ED_{50} ppm	Conidia production (10^7)	Inhibition (%)	ED_{50} ppm
Nano-CLH	0	5.00[a]	-	2.59	37.12[a]	-	1.2
	3	1.85[b]	62.50[e]		9.40[b]	74.31[c]	
	5	1.12[d]	77.50[c]		3.3[cd]	90.86[ab]	
	10	0.00[f]	100[a]		0.00[d]	100[a]	
	15	0.00[f]	100[a]		0.00[d]	100[a]	
Nano-CLE	0	5.00[a]	-	2.02	37.12[a]	-	1.03
	3	1.20[d]	76.00[b]		4.37[c]	88.49[ab]	
	5	0.00[f]	100[a]		0.00[d]	100[a]	
	10	0.00[f]	100[a]		0.00[d]	100[a]	
	15	0.00[f]	100[a]		0.00[d]	100[a]	
Nano-CLM	0	5.00[a]	-	2.45	37.12[a]	-	1.12
	3	1.57[c]	68.50[d]		5.30[c]	85.84[b]	
	5	0.06[e]	88.00[b]		0.27[d]	99.25[a]	
	10	0.00[f]	100[a]		0.00[d]	100[a]	

This material is reserved for educational use only, not allowed for commercial use.
Forbidden to modify the content, and cite the document when use.

	15	0.00[f]	100[a]		0.00[d]	100[a]
CV%		7.41	2.95		24.72	7.17

The average of four replications, the mean followed by the common letters are not significantly different by Duncan's multiple range test (DMRT) at $p<0.05$

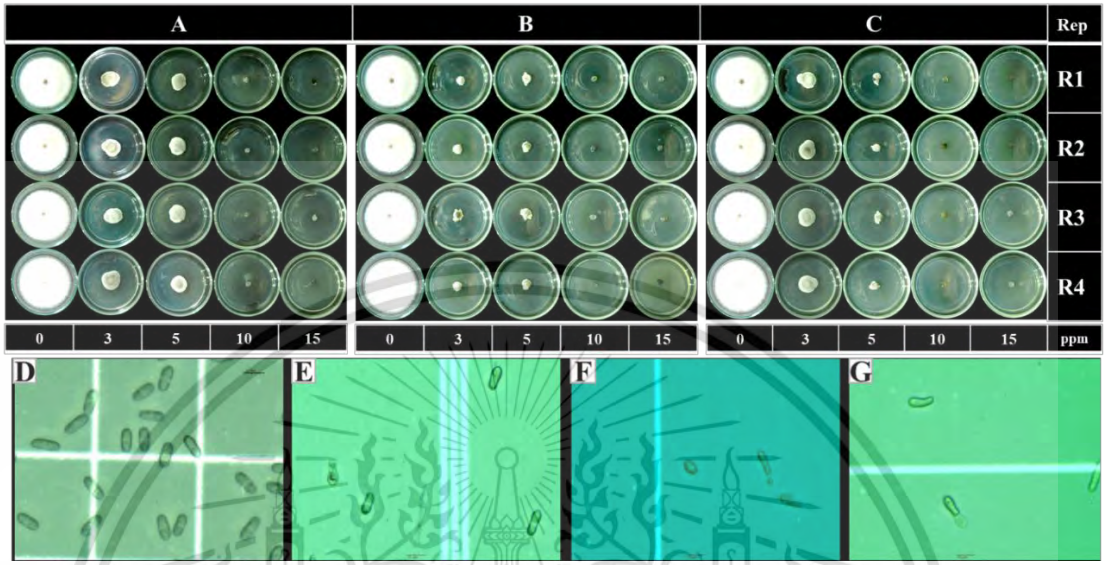

Figure 4.44 Inhibition of nanofibers from *Ch. lucknowense* CL against *C. gloeosporioides* C02. A, B, and C inhibition of nano-CLE, nano-CLE, and nano-CLM, respectively. D, normal conidia production produced from *C. gloeosporioides* C02 in control (0 ppm), E, F, and G abnormal conidia production caused by nano-CLE, nano-CLE, and nano-CLM, respectively

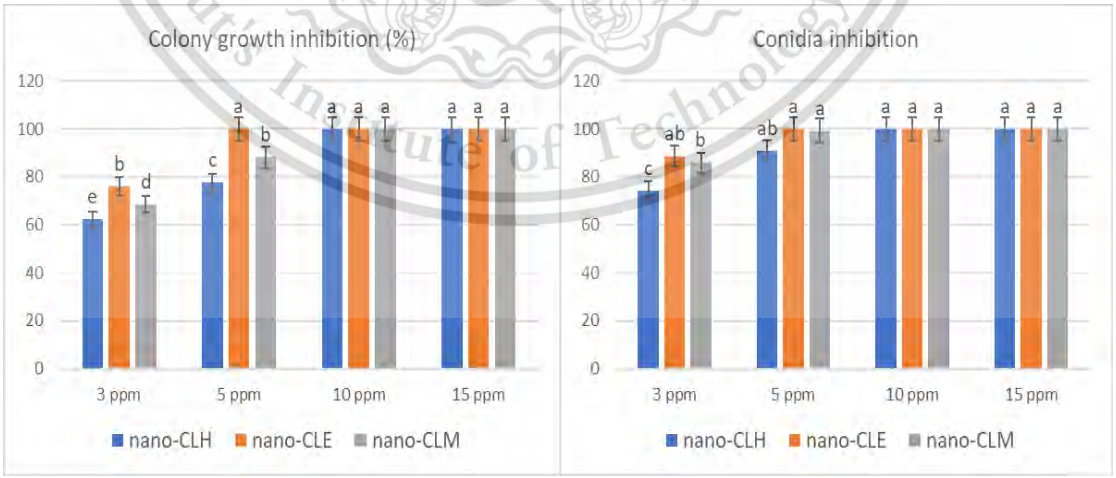

Figure 4.45 Inhibition of nanofibers from *Ch. lucknowense* CL against *C. gloeosporioides* C02

This material is reserved for educational use only, not allowed for commercial use.
Forbidden to modify the content, and cite the document when use.

4.6.4.2 Testing nanofibers from *Ch. lucknowense* CL against *P. palmivora* PYSC01 causing durian rot.

Natural product nanofibers (nano-CLH, nano-CLE, and nano-CLM) from *Ch. lucknowense* CL were also examined for their bioactive compounds to control *P. palmivora* PYSC01, which caused durian rot. The results indicated that both colony growth and sporangia formation of *P. palmivora* PYSC01 were inhibited by 100% at a concentration of 5 ppm for all test nanofibers. However, nano-CLE and nano-CLM exhibited the most antifungal potential against colony growth and sporangia production, with ED_{50} values lower than 1 and 2 ppm, respectively (Table 4.22., Figures 4.46 and 4.47). Moreover, the control mechanism of *Ch. lucknowense* CL was found to produce lysis enzymes, as evidenced by the nanofibers test, which resulted in abnormal sporangia formation, as shown in Figure 4.46.

Table 4.22 Nanofibres derived *Ch. lucknowense* against *P. palmivora* PYSC01, causing durian rot

Nanofibres	Concentration ppm	Colony growth (cm)	Growth inhibition (%)	ED_{50} ppm	Sporangia production (10^5)	Inhibition (%)	ED_{50} ppm
Nano-CLH	0	4.90[a]	0	2.82	103.50[a]	-	1.05
	3	2.22[b]	54.64[b]		2.25[b]	97.77[b]	
	5	0[c]	100[a]		0[c]	100[a]	
	10	0[c]	100[a]		0[c]	100[a]	
	15	0[c]	100[a]		0[c]	100[a]	
Nano-CLE	0	4.90[a]	0	2.0>	103.50[a]	-	1.0>
	3	0[c]	100[a]		0[c]	100[a]	
	5	0[c]	100[a]		0[c]	100[a]	
	10	0[c]	100[a]		0[c]	100[a]	
	15	0[c]	100[a]		0[c]	100[a]	
Nano-CLM	0	4.90[a]	0	2.0>	103.50[a]	-	1.0>
	3	0[c]	100[a]		0[c]	100[a]	
	5	0[c]	100[a]		0[c]	100[a]	
	10	0[c]	100[a]		0[c]	100[a]	
	15	0[c]	100[a]		0[c]	100[a]	

This material is reserved for educational use only, not allowed for commercial use.
Forbidden to modify the content, and cite the document when use.

CV%	6.83	1.40		37.96	1.11

The average of four replications, the mean followed by the common letters are not significantly different by Duncan's multiple range test (DMRT) at $p<0.05$

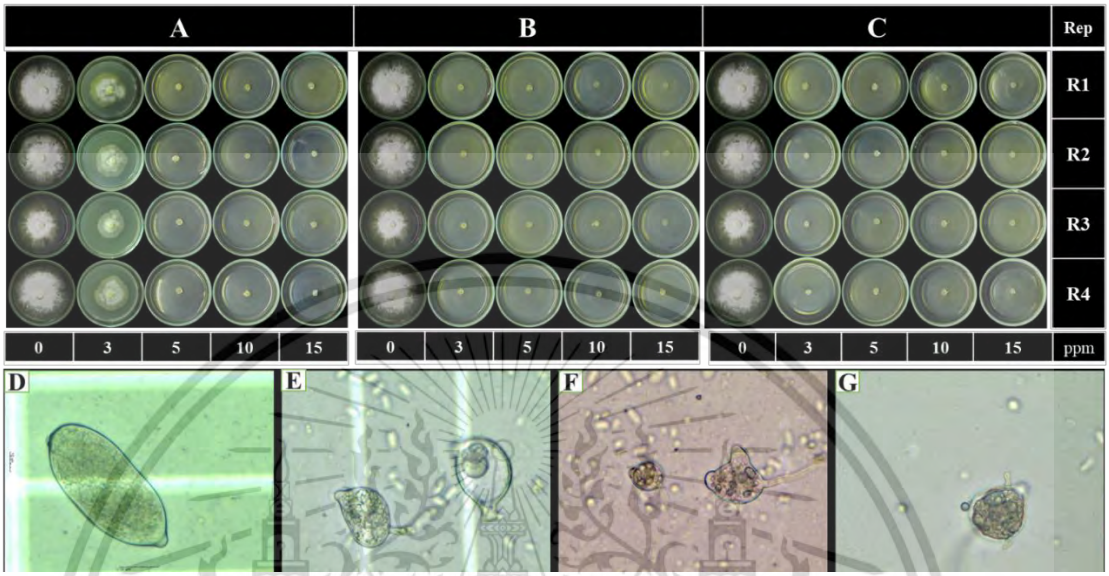

Figure 4.46 Inhibition of nanofibers from *Ch. lucknowense* CL against *P. palmivora* PYSC01, A; B, and C inhibition of nano-CLH, nano-CLE, and nano-CLM, respectively, D, normal sporangia formation produced by *P. palmivora* PYSC01 in control (0 ppm) E, F, and G, abnormal sporangia formation of *P. palmivora* PYSC01 causing by nano-CLH, nano-CLE and nano-CLM, respectively.

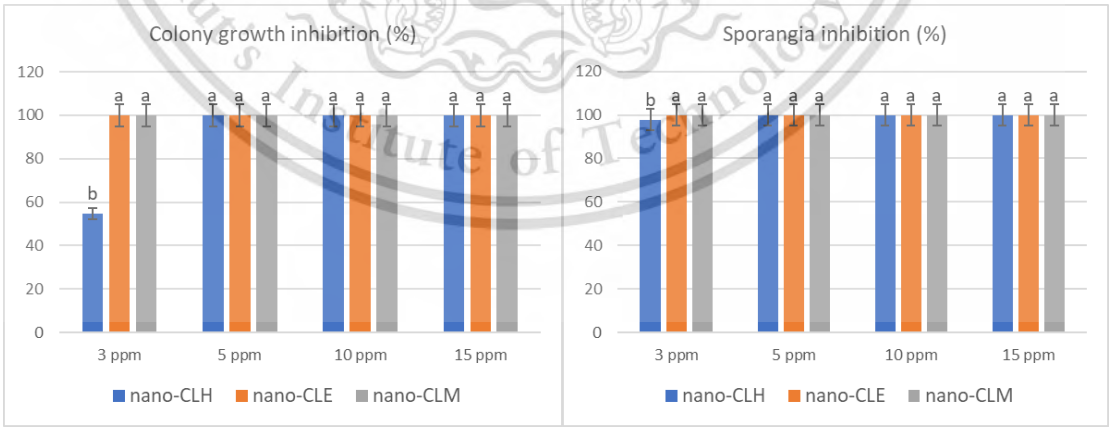

Figure 4.47 Inhibition of nanofibers from *Ch. lucknowense* CL against *P. palmivora* PYSC01

This material is reserved for educational use only, not allowed for commercial use.
Forbidden to modify the content, and cite the document when use.

4.7 Greenhouse experiments

The application of bioproducts (*T. hamatum* K01's product, *Ch. lucknowense* CL's product, microbial nanofiber from *T. hamatum* K01, microbial nanofiber from *Ch. lucknowense* CL) and chemical metalaxyl (Figure 4.48), were investigated for their effectiveness in reducing disease severity, phytoalexins production, photosynthetic pigments, and plant growth parameters of durian and citrus. Pathogenic fungi *P. palmivora* PYSC01 and *C. gloeosporioides* C02 were used for co-inoculated with durian, and *C. gloeosporioides* C01 was inoculated with citrus, which was adjusted at $2x10^6$ spores/mL using hemocytometer as shown in Figure 4.49.

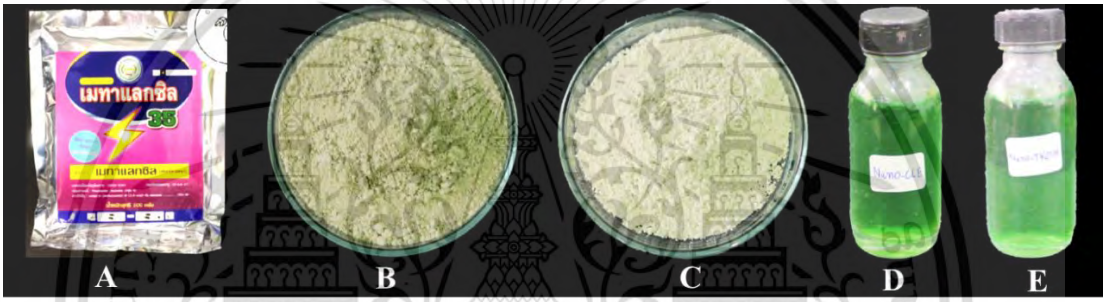

Figure 4.48 Agricultural inputs for durian production in pots experiment, A; Metalaxyl, B; *Ch. lucknowense* CL product, C; *T. hamatum* K01 products, D; microbial nanofiber loaded by crude ethyl acetate extracted from *Ch. lucknowense* CL and E; microbial nanofiber loaded by crude methanol extracted from *T. hamatum* K01

This material is reserved for educational use only, not allowed for commercial use.
Forbidden to modify the content, and cite the document when use.

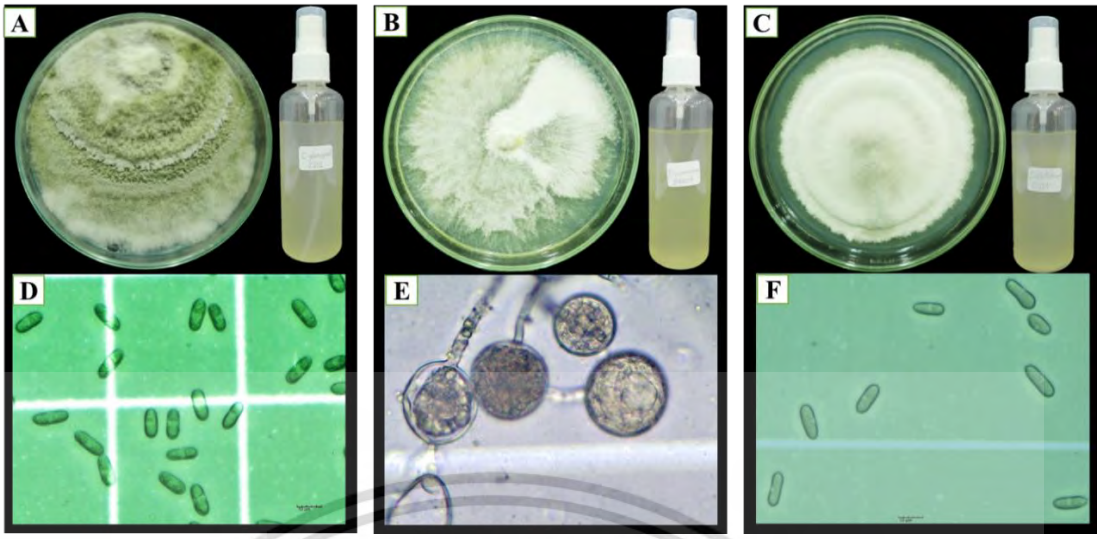

Figure 4.49 Pathogenic organisms for inoculation on durian and citrus, A, B, and C, colony growth of *C. gloeosporioides* C02, *P. palmivora* PYSC01, C; *C. gloeosporioides* C01, respectively, D, E, and F, sporulation of *C. gloeosporioides* C01, *P. palmivora* PYSC01 and *C. gloeosporioides* C01, respectively

4.7.1 Disease reduction

4.7.1.1 Disease reduction of durian

Disease severity of durian rot and durian anthracnose were assessed on days 30, 60, 90, and 120 after co-inoculated by *P. palmivora* PYSC01 and *C. gloeosporioides* C02 and treated with nanofiber from *T. hamatum* K01, nanofiber from *Ch. lucknowense* CL, *T. hamatum* K01' product, *Ch. lucknowense* CL's product and chemical metalaxyl compared to positive control and negative control. The result indicated that disease severity did not show in positive control. In contrast, the highest disease severity was recorded in negative control by 100%, in which the test plants completely died on day 120. However, disease severity was also recorded in *T. hamatum* K01's product by 13%, *Ch. lucknowense* CL product's treatment by 10%, chemical metalaxyl by 7.91%, nanofiber from *Ch. lucknowense* CL by 4.58%, and nanofiber from *T. hamatum* K01 by 0.83%.

Moreover, disease reduction was also recorded on days 30, 60, 90, and 120. The most effective treatment for disease reduction was found to be nanofiber from *T. hamatum* K01, achieving a reduction of 99.16%, followed by nanofiber from

This material is reserved for educational use only, not allowed for commercial use.
Forbidden to modify the content, and cite the document when use.

Ch. lucknowense CL by 95.41%, chemical metalaxyl by 92.08%, *Ch. lucknowense* CL's product by 90% and *T. hamatum* K01's product 86.66% on day 120, as shown in Table 4.23., Figures 4.50, 4.51 and 4.58-4.61.

Table 4.23 Disease assessment of durian plants after fungal inoculation and treatment by bioproducts and metalaxyl compared to negative and positive control

Treatments	Assessment of disease incident (DI%)			
	Day 30	Day 60	Day 90	Day 120
Positive control	0.00^{c}	0.00^{b}	0.00^{c}	0.00^{c}
Metalaxyl	16.67^{bc}	15.00^{b}	16.68^{bc}	18.40^{bc}
Ch. lucknowense	33.30^{b}	26.76^{b}	25.00^{b}	26.67^{b}
T. hamatum	25.00^{bc}	23.32^{b}	20.00^{bc}	21.66^{bc}
Nano-CL	30.00^{b}	13.32^{b}	10.00^{bc}	11.70^{bc}
Nano-TK01	15.00^{bc}	10.00^{b}	1.65^{bc}	3.34^{bc}
Negative control	66.67^{a}	78.32^{a}	93.33^{a}	100^{a}
CV%	42.52	53.88	42.22	41.19
Treatments	Assessment of disease severity (DI%)			
	Day 30	Day 60	Day 90	Day 120
Positive control	0.00^{b}	0.00^{b}	0.00^{c}	0.00^{c}
Metalaxyl	5.83^{b}	5.41^{b}	5.83^{bc}	7.91^{bc}
Ch. lucknowense	14.16^{b}	16.25^{b}	12.50^{b}	13.35^{b}
T. hamatum	10.80^{b}	10.83^{b}	9.58^{bc}	10.00^{cb}
Nano-CL	12.50^{b}	5.42^{b}	4.16^{bc}	4.58^{bc}
Nano-TK01	5.41^{b}	2.50^{b}	0.41^{bc}	0.83^{cb}
Negative control	50.00^{a}	64.58^{a}	93.30^{a}	100^{a}
CV%	51.73	70.43	29.48	27.66
Treatments	Assessment of disease reduction (DR%)			
	Day 30	Day 60	Day 90	Day 120
Positive control	100^{a}	100^{a}	100^{a}	100^{a}
Metalaxyl	88.50^{a}	92.26^{a}	93.97^{a}	92.08^{ab}
Ch. lucknowense	70.04^{a}	72.58^{a}	86.73^{a}	86.66^{b}
T. hamatum	79.41^{a}	82.14^{a}	90.35^{a}	90.00^{ab}
Nano-CL	75.36^{a}	89.40^{a}	91.70^{a}	95.41^{ab}

This material is reserved for educational use only, not allowed for commercial use.
Forbidden to modify the content, and cite the document when use.

Nano-TK01	87.73[a]	95.63[a]	99.52	99.16[ab]
Negative control	-	-	-	-
CV%	18.73	15.43	6.94	5.90

Treatment means followed by the same letter are not significantly different at $p<0.05$.

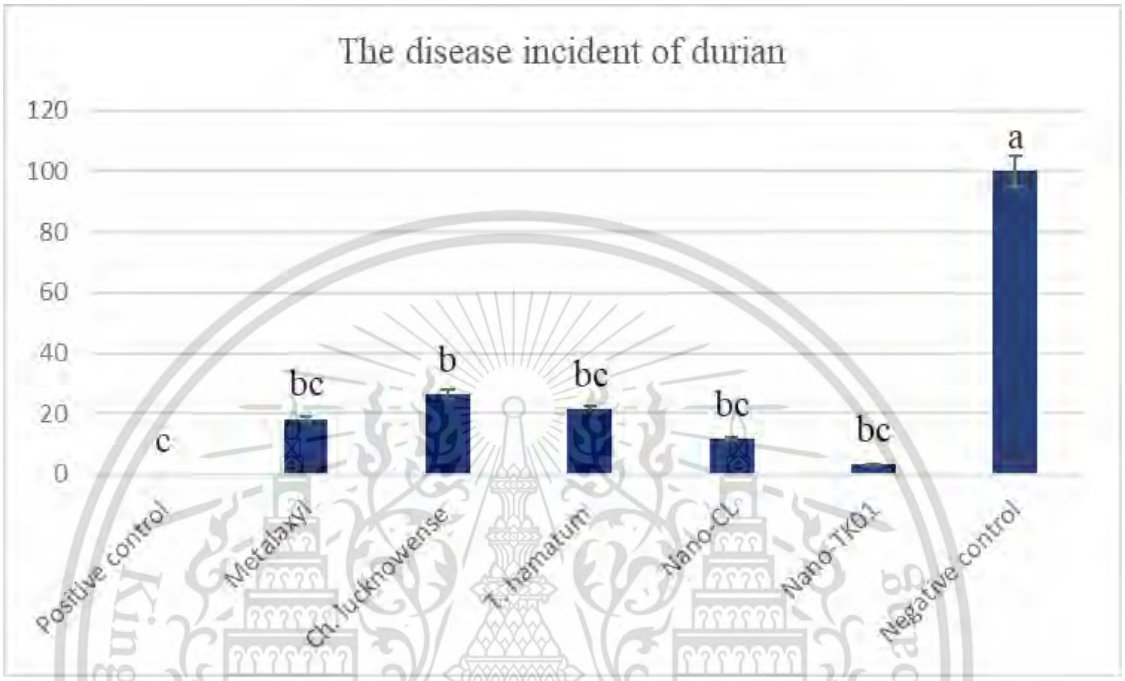

Figure 4.50 The disease incident of durian on day 120 after fungal inoculation and treatment

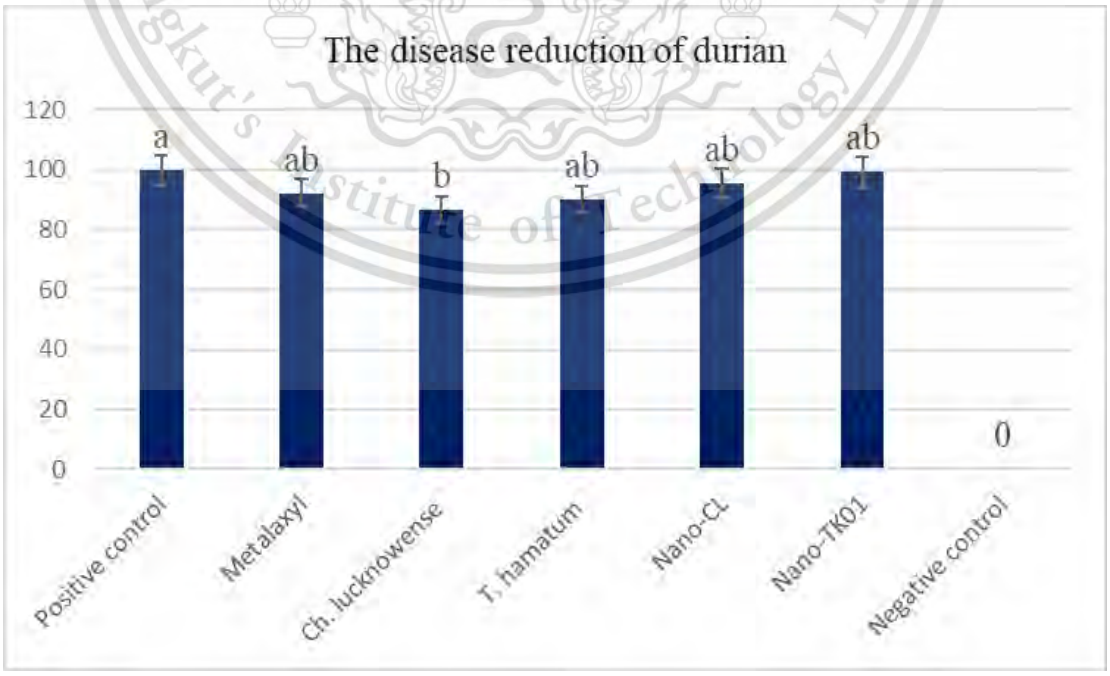

This material is reserved for educational use only, not allowed for commercial use.
Forbidden to modify the content, and cite the document when use.

Figure 4.51 The disease reduction of durian on day 120 after fungal inoculation and treatment

4.7.1.2 Disease reduction of citrus

The anthracnose disease of citrus was assessed after inoculation of *C. gloeosporioides* C02 and treatment. The result showed that the highest disease severity was recorded in negative control by 98.30%. However, the severity of the disease was also recorded with the treatment of *Ch. lucknowense* CI's product 6.67%, Metalaxyl 3.33%, *T. hamatum* K01's product 2.50%, nanofiber from *Ch. lucknowense* Cl 1.25% and nanofiber from *T. hamatum* K01 0.84%, while the disease severity of citrus anthracnose did not show in positive control.

Treatment of nanofiber from *T. hamatum* K01 was found to be the most effective in the reduction of severity of disease, in which the durian rot and durian anthracnose was decreased by 99.13%, followed by the treatment of nanofiber from Ch. lucknowense CL 98.72%, *T. hamatum* K01's product 97.50% and *Ch. lucknowense* Cl's product 93.30% the same the treatment of metalaxyl 96.67%, compared to the negative control, as shown in Table 4.24., Figures 4.52, 4.53, and 4.63-4.67.

Table 4.24 Disease assessment of citrus plants after fungal inoculation and treated by bioproducts and metalaxyl compared to negative and positive control

Treatments	Assessment of disease incident (DI%)			
	Day 30	Day 60	Day 90	Day 120
Positive control	0.00^{b}	0.00^{b}	0.00^{c}	0.00^{c}
Metalaxyl	6.60^{ab}	18.33^{b}	21.65^{b}	13.30^{cb}
Ch. lucknowense	8.33^{ab}	18.30^{b}	23.30^{b}	18.33^{b}
T. hamatum	3.30^{ab}	10.00^{b}	13.33^{bc}	10.00^{cb}
Nano-CL	1.67^{ab}	6.68^{b}	10.00^{bc}	5.00^{cb}
Nano-TK01	0.00^{b}	1.70^{b}	5.00b^{c}	3.34^{cb}
Negative control	23.30^{a}	63.43^{a}	86.67^{a}	98.30^{a}
CV%	156.91	69.29	39.78	32.32
Treatments	Assessment of disease severity (DS%)			

This material is reserved for educational use only, not allowed for commercial use.
Forbidden to modify the content, and cite the document when use.

	Day 30	Day 60	Day 90	Day 120
Positive control	0.00[b]	0.00[b]	0.00[b]	0.00[b]
Metalaxyl	3.33[b]	6.25[b]	7.19[b]	3.33[b]
Ch. lucknowense	4.16[b]	8.30[b]	9.58[b]	6.67[b]
T. hamatum	0.83[b]	2.50[b]	3.30[b]	2.50[b]
Nano-CL	0.41[b]	1.25[b]	2.50[b]	1.25[b]
Nano-TK01	0.00[b]	0.42[b]	1.25[b]	0.84[b]
Negative control	9.98[a]	44.58[a]	82.50[a]	98.30[a]
CV%	192.73	89.86	61.50	18.83

Treatments	Assessment of disease reduction (DR%)			
	Day 30	Day 60	Day 90	Day 120
Positive control	100[a]	100[a]	100[a]	100a
Metalaxyl	83.33[a]	82.14[a]	90.76[a]	96.67[a]
Ch. lucknowense	68.75[a]	83.35[a]	86.35[a]	93.30[a]
T. hamatum	93.75[a]	94.43[a]	95.22[a]	97.50[a]
Nano-CL	96.88[a]	98.07[a]	97.27[a]	98.72[a]
Nano-TK01	100[a]	98.21[a]	98.69[a]	99.13[a]
Negative control	-	-	-	-
CV%	32.15	13.23	6.51	3.26

Treatment means followed by the same letters are not significantly different at $p<0.05$.

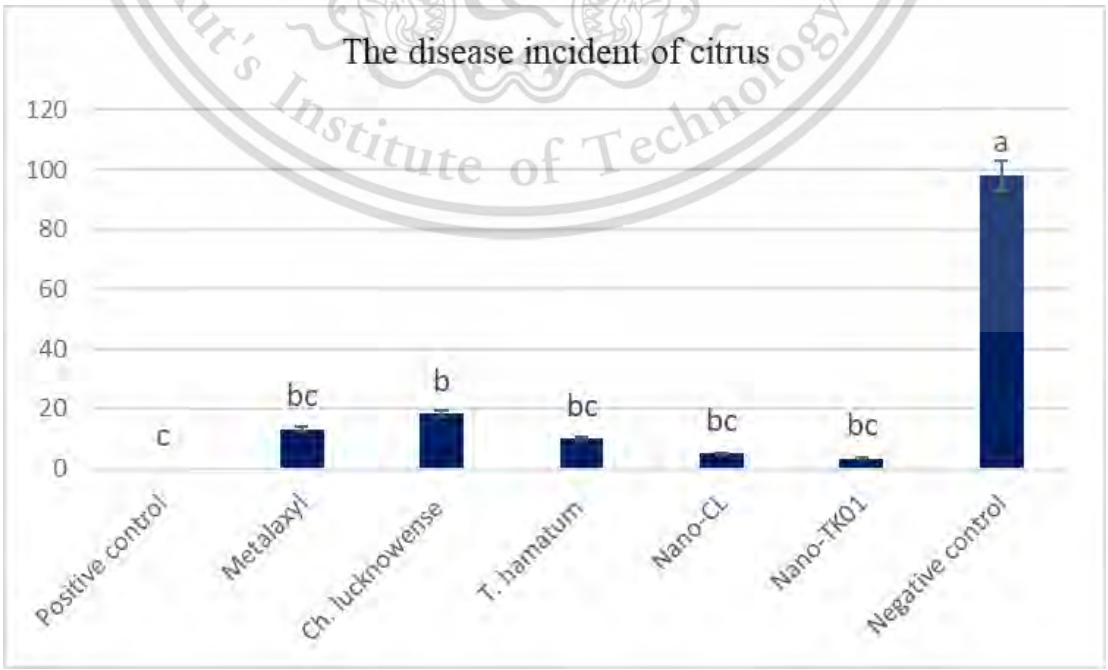

This material is reserved for educational use only, not allowed for commercial use.
Forbidden to modify the content, and cite the document when use.

Figure 4.52 The disease incident of citrus on day 120 after fungal inoculation and treatment

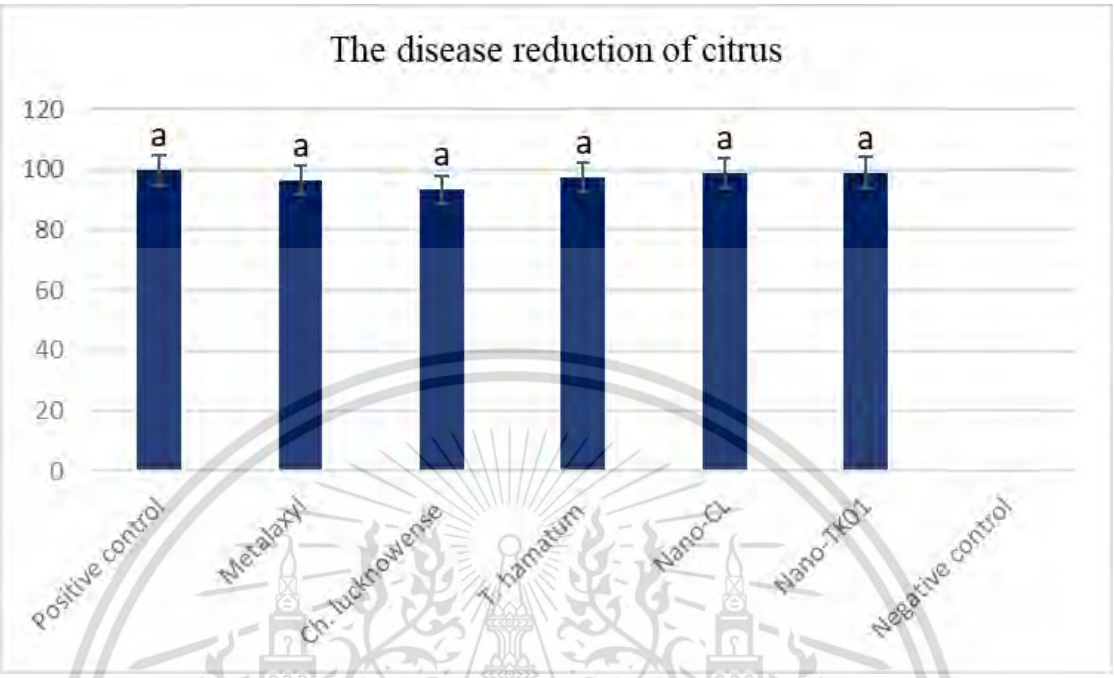

Figure 4.53 The disease reduction of citrus on day 120 after fungal inoculation and treatment

4.7.2 Phytoalexins production

4.7.2.1 Phytoalexins production of durian

Durian plants were examined for phytoalexin production after fungal inoculation, treated with bioproducts and metalaxyl, and compared to positive and negative control on days 3, 5, 7, 14, and 21. The durian leaves from each treatment were extracted by methanol and then evaporated to produce a crude methanol extract, as shown in Figure 41. Each crude extract was spotted on a TLC plate. The result revealed that the phytoalexin was detected on day 21 as the spots on the TLC plates. The R_f value was computed at 0.77 in 12% acetic acid, known as scopoletin, which is considered systemic resistance of the plants against pathogens. Among these, treatment nano-TK01 from *T. hamatum* K01 and nano-CL from *Ch. lucknowense* CL showed the most apparent spots compared to standard scopoletin. However, treatments of metalaxyl, *T. hamatum* K01, *Ch. lucknowense* CL products, and negative control also showed the presence of spots on TLC plates, while positive control did not show spots on TLC plates, as shown in (Figures 4.54 and 4.55).

This material is reserved for educational use only, not allowed for commercial use.
Forbidden to modify the content, and cite the document when use.

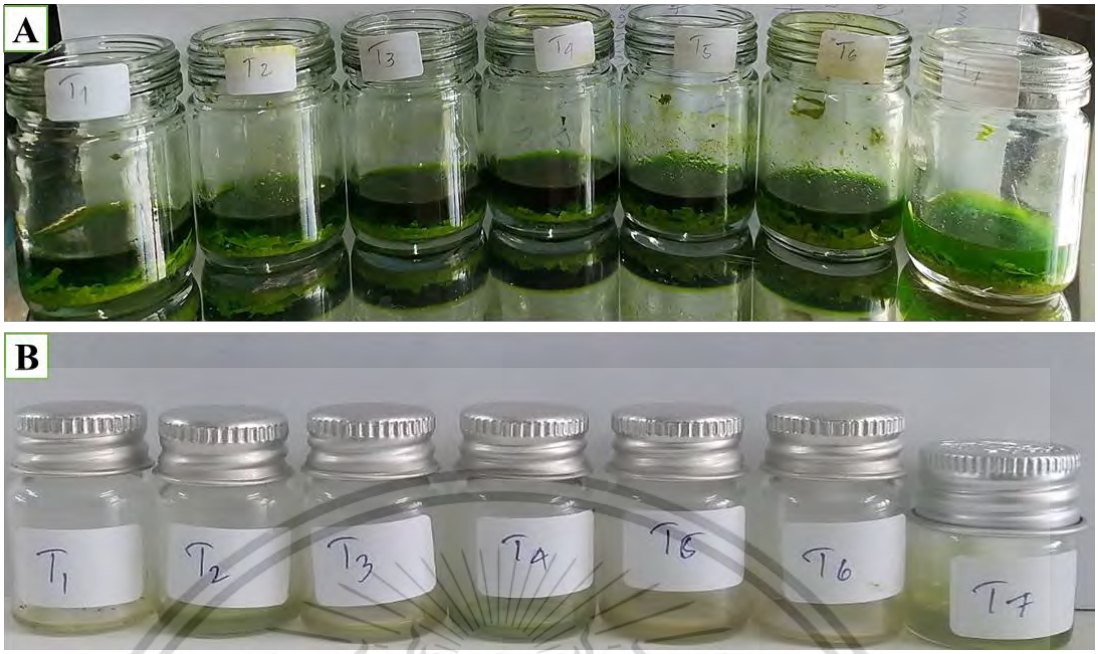

Figure 4.54 Extraction leaves of durian for phytoalexin production; A, durian leaves extracted by methanol from each treatment; B, crude extract of durian from each treatment

Figure 4.55 The phytoalexin production was induced by durian, S-standard scopoletin, T1-positive control, T2-metalaxyl, T3-*Ch. lucknowense* CL product, T4-*T. hamatum* K01 product, T5-nano-CL from *Ch. lucknowense* CL, T6-nano-TK01 from *T. hamatum* K01 and T7-negative control

This material is reserved for educational use only, not allowed for commercial use.
Forbidden to modify the content, and cite the document when use.

4.7.2.2 Phytoalexins production of citrus

After fungal inoculation and treatment, phytoalexin production in citrus was examined on day 3. Citrus leaves from each treatment were extracted with sterilized distilled water and ethyl acetate, then evaporated using a rotary vacuum evaporator to yield crude extracts. Each crude extract was spotted on a TLC plate. The results indicated the detection of phytoalexin, visible as blue spots on the TLC plate under UV light at 254 nm, with an R_f value computed at 0.58 in toluene:ethyl acetate (1:1). Among these spots, the nano-TK01 treatment from *T. hamatum* K01 and nano-CL from *Ch. lucknowense* CL showed the most apparent spots on the TLC plate compared to all other treatments. However, there was no detection of spots on the TLC plate from the positive control (Figures 4.56 and 4.57).

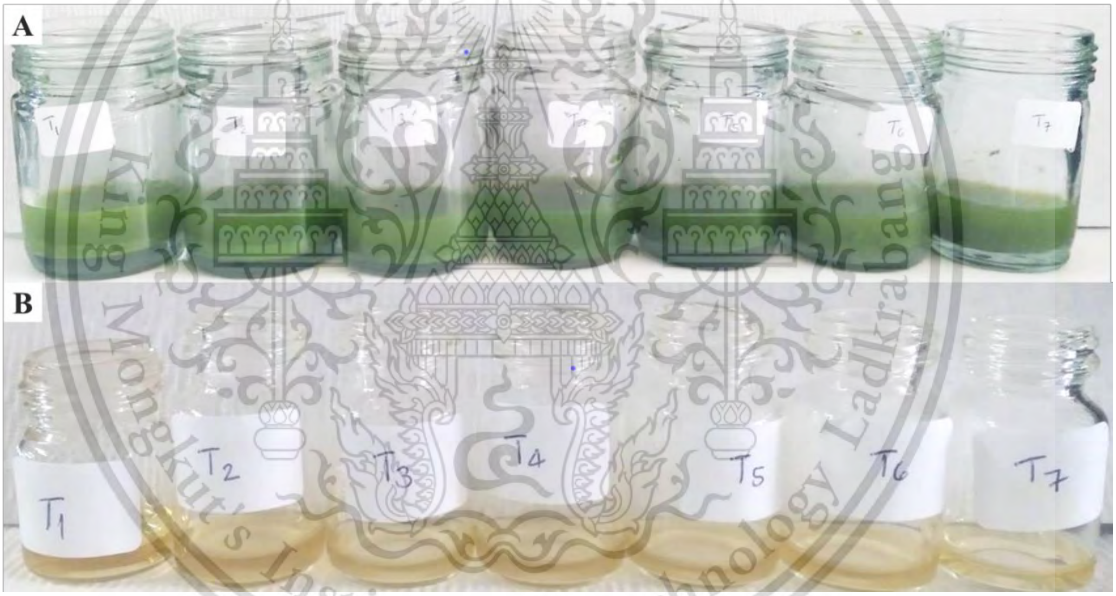

Figure 4.56 Extraction leaves of citrus for phytoalexin production by toluene: ethyl acetate (1:1); A, citrus leaves from each treatment extracted by sterilized distill water; B, crude ethyl acetate extract of citrus leaves from each treatments

This material is reserved for educational use only, not allowed for commercial use.
Forbidden to modify the content, and cite the document when use.

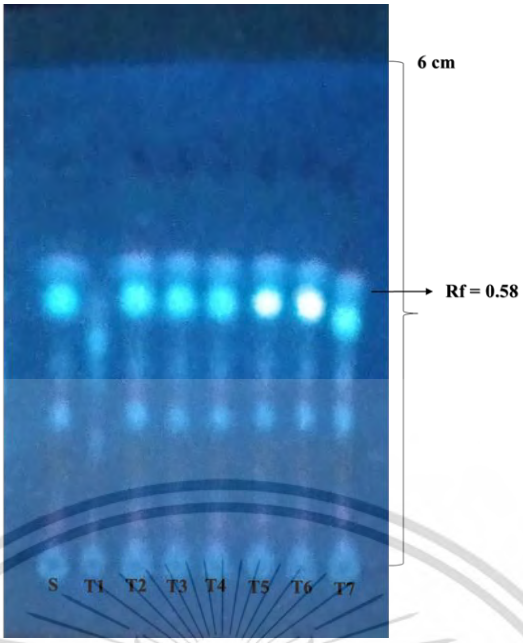

Figure 4.57 The phytoalexin production was induced by citrus, S-standard scoparone, T1-positive control, T2-metalaxyl, T3-*Ch. lucknowense* CL product, T4-*T. hamatum* K01 product, T5-nano-CL from *Ch. lucknowense* CL, T6-nano-TK01 from *T. hamatum* K01 and T7-negative control

4.7.3 Assessment of growth parameters

4.7.3.1 Plant growth parameters of durian

The plant growth parameters of durian, regarding plant height were assessed before and after co-inoculation with *P. palmivora* and *C. gloeosporioides*, the causal agents of durian rot and durian anthracnose disease. At 24 hours after fungal inoculation, durian plants were treated with agricultural inputs, including chemical metalaxyl, products from *Ch. lucknowense* and *T. hamatum* K01, and nanofibers from *Ch. lucknowense* CL and *T. hamatum* K01, in comparison to positive and negative controls. In table 4.25 showed that the plant height of durian before and day 30 after fungal inoculation and treatment were not significantly different for all treatments. However, 120 days after treatment, the lowest plant height was recorded with negative control 72 cm, while the most effective treatment was observed in nanofiber from *T. hamatum* K01 treatment 82 cm, as shown in Figure 4.58-4.62.

This material is reserved for educational use only, not allowed for commercial use.
Forbidden to modify the content, and cite the document when use.

Table 4.25 Plant height of durian was assessed before treatment and after treatment

Methods	Plant height parameter of durian (cm)				
	Before treatment	After treatment			
		Day 30	Day 60	Day 90	Day 120
Positive control	67.00[a]	69.00[a]	71.20[a]	72.00[a]	72.00[b]
Metalaxyl	70.00[a]	71.25[a]	71.80[a]	75.25[a]	76.00[ab]
Ch. lucknowense	69.25[a]	71.75[a]	72.25[a]	73.50[a]	74.00[ab]
T. hamatum	69.70[a]	72.25[a]	74.74[a]	75.75[a]	76.75[ab]
Nano-CL	69.80[a]	71.00[a]	74.50[a]	80.25[a]	81.00[ab]
Nano-TK01	71.50[a]	75.50[a]	75.80[a]	81.00[a]	82.00[a]
Negative control	71.00[a]	70.00[a]	59.75[b]	53.20[b]	53.25[c]
CV%	6.99	6.38	6.20	5.52	5.39

Treatment means followed by the same letter are not significantly different at $p<0.05$.

Figure 4.58 Durian plants from the pots experiment were measured before fungal inoculation and treatment

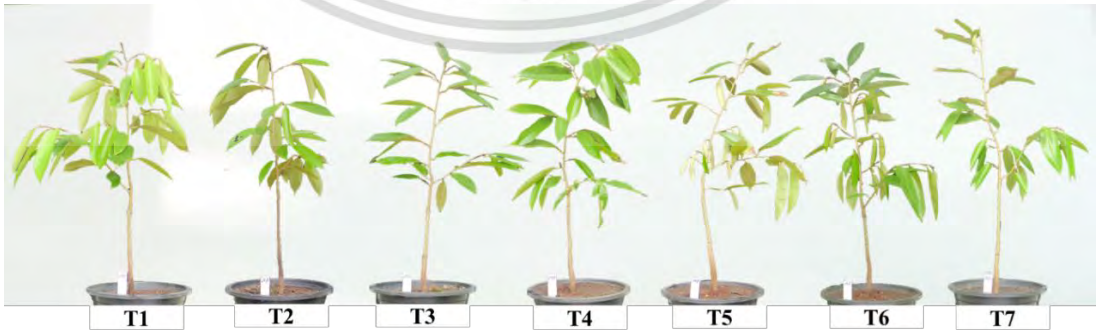

Figure 4.59 Durian plants from the pots experiment were measured 30 days after fungal inoculation and treatment

This material is reserved for educational use only, not allowed for commercial use.
Forbidden to modify the content, and cite the document when use.

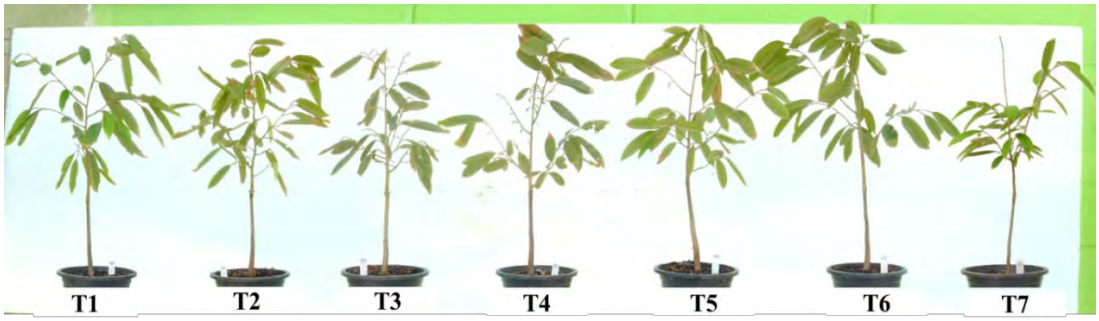

Figure 4.60 Durian plants from the pots experiment were measured on day 60 after fungal inoculation and treatment

Figure 4.61 Durian plants from the pots experiment were measured on day 120 after fungal inoculation and treatment

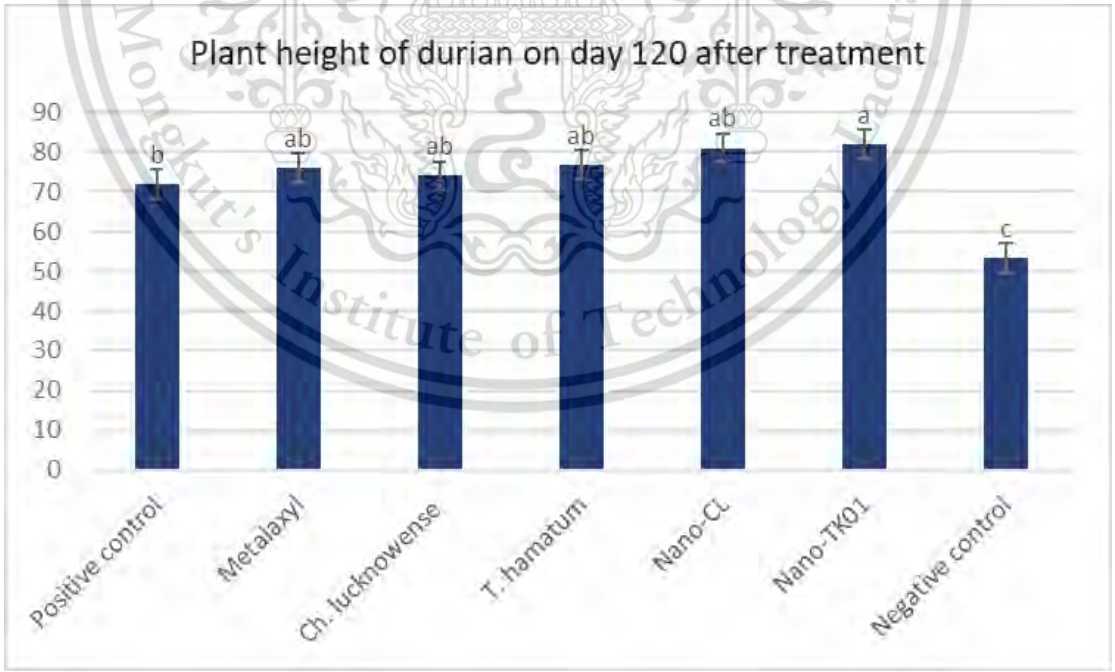

Figure 4.62 The effect of bioproducts and metalaxyl compared to positive and negative control on the growth of durian plants

This material is reserved for educational use only, not allowed for commercial use.
Forbidden to modify the content, and cite the document when use.

4.7.3.2 Plant growth parameter of citrus

The growth parameters of citrus, regarding plant height, were measured before and after fungal inoculation of *C. gloeosporioides* C02, is known a causal agent of citrus anthracnose and Treatment of agricultural inputs, including chemical metalaxyl, products of *Ch. lucknowense* Cl and *T. hamatum* K01, and nanofiber from *Ch. lucknowense* CL and *T. hamatum* K01 compared to positive and negative control. The result indicated that plant height was not significantly different on days 30 and 60 after fungal inoculation and treatment. However, on day 120, after fungal inoculation and treatment, the highest plant height was observed from the treatment of nanofiber from *T. hamatum* K01 76.50 cm, compared to the negative control 51.73 cm as shown in Table 4.26, Figures 4.63-4.68.

Table 4.26 Assessment of plant growth of citrus before and after fungal inoculation and treatment

Methods	Plant height parameter of citrus (cm)				
	Before treatment	After treatment			
		Day 30	Day 60	Day 90	Day 120
Positive control	64.75[a]	70.70[a]	71.00[a]	72.75[a]	73.25[a]
Metalaxyl	65.25[a]	67.00[a]	68.25[a]	69.50[a]	70.75[a]
Ch. lucknowense	64.25[a]	67.75[a]	70.00[a]	71.00[a]	71.50[a]
T. hamatum	64.00[a]	68.75[a]	71.30[a]	74.25[a]	75.25[a]
Nano-CL	63.70[a]	66.50[a]	71.00[a]	73.30[a]	75.30[a]
Nano-TK01	62.50[a]	67.00[a]	70.13[a]	74.50[a]	76.50[a]
Negative control	64.70[a]	63.75[a]	60.30[a]	51.75[b]	51.75[b]
CV%	3.14	8.17	7.58	8.38	7.40

Treatment means followed by the same letter are not significantly different at $p<0.05$.

This material is reserved for educational use only, not allowed for commercial use.
Forbidden to modify the content, and cite the document when use.

Figure 4.63 Citrus plants from the pots experiment were measured before fungal inoculation and treatment

Figure 4.64 Citrus plants from the pots experiment were measured on day 30 after fungal inoculation and treatment

Figure 4.65 Citrus plants from the pots experiment were measured on day 60 after fungal inoculation and treatment

This material is reserved for educational use only, not allowed for commercial use.
Forbidden to modify the content, and cite the document when use.

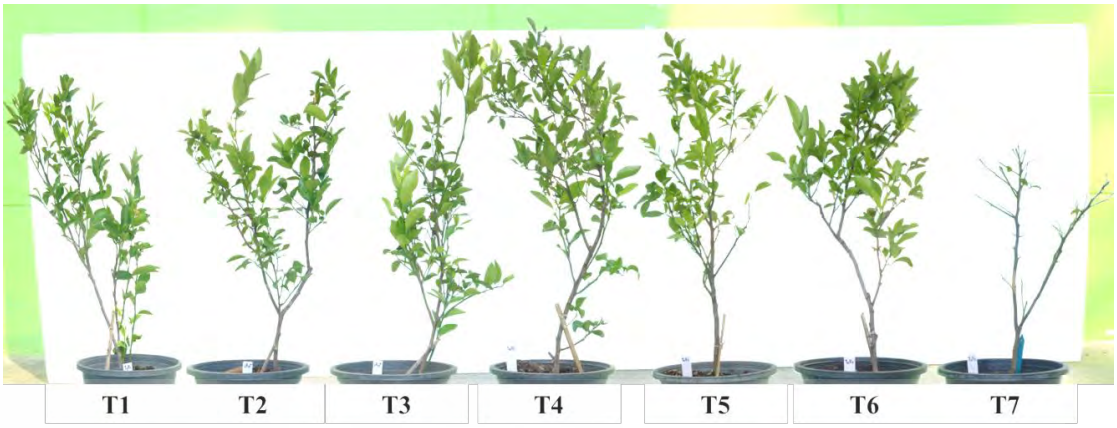

Figure 4.66 Citrus plants from the pots experiment were measured on day 90 after fungal inoculation and treatment

Figure 4.67 Citrus plants from the pots experiment were measured on day 120 after fungal inoculation and treatment

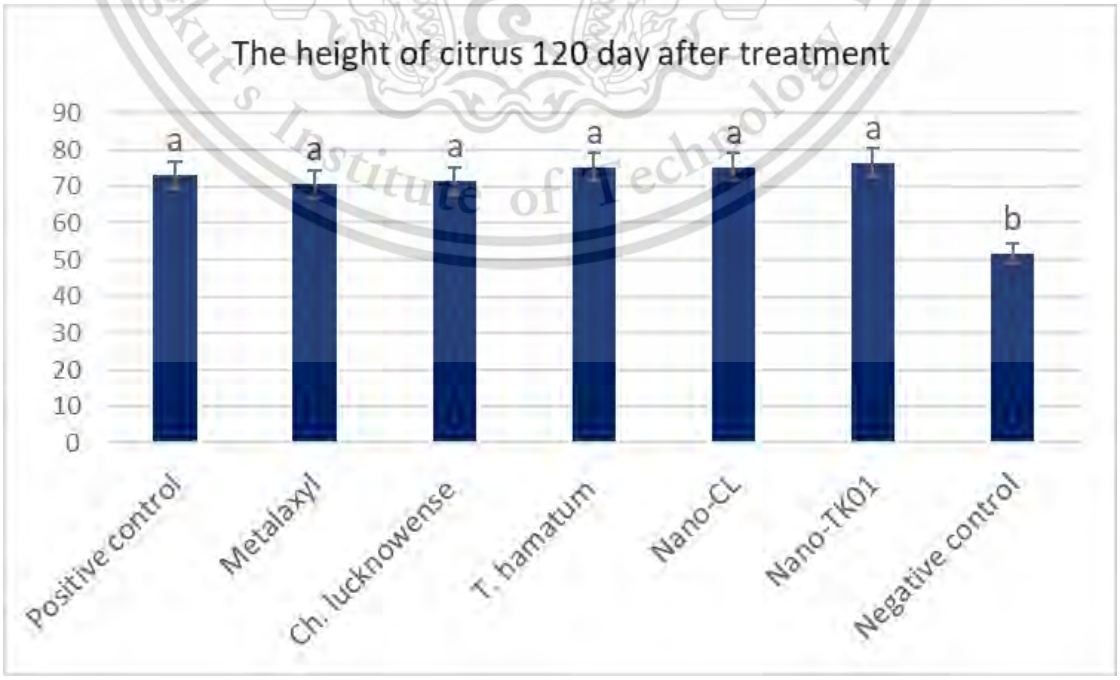

This material is reserved for educational use only, not allowed for commercial use.
Forbidden to modify the content, and cite the document when use.

Figure 4.68 The plant height of citrus was measured on days 120 after treatment

4.7.4 Plant physiological parameters

4.7.4.1 Photosynthesis pigment of durian

Photosynthesis pigment of durian regarding total chlorophyll and carotenoid contents were examined 90 days after treatment. The result indicated that nanofiber from *T. hamatum* K01 was the most effective treatment on photosynthetic pigments, in which chlorophyll and carotenoid contents were computed 25.98 and 3.70 µg/g, respectively. However, All treatments significantly increased photosynthesis pigments compared to the negative control, which was recorded to have a lesser effect on total chlorophyll and carotenoid contents 8.07 and 1.65 µg/g, respectively, as shown in Table 4.27., Figures 4.69 and 4.70.

Table 4.27 The chlorophyll and carotenoid contents of durian were examined on day 90 after treatment

Treatments	Photosynthetic pigment (µg/g)			
	Chlorophyll a	Chlorophyll b	Total chlorophyll	Carotenoid
Positive control	14.04^{a}	5.99^{a}	22.36^{a}	1.69^{b}
Metalaxyl	12.13^{ab}	4.16^{ab}	16.30^{ab}	2.15^{ab}
Ch. lucknowense	14.37^{a}	7.31^{a}	21.68^{a}	1.29^{b}
T. hamatum	15.06^{a}	5.05^{ab}	20.12^{a}	2.93^{ab}
Nano-CL	14.92^{a}	4.94^{ab}	20.07^{a}	3.01^{ab}
Nano-TK01	18.84^{a}	7.14^{a}	25.98^{a}	3.70^{a}
Negative control	5.49^{a}	2.57^{ab}	8.07^{b}	1.65^{ab}
CV%	21.99	21.41	20.12	29.63

Treatment means, followed by the same letters are not significantly different at $p<0.05$.

This material is reserved for educational use only, not allowed for commercial use.
Forbidden to modify the content, and cite the document when use.

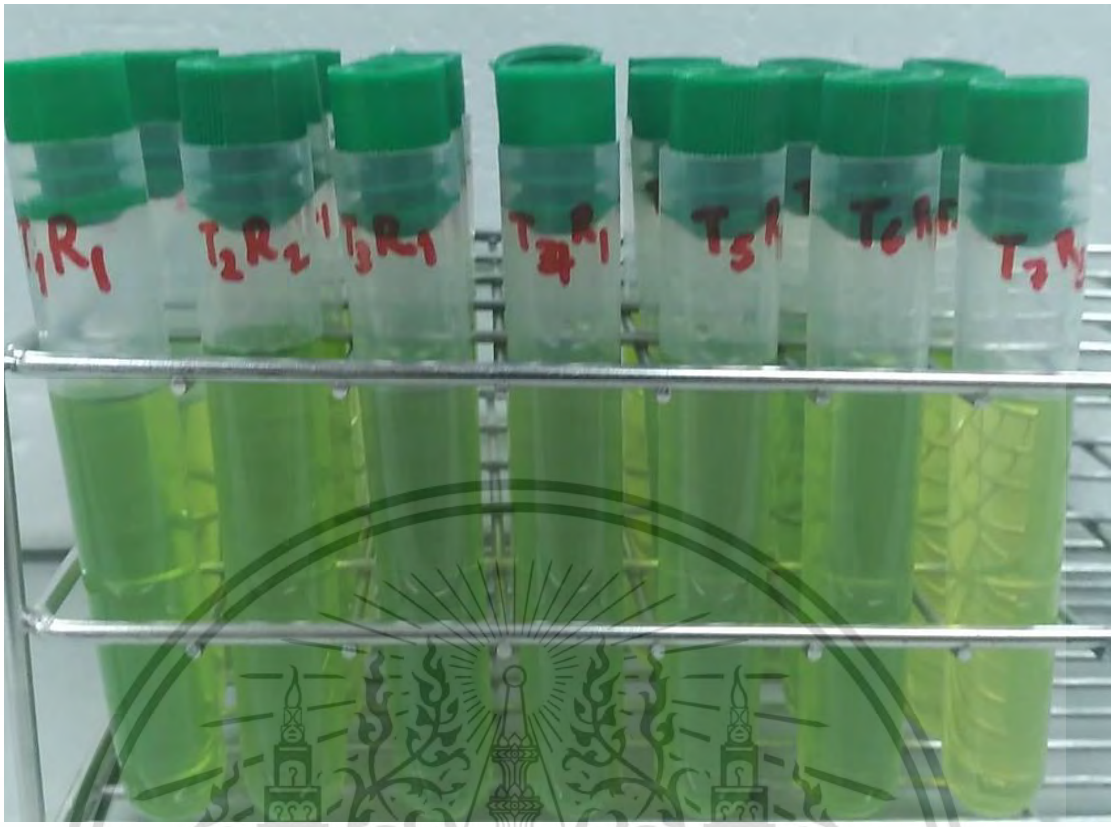

Figure 4.69 Each treatment's solution of durian leaves was extracted by 20 mL of 80% acetone for photosynthetic pigments

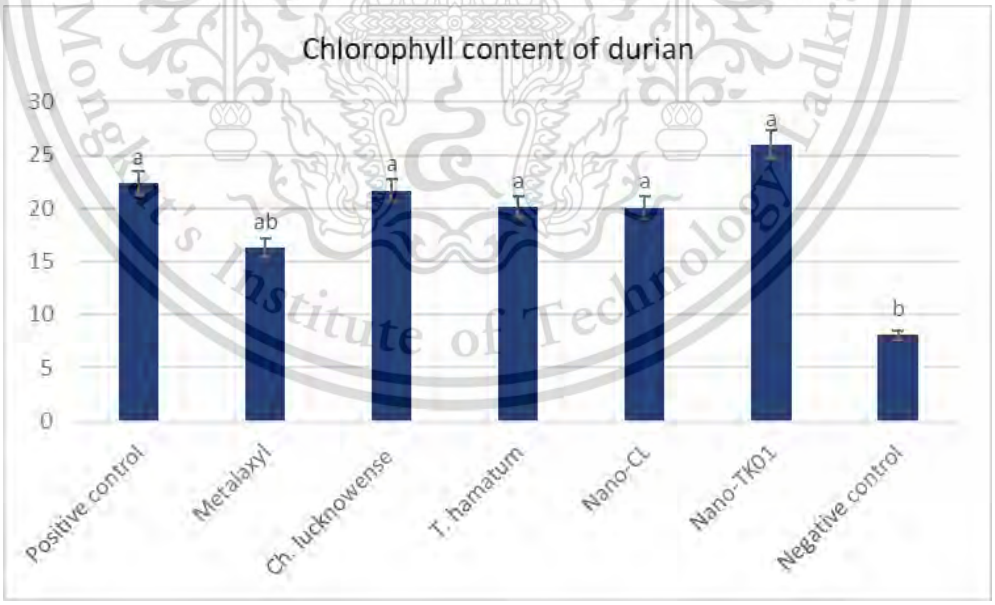

Figure 4.70 The Chlorophyll content of durian was measured on day 120 after fungal inoculation and treatment

This material is reserved for educational use only, not allowed for commercial use.
Forbidden to modify the content, and cite the document when use.

4.7.4.2 Photosynthesis pigments of citrus

Photosynthesis pigments, including chlorophyll and carotenoid contents of citrus plant from pots experiment, were examined on day 90 after fungal inoculation and treatment of nanofibers from *T.hamtum* K01, nanofiber from *Ch. lucknowense* CL, *T. hamatum* K01's product, *Ch. lucknowense* CL's product, and chemical metalaxyl compared to positive and negative control. The results showed that the highest chlorophyll and carotenoid contents were recorded in nanofiber from *T. hamatum* K01 's treatment, which were measured 15.98 µg/g and 0.78µg/g, followed by the positive control 14.36 µg/g and 1.12 µg/g, while the lowest chlorophyll and carotenoid contents were from negative control 6.13 µg/g and 0.16 µg/g, respectively Table 4.28., Figures 4.71 and 4.72.

Table 4.28 The chlorophyll and carotenoid contents of citrus leaves were examined on day 90 after treatment

Treatments	Photosynthetic pigment (µg/g)			
	Chlorophyll a	Chlorophyll b	Total chlorophyll	Carotenoid
Positive control	6.67^{a}	7.69^{a}	14.36^{a}	1.12^{a}
Metalaxyl	4.47^{ab}	4.24^{a}	9.13^{ab}	0.59^{a}
Ch. lucknowense	583^{ab}	3.70^{a}	9.58^{ab}	0.65^{a}
T. hamatum	6.12^{ab}	385^{a}	9.98^{ab}	1.18^{a}
Nano-CL	6.48^{a}	4.56^{a}	11.05^{ab}	1.06^{a}
Nano-TK01	7.83^{a}	8.15^{a}	15.98^{a}	0.78^{a}
Negative control	3.08^{b}	3.23^{a}	6.13^{b}	0.16^{a}
CV%	19.41	43.76	22.93	65.39

Treatment means, followed by the same letter, is not significantly different at $p<0.05$.

This material is reserved for educational use only, not allowed for commercial use.
Forbidden to modify the content, and cite the document when use.

Figure 4.71 Each treatment's solution of citrus leaves was extracted by 10 mL of 80% acetone for photosynthetic pigments

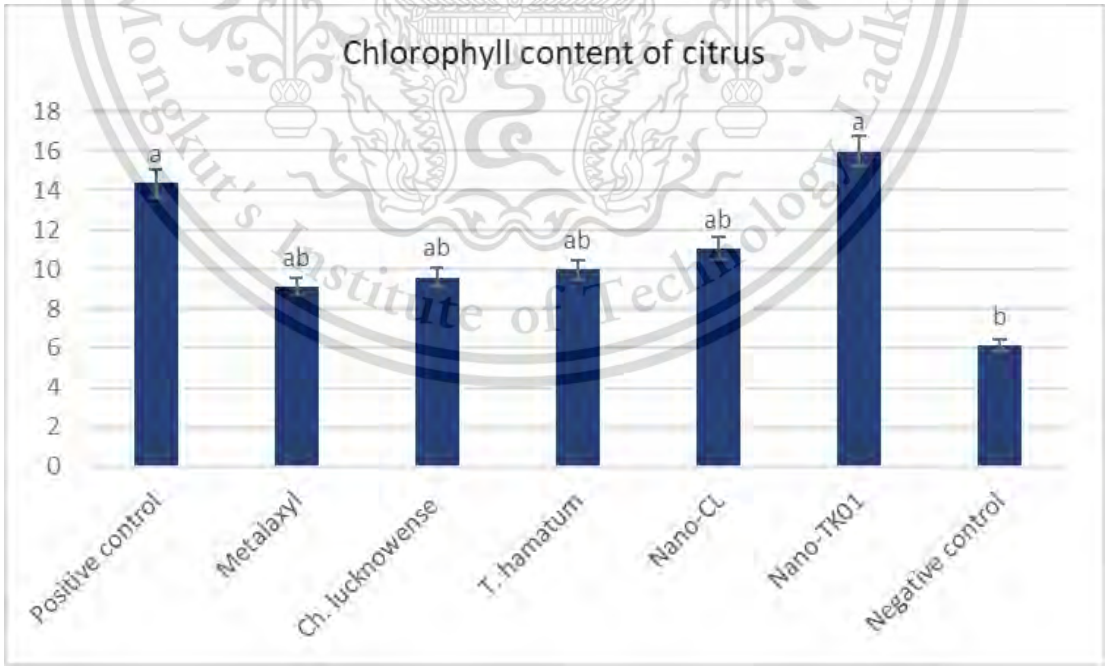

Figure 4.72 Chlorophyll content of citrus was measured on day 120 after fungal inoculation and treatment

This material is reserved for educational use only, not allowed for commercial use.
Forbidden to modify the content, and cite the document when use.

CHAPTER 5

DISCUSSION

The tested pathogens were isolated from the host plant, durian, and citrus. *C. gloeosporioides* C01 was obtained from the anthracnose disease of citrus. Morphological characterization showed that *C. gloeosporioide*s produces septate mycelia that are hyaline, one-cell conidium, ovoid, and slightly carved. These characteristics are similar to the reports of Ajay Kumar (2014), who also characterized *C. gloeosporioide*s. Meanwhile, molecular identification results showed that *C. gloeosporioides* C01, the pathogenic isolate, was closely related to the clade of *C. gloeosporioides* with GenBank accession numbers KM519999, KY033215, MT993622, HQ264182, and MT919170. KY930619 was compared as the outgroup, similar to Hassan *et al.* (2018)' s finding. The pathogenicity test proved *C. gloeosporioides* to be the causal agent of citrus anthracnose disease. Similarly, Wang *et al.* (2021b) found that *C. gloeosporioides* is a causal agent of citrus anthracnose.

C. gloeosporioides isolate C02 was obtained from anthracnose lesions of durian leaves. The observation of morphological characteristics was also similar to the work of Freeman *et al.* (2007). Furthermore, the rDNA-ITS sequence analysis revealed that isolate C02-ITS1 common ancestors with GenBank accession numbers KJ777830, MT729939, KJ777825, KF697685, MZ021314, CBS112999, and HQ264183. LC684558 was being compared as an outgroup. This study corresponded with the report of (Bhunjun *et al.*, 2021); Chithra *et al.* (2014). This isolate was proven to be pathogenic, as confirmed by Koch's postulate, which was confirmed by the study of Alahakoon *et al.* (1994).

Phytophthora root rot was the most severe disease for durian plantations in Thailand and other Southeast Asian countries. *P. palmivora* PYSC01 was obtained from the root zone of durian infected by root rot disease. The external characteristics observed that *P. palmivora* PYSC01 produced a different shape of sporangia with one papilla, branched hyphae, and globose chlamydospore, which was similar to the report by Suksiri *et al.* (2018). The results of molecular characterization indicated that the isolated PYSC01 common ancestors GenBank accession number HQ237479, MH219857, MH219852L, C688458, LC684540, GU111683, and

This material is reserved for educational use only, not allowed for commercial use.
Forbidden to modify the content, and cite the document when use.

KP050545. EF025942 as the outgroup, similar to the one reported by Tongon and Soytong (2021). It was proved to be an aggressive pathogen causing the root rot of durian using Koch's. This is similar to the study of (Thongkham *et al.*, 2017a); Tongon *et al.* (2018); (Vawdrey *et al.*, 2005), who reported that *P. palmivora* is a causal agent of durian rot.

Antagonistic fungi, *Ch. lucknowense* CL was observed colony appearance, color, hairs, shape, and size also confirmed by the study of Ruppavalli *et al.* (2019). rDNA-ITS sequence analysis showed that *Ch. lucknowense* CL-ITS1 is closely related to accession numbers MH080360, JX280827, MH860312, and MT186188. MZ799225 was being compared as an outgroup, which the database supported by the 100% bootstrap value. This study was similar to the one reported by Song *et al.* (2020).

T. hamatum K01 was confirmed at the species level based on morphological characteristics and molecular phylogeny. The general structures of *T. hamatum* K01 were confirmed by the study of Mao *et al.* (2020). For molecular phylogeny, *T. hamatum* K01 was closed, related to the sequences of *T. hamatum* with GenBank accession numbers AB737864, MW750434, OL439486, MW763159, MN880214, KX424842. Furthermore, identification was recorded with a 100% bootstrap value constructed after the distance-based analysis of the universal primer ITS1, ITS4, and 5.8S region of the rDNA, consistent with the study of Abdelkhalek *et al.* (2022).

Trichoderma species were reported to produce cell wall degrading enzymes (β-1, 3 glucanases, chitinases, proteases, and β-1,4 glucanases) (Baazeem *et al.*, 2021; Rajani *et al.*, 2021). Antifungal activities of *T. hamatum* K01 have also proved to antagonize against pathogenic fungi, *C. gloeosporioides* C01, and *P. palmivora* PYSC01 causing, anthracnose disease and durian rot respectively, in the dual culture assay, *T. hamatum* K01 significantly inhibited colony growth ranging from 48% to 77% and reduced sporulation ranging from 64% to 92%. Such findings confirmed with Khonglah and Kayang (2018) found that *T. hamatum* could inhibit the colony growth of *Botrytis cineria* by 63.77%. This might be because *T. hamatum* K01 released the secretion of lytic enzymes to degrade the pathogens' mycelia growth and cell wall, which was proved by causing abnormal colony growth and sporulation of test pathogens. Our study was similar to the obtained by Osorio-Hernández *et al.*

This material is reserved for educational use only, not allowed for commercial use.
Forbidden to modify the content, and cite the document when use.

(2011), which revealed that volatile compounds produced from *T. hamatum* T25 exhibited a high antagonist level against *P. capsici,* causing leaf blight of pepper, which the colony growth was inhibited by 48.8%. Similarly, Andrade-Hoyos *et al.* (2020) found that *T. hamatum* strain T-A12 expressed fungal activity against the colony growth of *P. cinnamomi* strain CPO-CPU, causing root rot disease Avocado by 50.99%. Khatri *et al.* (2017) confirmed that lytic enzyme (protease) produced from *T. hamatum* exhibited strong antifungal activity against radial growth of *Aspergillus niger, F. oxysporum*, and *Sclerotium rolfsii*. In addition, several authors have also reported the antagonistic potential of Trichoderma species in controlling plant pathogenic fungi (Hoitink *et al.*, 2006; Khan *et al.*, 2004). Other biological control agent species (i.e., *Emericella nidulans*) reported by Talubnak and Soytong (2010) were also found to inhibit colony growth and conidia production of *C. gloeosporioides* causing anthracnose of *Vanilla planifolia* by 49.44% and 75.31% respectively.

Chaetomium spp. has been reported for its control mechanism, including mycoparasitism, clear zone and nutrient competition, and antibiosis against pathogenic fungi (Madbouly & Abdel-Wareth, 2020). In this study, *Ch. lucknowense* CL effectively controlled *C. gloeosporioides* C02 and *P. palmivora* PYSC01 in a dual culture test. It was more effective in inhibiting sporulation, ranging from 60% to 94 %, than its affected colony growth, from 48% to 52%. This finding was similar to the study of Phung *et al.* (2014), who reported that *Ch. lucknowense* CL was able to suppress colony growth of *C. gloeosporioides* by 34.86% and conidia production by 60.54%, showing its control mechanisms against Pomelo anthracnose and also inhibited spore production of *P. aphanidermatum* PY. S02 causal agent of pomelo root rot by 86.41%. *Ch. lucknowense* CL also shows parasitic activity against other plant diseases. For instance, control mechanisms were expressed by *Ch. lucknowense* CL01 in suppressing the colony growth by 52.5% of *P. nicotianae* KA1, a causal agent of citrus rot disease (Hung *et al.*, 2015). Similarly, Phung *et al.* (2015b) indicated that *Ch. lucknowense* CL showed antifungal activity against *P. palmivora* PHY02, causing root rot of pomelo, resulting in inhibition of the colony growth and mycelia formation by 59.2% and 97.5%, respectively. It was likely to release lytic enzymes in PDA media to inhibit the mycelia growth, which is usually produced by *Chaetomium* species (Longoni *et*

This material is reserved for educational use only, not allowed for commercial use.
Forbidden to modify the content, and cite the document when use.

al., 2012; Phong *et al.*, 2015), which was confirmed by several authors who have also reported the biocontrol potential of *Chaetomium* spp. to control plant pathogens (Phong *et al.*, 2015; Song *et al.*, 2017). Other species of *Chaetomium* have also been reported to control *C. gloeosporioides* and *P. palmivora*. A study by Somdej *et al.* (2018) showed that *Ch. cupreum* CC3003 can control *C. gloeosporioides*, also known as a causal agent of anthracnose disease of coffee var. Arabica in Laos. Their study reduced conidia production by 42.60 % within 30 days. Soytong (2010) revealed that the antagonistic activity of *Ch. globosum* implicated the control mechanism on the radial growth of *P. palmivora*, the causal pathogen of durian root rot var. Chanee by 63.33%. Tongon and Soytong (2021) cited that the biological agent of *Ch. cochliodes* CTh02 significantly suppressed the mycelia growth 61.11% and sporangia formation 68.55% of *P. palmivora* RT01, causing durian root rot.

T. hamatum exerted several modes of activity, mainly mycoparasitism through cell wall degrading enzymes such as glycoside hydrolases and chitinases, *N*-acetyl-β-D-glycosaminidases, and β-1,3-glucanases, which play an essential role in degrading carbohydrates of the pathogenic microorganism (Studholme *et al.*, 2013). The difference between crude extract produces a variety of bioactive compounds with various fungal activity and molecular weights, resulting in variations of efficacy (Charoenporn *et al.*, 2010; Phal *et al.*, 2021), which can be illustrated by the difference in crude extract in variation response against plant pathogens. Crude metabolites extracted from *T. hamatum* K01 effectively inhibited the growth of *C. gloeosporioides,* causing anthracnose disease, and *P. palmivora,* causing durian rot. This study indicated that crude TK01-MeOH from *T. hamatum* K01 showed the highest inhibitory effect against the growth of test pathogens, in which the colony growth was inhibited at ED_{50} values ranging from 373 to 288 ppm. Sporulation was inhibited at ED_{50} values ranging from 375 to 118 ppm, followed by crude TK01-EtOAc, which expressed a better effect, in which sporulation was inhibited at ED_{50} values 607 to 185. Colony growth inhibition required more than 1000 ppm, while crude TK01-Hexane recorded the lesser effect, in which ED_{50} values were computed more than 1000 ppm in both colony growth and sporulation suppression. This was confirmed by a previous report by Kaewchai and Soytong (2010) found that metabolite crude methanol from *T. hamatum* STN07 exert the best potential activities in the host plant directly by the production of the bioactive compound to suppress

This material is reserved for educational use only, not allowed for commercial use.
Forbidden to modify the content, and cite the document when use.

Rigidoporus microporus causal agent of rubber white root disease, which the colony growth was inhibited by 80% at 500 µg/mL concentration with the ED_{50} values of 187 µg/mL, while crude hexane extract gave the least effective. Similarly, the biological control agent *T. hamatum* THSW13 was reported to suppress the growth of *P. capsici* causing damping-off collar rot pathogen of chili pepper seedlings by 61% (Chemeltorit *et al.*, 2017). This study agrees with the previous report by Khan *et al.* (2004), which indicated that *T. hamatum* 382 significantly inhibited the population growth of *P. capsici,* causing crown rot and leaf blight disease in cucumbers. The previous study also reports antifungal activities of the same ethyl acetate crude extract derived from *T. hamatum* PC02, which inhibited conidia production of *C. gloeosporioides* by 67.73% (Kasem *et al.*, 2005). Sour *et al.* (2015) found that crude hexane, ethyl acetate, and methanol derived from *Ch. cupreum* expressed fungal activity against *C. gloeosporioides* pathogen causing anthracnose disease on orchids. Their study inhibited conidia production by 51.35%, 51.27%, and 58.65% at 1000 µg/mL concentrations, yielding ED_{50} values of 794, 624, and 879 µg/mL, respectively. Additionally, *Trichoderma* species have been successfully reported as biological control agents due to cell wall degrading enzyme production, fast growth organisms, competition for clear zone and nutrients, tolerance or resistance to metalaxyl fungicide, and significant aggressiveness toward pathogenic microorganisms (Benitez *et al.*, 2004).

Metabolite crude extracts derived from *Ch. lucknowense* CL are an effective and potential biological control agent against durian anthracnose disease caused by *C. gloeosporioides* C02 and root rot disease caused by *P. palmivora*, as shown by its inhibitory effect from crude CL-EtOAc from *Ch. lucknowense* CL was significantly inhibited colony growth and sporulation at the ED_{50} values ranging from 618 to 95 ppm, and 37 to 13 ppm respectively. However, crude CL-Hexane gave a better result for inhibition than crude CL-MeOH. This study was supported by the report of Song *et al.* (2020), who found that crude ethyl acetate from *Ch. lucknowense* exhibited a strong inhibitory effect on conidia production of *M. oryzae* causing rice blast pathogens which the ED_{50} values required only 57 ppm, in comparison to crude hexane and methanol were required a higher ED_{50} values for inhibition by 103 and 422 ppm respectively. A previous study by Phong *et al.* (2016) found that crude ethyl acetate from *Ch. lucknowense* CL01 strains showed the best

This material is reserved for educational use only, not allowed for commercial use.
Forbidden to modify the content, and cite the document when use.

inhibitory effects against Fusarium wilt of tea caused by *F. oxysporum*, suppressing conidia germination at the ED_{50} values by 62.17 µg/ml, followed by crude hexane gave the better inhibitive efficiency on conidia production at the ED_{50} values of 151.78 µg/ml, while, crude methanol gave the most negligible effect on conidia production at the ED_{50} of 174.57 µg/ml. Moreover, a review by Phong *et al.* (2014) revealed that metabolite crude ethyl acetate extracted from *Ch. lucknowense* exhibited strong antifungal effects on spore production of *Pestalotia* spp. are known as a causal agent of grey blight disease of tea with an inhibition rate of 81.08% at the ED_{50} value of 86.99 µg/ml. Similarly, Phung *et al.* (2015b) demonstrated that crude extracts from *Ch. lucknowense* CL01 expressed vigorous antifungal activity toward *P. palmivora* PHY02 causal agent of pomelo root rot, while crude ethyl acetate gave the best result for inhibition of colony growth and sporangia production with the ED_{50} values was required only 77 µg/mL and 3.5 µg/mL, respectively, which was more effective than crude methanol and hexane, ED_{50} values were computed at 143.9, 919 µg/mL and 4, 16.7 µg/mL, respectively. In contrast, previous results of Sibounnavong *et al.* (2011a) found that the highest inhibitory effect from crude methanol extracted from *Ch. lucknowense*, followed by crude ethyl acetate on colony growth of *Fusarium oxysporum f. sp. lycopersici,* a causal pathogen for tomato wilt. Meanwhile, consistent with the previous research, the results of this study showed that crude hexane had a lesser effect on colony growth inhibition. Several secondary metabolites are produced from *Chaetomium* spp., which plays an essential role against fungal pathogens (Hamed *et al.*, 2020; Sun *et al.*, 2006). *Chaetomium* spp. have been reported to produce an antibiotic substance named Chaetoglobosin-C (Sibounnavong *et al.*, 2011b), Chaetoglobosin-A (Ishiuchi *et al.*, 2013; Rajendran *et al.*, 2023) and synthetic volatiles compounds (Hexadecanoic acid, 9,12-Octadecadienoic acid (Z), octadecanoic acid) (Kamat *et al.*, 2020).

Nanofibers from *T. hamatum* K01 and *Ch. lucknowense* CL were characterized and measured. The Scanning electron microscopy result indicated particle size of nano-TK01H, nano-TK01E, and nano-TK01M from *T. hamatum* K01 averaged of 122, 187, and 136 nm, respectively. Nanofibers from *Ch. lucknowense* CL, namely, nanofibers nano-CLH, nano-CLE, and nano-CLM were measured at average of 155.62nm, 207.91nm, and 156.87 nm, respectively. This

This material is reserved for educational use only, not allowed for commercial use.
Forbidden to modify the content, and cite the document when use.

research finding corresponded to the report by (Song *et al.*, 2020); Tongon and Soytong (2022), who characterized and measured the size of nanofibers.

The antimicrobial agent of nanofiber derived from *T. hamatum* K01 (nano-TK01H, nano-TK01E, and nano-TK01M) could effectively inhibit *P. palmivora, C. gloeosporioides* C01, and *C. gloeosporioides* C02 at low concentrations. Nano-TK01M demonstrated the most potent antifungal activity, inhibiting colony growth with ED_{50} values ranging from 14 to 11 ppm and sporulation with ED_{50} values of 3 to 2 ppm, respectively. In comparison, nano-TK01E had a good effect on colony growth, with ED_{50} values ranging from 36 to 16 ppm, and sporangia inhibition was computed with ED_{50} values ranging from 9 to 5 ppm, respectively. At the same time, nano-TK01H had the lesser effect in inhibition, in which colony growth was computed with ED_{50} values ranging from 40 to 19 ppm, and sporulation inhibition was computed with ED_{50} values ranging from 15 to 9 ppm, respectively. This study was supported by the El-Wakil (2020), who found that nanofibers from *T. hamatum* significantly suppressed *Fusarium* spp., *F. solani*, *F. semitectum, F. oxysporum* and *F. roseum,* which was known as a causal agent of soil-borne pathogens. This study indicated that the inhibitory effect is attributed to major organic compounds, including benzoic acid, hexadecane, 6-pentyl-2H-pyran-2-one, and tetracosane. Additionally, Alpha-phenylacetamide ((R)-5,6-dihydro-6-pentyl-2H-pyran-2-one), fatty acids such as palmitic acid, linoleic acid, Tetradecanoic acid, pentadecanoic acid, hexadecenoic acid, as well as their ethyl esters (linoleic acid ethyl ester and ethyl oleate), and sorbicillin, which *T. hamatum* K01 produces, were found to exhibit antifungal activity toward plant pathogenic organisms. This research finding was confirmed by the study of Reino *et al.* (2008), who reported that pyrone name (6-pentyle-2H-pyran-2-one) and sorbicillin metabolites produced from *Trichoderma* species exhibited a robust antifungal activity against *Rhizoctonia solani* and *F. oxysporum f.* sp. *lycopersici*. Similarly, the pyrone fungal metabolite, specifically 6-Pentyl-α-pyrone, derived from *T. koningii*, has also been reported to suppress the Rhizoctonia root rot pathogen (Khan *et al.*, 2020). (6-pentyle-2H-pyran-2-one) from *T. atroviride* decreased spores population of *Clarireedia jacksonii* turf dollar spot of bent-grass at EC_{50} value of 83 µL/mL (Liu *et al.*, 2023). *Trichoderma* species were also reported to produce antifungal metabolite ((R)-5,6-dihydro-6-pentyl-2H-pyran-2-one). This metabolite significantly inhibited *Sphaeropsis sapinea (syn. Diplodia pinea)*, causing *Pinus*

This thesis is reserved for academic and non-commercial use.
Forbidden to modify the content, and cite the document when use.

radiata sapwood (Vanneste *et al.*, 2002) and 6-pentyle-2H-pyran-2-one produced from *T. atroviride* LZ42, this compound was inhibited *F. oxysporum* at EC_{50} values of 5.76 µL/mL (Rao *et al.*, 2022).

Natural product nanofibers derived from *Ch. lucknowense* CL exhibited antifungal activity against three test pathogens: *P. palmivora* PYSC01, *C. gloeosporioides* C01, and *C. gloeosporioides* C02, which are known as causal agents of durian rot, citrus anthracnose, and durian anthracnose, respectively. Germination of spores is a crucial phase in the pathogen life cycle (Yun *et al.*, 2023). These nanofibers, namely nano-CLH, nano-CLE, and nano-CLM, inhibited both colony growth and sporulation of *P. palmivora* PYSC01, *C. gloeosporioides* C01, and *C. gloeosporioides* C02 by 100% at a concentration of 10 ppm. Among them, nano-CLE exhibited the highest inhibition of colony growth, with an ED_{50} value computed at 2.2 to 2.02 ppm, and sporulation inhibition required only 1.03 to 0.2 ppm. This research finding was confirmed by Song *et al.* (2020), who found that nanofiber from *Ch. lucknowense* loaded with crude hexane, crude ethyl acetate, and methanol showed the best inhibitory effect against spore production of *M. oryzae,* causing rich blast disease at ED_{50} of 10.72, 7.01 and 5.24 ppm respectively. Similarly, nanofibers constructed from *Ch. cupreum* CC3003 (Nano-CC-H, Nano-CC-E, and Nano-CC-M) exhibited significant inhibition against *P. palmivora*, the causal agent of durian root rot. The inhibition of colony growth was calculated at ED_{50} values ranging from 1.78 to 1.19 ppm, while the suppression of sporangia required ED_{50} values ranging from 11.01 to 16.48 ppm, respectively (Tongon & Soytong, 2022).

Under greenhouse trails, the highest severity disease of anthracnose and root rot of durian caused by *C. gloeosporioides* and *P. palmivora* inoculation was recorded with negative control. However, the disease symptoms were not shown in non-inoculated positive control. The treatments of metalaxyl, *Ch. lucknowense* CL, *T. hamatum* K01 products, and nanofibers from *Ch. lucknowense* CL and *T. hamatum* K01 significantly decreased the disease severity compared to negative control on days 30 to 120 after treatment. Nanofibers from *T. hamatum* K01 and *Ch. lucknowense* CL treatments reduced disease severity by 99.16 % and 95.41%, respectively, the same as the effect by chemical metalaxyl 92.08%. However, *T. hamatum* K01 product and *Ch. lucknowense* CL product exhibited a good result in

This material is reserved for educational use only, not allowed for commercial use.
Forbidden to modify the content, and cite the document when use.

reducing the severity of disease by 90% and 86.66%, respectively, compared to negative control. The inhibitory effects were attributed to antifungal metabolite production and elicited systemic resistance. GC-MS analysis showed that *T. hamatum* K01 was found to produce antifungal compounds pyrone (6-pentyl-2H-Pyran-2-one), sorbicillin, and fatty acid (palmitic acid, octadecadienoic acid, pentadecanoic acid and linoleic acid). This study was confirmed by Lazazzara *et al.* (2021), who discovered that pyrone metabolite (6-pentyl-2H-Pyran-2-one) produced by *T. atroviride* significantly reduced the severity of downy mildew on grapevine leaves (82.1%) causing by *Plasmopara viticola.* Active metabolite 6-pentyl-2H-Pyran-2-one from *T. atroviride* T2 showed a strong effect in inhibition of the growth of *Cylindrocarpon destructans* is known acausal agent of root rot pathogen of *Panax notoginseng* (Jin *et al.*, 2020). The pyrone metabolite 6-pentyl-2H-Pyran-2-one suppressed the growth of the pathogenic organism by damaging the cell walls and membranes (Liu *et al.*, 2023). Cell membranes of pathogenic fungi involve sterol, phospholipids, and fatty acids (Dupont *et al.*, 2021). Phospholipase is a main enzyme that catalyzes phospholipid decomposition and plays a role as a signal molecule to mediate cell death, growth, migration, proliferation, and other physiological reactions, changing their structure and content, which affects fungal activities (Ecker & Liebisch, 2014). This is consistent with the study by Liu *et al.* (2023), who found that 6-pentyl-2H-Pyran-2-one treatment resulted in degraded phospholipid of *C. jacksonii* fungus. Some fatty acids (linoleic acid, palmitic acid, and oleic acid) have also been reported to possess antifungal activity against plant pathogens (Altieri *et al.*, 2007; Liu *et al.*, 2008). This inhibitory effect is related to sterol content in fungal pathogen's cell membrane (Liu *et al.*, 2008). Antifungal activity of fatty acid exhibited a strong biocontrol potential against pathogens, observed by reducing sterol content in cell membranes (Lanzuise *et al.*, 2022). Palmitic acid, linoleic acid, and oleic acid from *Trichoderma spirale* was able to inhibit *Moniliophthora perniciosa*' growth by 33–47% at 10 µg/mL (Choez-Guaranda *et al.*, 2023). The effectiveness of *Ch. lucknowense* CL was associated with major bioactive compounds, regarding volatile organic compounds (Hexadecanoic acid, Hexadecanoic acid, ethyl ester), aliphatic compounds (9, 12-Octadecadienoic acid, and Oleic acid) compounds were identified in crude ethyl extract by GC-MS analysis. These compounds have been reported to possess antifungal activity and antioxidants toward plant pathogens (Huang *et al.*, 2007;

This material is restricted for educational use only. Not allowed for commercial use.
Forbidden to modify the content, and cite the document when use.

Shaker *et al.*, 2022). This study is confirmed by Kumar and Prasher (2023), who discovered that volatile organic compounds (hexadecanoic acid and 9,12-octadecadienoic acid (z)) from *Ch. globosum* exhibited antifungal activity and antioxidant potential against pathogenic organisms. Another supporting evidence is that hexadecanoic acid, ethyl ester, and 9, 12-Octadecadienoic acid derived from *Cheatomium* sp. significantly inhibited the population of *F. solani*, *F. oxysporum*, *R. solani,* and *M. phaseolina* in pot trial (Farhat *et al.*, 2023). Furthermore, in this current study, durian and citrus plants were also found to synthesize phytoalexins, as demonstrated by the presence of spots on TLC plates with an R_f value of 0.77 in 12% acetic acide for durian and 0.58 in toluene:ethyl acetate (1:1) for citrus. These spots were identified as containing the scopoletin and scoparone compound respectively, as confirmed by comparison with standard compounds. These compounds served as a defense mechanism of durian and citrus against pathogens. Interestingly, treatment with nano-TK01 and nano-CL produced the clearest spots on the TLC plate, suggesting their involvement in stimulating systemic resistance in durian and citrus plants. In contrast, the positive control did not show a spot on the TLC plate. This study corresponded to the findings of Tongon and Soytong (2022) who discovered that durian plants treated with nanoparticles from *Ch. cupreum* induced the production of scopoletin with an R_f value of 0.75. Scopoletin is known as a defense mechanism of the plant against durian root rot caused by *P. palmivora*. Similarly, rice seedling treated with nanoparticle derived *Ch. brasiliense* was also found inducing of Sakuranertin and Oryzalexin B with R_f of value of 0.08 and 0.28, respectively, that act as plant immunity against rice blast disease causing by *M. oryzae* (Song *et al.*, 2020). Citrus plant was also found to produce phytoalexin after treatment of nano-elicitor from *Ch. cochliodes*, in which the R_f values was computed 0.6 (Mongkutkarn, 2020). Another study stated by Afek and Sztejnberg (1988) who found that scoparone compound was detected in citrus 1-8 after inoculation with *P. citrophthora,* which is considered as the disease resistance of the citrus against fungal infection.

Plant physiology in both durian and citrus was significantly affected after treatment. Photosynthesis parameters, including total chlorophyll and carotenoid contents, were assessed on day 60 after fungal inoculation and treatment. The lowest chlorophyll and carotenoid contents were recorded in the negative control, possibly

This material is reserved for educational use only, not allowed for commercial use.
Forbidden to modify the content, and cite the document when use.

due to pathogenic activity in the plants after inoculation. El-Sharkawy and Abdelrazik (2022) reported that a reduction in chlorophyll and carotenoid content in the plant is caused by pathogenic infection, releasing toxins that lead to xylem vessel choking. The positive control gave a higher total chlorophyll and carotenoid contents than the negative control, possibly indicating free from pathogenic infection, making it available for nitrogen distribution. Nanofiber from *T. hamatum* K01 was the most effective in synthesizing total chlorophyll and carotenoid contents, followed by nanofiber from *Ch. lucknowense* CL, metalaxyl, *T. hamatum* K01, and *Ch. lucknowense* CL's products. This may be attributed to reduce fungal toxins produced due to pathogenic inoculation.

Moreover, all treatments have various effects on durian and citrus growth parameters. Among these treatments, nanofiber from *T. hamatum* K01 was the most effective on durian and citrus plant height, followed by nanofiber from *Ch. lucknowense* CL. At the same time, the lowest effect was recorded with negative control. Plant growth is associated with the nutrient absorption ability of the plant (Asghar & Kataoka, 2021). *Trichoderma* spp. have been reported on their ability to improve plant nutrient assimilation (Asghar & Kataoka, 2021) and change soil pH that is available for plant growth (Li *et al.*, 2015). Asghar and Kataoka (2021) discovered that *Trichoderma* sp. strain RW309 was able to degrade organic material in soil, resulting in the release of nutrients available for plants. This current study was supported by Marra *et al.* (2019), who discovered that 6-pentyl-α-pyrone (6PP) from *T. harzianum* treatment significantly promoted soybean plant growth compared to control. Rao et al. (2022) reported a similar result, found that 6-pentyl-2H-pyran-2-one (6-PP) released from *Trichoderma* strain LZ42 promoted tomato seedling growth. *Chaetomium* spp. has also been reported for its ability to promote plant growth. Kumar *et al.* (2021) indicated that the ethyl acetate fraction of *Ch. globosum* CG5157 significantly affected the growth promotion of *Brassica* seeding (regarding shoot length and root length) compared to the non-treated control.

This material is reserved for educational use only, not allowed for commercial use.
Forbidden to modify the content, and cite the document when use.

CHAPTER 6

CONCLUSION

C. gloeosporioides isolate C01, *C. gloeosporioides* isolate C02, and *P. palmivora* PYSC01 were obtained from citrus anthracnose, durian anthracnose, and durian root rot. They were proven to infect the citrus, durian leaves, and durian rot. They were confirmed at the species level based on morphological and molecular characterizations. The findings show that *Ch. lucknowense* CL and *T. hamatum* K01 were able to compete for space on radial colony growth and reduce sporulation of the test pathogens in dual culture tests. Moreover, crude extracts and nanofibers from *Ch. lucknowense* CL and *T. hamatum* K01 significantly suppressed the test pathogens, and applying of nanofibers from *T. hamatum* K01 and *Ch. lucknowense* significantly reduced the disease severity of durian rot and durian anthracnose caused by *P. palmivora* and *C. gloeosporioides*, and decreased the disease severity of citrus anthracnose caused by *C. gloeosporioides,* and induced the production of phytoalexins against plant pathogens. These inhibitory effects were associated with active metabolites of pyrone (6-pentyl-2H-Pyran-2-one), sorbicillin, and fatty acid produced by *T. hamatum* K01 and bioactive compounds, namely hexadecanoic acid, 9, 12-octadecadienoic acid (Z), and octadecanoic acid derived from *Ch. lucknowense* CL. This study suggests that natural products nanofibers from *Ch. lucknowense* CL and *T. hamatum* K01 can be a promising option for plant disease management while ensuring sustainable production that is friendly for farmers, consumers, and the environment.

This material is reserved for educational use only, not allowed for commercial use.
Forbidden to modify the content, and cite the document when use.

REFERENCES

Abdelkhalek, A.,Al-Askar, A. A.,Arishi, A. A., & Behiry, S. I. (2022). *Trichoderma hamatum* Strain Th23 Promotes Tomato Growth and Induces Systemic Resistance against Tobacco Mosaic Virus. *Journal of Fungi*, *8*(3), 228.

Abobatta, W. (2019). Nutritional benefits of citrus fruits. *American Journal of Biomedical Science & Research 3*(1), 303-306.

Afek, U., & Sztejnberg, A. (1988). Accumulation of scoparone, a phytoalexin associated with resistance of Citrus to *Phytophthora citrophthora*. *Phytopathology*, *78*(12), 1678-1682.

Ahuja, I.,Kissen, R., & Bones, A. M. (2012). Phytoalexins in defense against pathogens. *Trends in Plant Science*, *17*(2), 73-90.

Ajay Kumar, G. (2014). *Colletotrichum gloeosporioides*: biology, pathogenicity and management in India. *Journal of Plant Physiology & Pathology*, *2*(2), 2.

Alahakoon, P. W.,Brown, A. E., & Sreenivasaprasad, S. (1994). Cross-infection potential of genetic groups of *Colletotrichum gloeosporioides* tropical fruits. *Physiological and Molecular Plant Pathology*, *44*(2), 93–103.

Altieri, C.,Cardillo, D.,Bevilacqua, A., & Sinigaglia, M. (2007). Inhibition of Aspergillus spp. and Penicillium spp. by fatty acids and their monoglycerides. *Journal of food protection*, *70*(5), 1206-1212.

Altschul, S.,Madden, T. L.,Schaffer, A.,Zhang, Z.,Miller, W. E., & Lipman, D. J. (1997). Gapped BLAST and PSI-BLAST: a new generation of protein databases search programs. *Nucleic Acids Research*, *25*(17), 3389-3402.

Andrade-Hoyos, P.,Silva-Rojas, H., & Romero Arenas, O. (2020). Endophytic *Trichoderma* Species Isolated from *Persea americana* and Cinnamomum verum Roots Reduce Symptoms Caused by *Phytophthora cinnamomi* in Avocado. *Plants*, *9*(9), 1220.

Arruda, R. L.,Paz, A. T. S.,Bara, M. T. F.,Cortes, M. V. d. C. B.,Filippi, M. C. C. d., & Conceicao, E. C. d. (2016). An approach on phytoalexins: function, characterization and biosynthesis in plants of the family Poaceae. *Ciencia Rural*, *46*, 1206-1216.

Asghar, W., & Kataoka, R. (2021). Effect of co-application of Trichoderma spp. with organic composts on plant growth enhancement, soil enzymes and fungal community in soil. *Archives of Microbiology*, *203*(7), 4281-4291.

Baazeem, A.,Almanea, A.,Manikandan, P.,Alorabi, M.,Vijayaraghavan, P., & Abdel-Hadi, A. (2021). In vitro antibacterial, antifungal, nematocidal and growth promoting activities of *Trichoderma hamatum* FB10 and its secondary metabolites. *Journal of Fungi*, *7*(5), 331.

Beakes, G. W.,Glockling, S. L., & Sekimoto, S. (2012). The evolutionary phylogeny of the oomycete "fungi". *Protoplasma*, *249*(1), 3-19.

Benitez, T.,Rincon, A. M.,Limon, M. C., & Codon, A. C. (2004). Biocontrol mechanisms of Trichoderma strains. *International Microbiology*, *7*(4), 249-260.

Bhunjun, C. S.,Phukhamsakda, C.,Jayawardena, R. S.,Jeewon, R.,Promputtha, I., & Hyde, K. D. (2021). Investigating species boundaries in Colletotrichum. *Fungal diversity*, *107*(1), 107-127.

Brent, K. J., & Hollomon, D. W. (2007). Fungicide resistance: The assessment of risk (Vol. 2). Fungicide Resistance Action Committee

This material is reserved for educational use only, not allowed for commercial use.

Forbidden to modify the content, and cite the document when use.

Brown, M. J. (1997). *Durio, a bibliographic review*. Internation Plant Genitic Resources Institute.

Cannon, P.,Damm, U.,Johnston, P., & Weir, B. (2007). Colletotrichum–current status and future directions. *Studies in Mycology*, *59*(1), 129-145.

Charoenporn, C.,Kanokmedhakul, S.,Lin, F.,Poeaim, S., & Soytong, K. (2010). Evaluation of bio-agent formulations to control Fusarium wilt of tomato. *African Journal of Agricultural Research*, *9*(36).

Chemeltorit, P. P.,Mutaqin, K. H., & Widodo, W. (2017). Combining *Trichoderma hamatum* THSW13 and Pseudomonas aeruginosa BJ10–86: a synergistic chili pepper seed treatment for *Phytophthora capsici* infested soil. *European Journal of Plant Pathology*, *147*(1), 157-166.

Chithra, S.,Jasim, B.,Sachidanandan, P.,Jyothis, M., & Radhakrishnan, E. (2014). Piperine production by endophytic fungus Colletotrichum gloeosporioides isolated from Piper nigrum. *Phytomedicine*, *21*(4), 534-540.

Choez-Guaranda, I.,Espinoza-Lozano, F.,Reyes-Araujo, D.,Romero, C.,Manzano, P.,Galarza, L., & Sosa, D. (2023). Chemical Characterization of Trichoderma spp. Extracts with Antifungal Activity against Cocoa Pathogens. *Molecules*, *28*(7), 3208.

Cooke, D.,Drenth, A.,Duncan, J.,Wagels, G., & Brasier, C. (2000). A molecular phylogeny of Phytophthora and related oomycetes. *Fungal Genetics Biology*, *30*(1), 17-32.

Cooke, D.,Schena, L., & Cacciola, S. (2007). Tools to detect, identify and monitor Phytophthora species in natural ecosystems. *Journal of Plant Pathology*, *89*(1), 13-28.

Daoud, H. B.,Baraldi, E.,Iotti, M.,Leonardi, P., & Boughalleb-M'hamdi, N. M. (2019). Characterization and pathogenicity of Colletotrichum spp. causing citrus anthracnose in Tunisia. *Phytopathologia*, *58*, 175-185.

Dar, J., & Soytong, K. (2014). Construction and characterization of copolymer nanomaterials loaded with bioactive compounds from Chaetomium species. *Internal Journal of Agricultural Technology*, *10*(4), 823-831.

David, S. (1998). Phytophthora Diseases Worldwide *Journal of Agricultural Science*, *131*(2), 245-249.

Dawson, C. J., & Hilton, J. (2011). Fertiliser availability in a resource-limited world: Production and recycling of nitrogen and phosphorus. *Food Policy*, *36*, 14-14.

Di Pietro, A.,Gut-Rella, M.,Pachlatko, J., & Schwinn, F. J. P. (1992). Role of antibiotics produced by *Chaetomium globosum* in biocontrol of *Pythium ultimum*, a causal agent of damping-off. *Phytopathology*, *82*(2), 131-135.

Dupont, S.,Fleurat-Lessard, P.,Cruz, R. G.,Lafarge, C.,Grangeteau, C.,Yahou, F., Simon-Plas, F. (2021). Antioxidant properties of ergosterol and its role in yeast resistance to oxidation. *Antioxidants*, *10*(7), 1024.

Ecker, J., & Liebisch, G. (2014). Application of stable isotopes to investigate the metabolism of fatty acids, glycerophospholipid and sphingolipid species. *Progress in lipid research*, *54*, 14-31.

El-Sharkawy, E. E. S., & Abdelrazik, E. (2022). Biocontrol of Fusarium root rot in squash using mycorrhizal fungi and antagonistic microorganisms. *Egyptian Journal of Biological Pest Control*, *32*(1), 13.

El-Sharkawy, H. H. A.,Abo-El-Wafa, T. S. A.,Mostafa, N. A., & Yousef, S. A. M. (2023). Boosting biopesticide potential of *Trichoderma harzianum* for controlling the downy mildew and improving the growth and the

This material is reserved for educational use only, not allowed for commercial use.

Forbidden to modify the content, and cite the document when use.

productivity of King Ruby seedless grape. *Egyptian Journal of Biological Pest Control*, *33*(1), 61.
El-Wakil, D. A. (2020). Antifungal activity of silver nanoparticles by Trichoderma species: synthesis, characterization and biological evaluation. *Egyptian Journal of Phytopathology*, *48*(1), 71-80.
Erwin, D. C., & Ribeiro, O. K. (1996). *Phytophthora: diseases worldwide*. Minnesota, US: APS Press.
FAO. (2017). *Citrus fruit fresh and processes statistical bulletin*. Food and Agriculture Organization of the United Nations. Retrieved 27 April from
Farhat, H.,Urooj, F.,Sohail, N.,Ullah, S., & Ali, M. S. (2023). Plant disease management with amelioration of systemic resistance in soybean by endophytic fungi associated with GC-MS metabolic profiling of Chaetomium sp. *Physiological Molecular Plant Pathology*, *126*, 102049.
Farr, D. F.,Aime, M. C.,Rossman, A. Y., & Palm, M. E. (2006). Species of Colletotrichum on agavaceae. *Mycological Research*, *110*(12), 1395-1408.
Flier, W.,Grunwald, N.,Kroon, L.,van den Bosch, T.,Garay-Serrano, E., & Bonants, P. (2001). *Phytophthora ipomoeae, a new homothallic species causing leaf blight onIpomoea longipedunculata in the Toluca Valley of central Mexico* [PhD Thesis,
Freeman, S.,Katan, T., & Shabi, E. (1998). Characterization of Colletotrichum species responsible for anthracnose diseases of various fruits. *Plant Disease*, *82*(6), 596-605.
Freeman, S.,Katan, T., & Shabi, E. (2007). Characterization of Colletotrichum species responsible for anthracnose diseases of various fruits. *Plant Disease*, *82*(6), 596-605.
Fry, W. (2008). *Phytophthora infestans*: the plant (and R gene) destroyer. *Molecular Plant Pathology*, *9*(3), 385-402.
Gams, W.,Bissett, J., & Gliocladium. (2002). Trichoderma and Gliocladium In (Vol. 1, pp. 3-31). Toylor and Francis.
Gnonlonfin, G. B.,Sanni, A., & Brimer, L. (2012). Review scopoletin–a coumarin phytoalexin with medicinal properties. *Critical Reviews in Plant Sciences*, *31*(1), 47-56.
Grunwald, N. J.,Martin, F. N.,Larsen, M. M.,Sullivan, C. M.,Press, C. M.,Coffey, M. D., Parke, J. L. (2011a). Phytophthora-ID. org: a sequence-based Phytophthora identification tool. *Plant Disease*, *95*(3), 337-342.
Grunwald, N. J.,Martin, F. N.,Larsen, M. M.,Sullivan, C. M.,Press, C. M.,Coffey, M. D., Parke, J. L. (2011b). Phytophthora-ID.org: A sequence-based Phytophthora identification tool. *Plant Disease*, *95*(3), 337-342.
Hahn, M. (2014). The rising threat of fungicide resistance in plant pathogenic fungi: Botrytis as a case study. *Journal of Chemical Biology*, *7*(4), 133-141.
Hamed, S. R.,Abdel-Azeem, A. M., & Dar, P. M. (2020). Recent advancements on the role of biologically active secondary metabolites from Chaetomium. In *Recent Developments on Genus Chaetomium* (pp. 177-204). Springer.
Hammerschmidt, R. (1999). Phytoalexins: what have we learned after 60 years? *Annual Review of Phytopathology*, *37*(1), 285-306.
Hassan, O.,Jeon, J.,Chang, T.,Shin, J.,Oh, N., & Lee, Y. (2018). Molecular and morphological characterization of *Colletotrichum* species in the *Colletotrichum gloeosporioides* complex associated with persimmon anthracnose in South Korea. *Plant Disease*, *102*(5), 1015-1024.

This material is reserved for educational use only, not allowed for commercial use.
Forbidden to modify the content, and cite the document when use.

Heydari, A., & Pessarakli, M. (2010). A review on biological control of fungal plant pathogens using microbial antagonists. *Journal of Biological Sciences*, *10*(4), 273-290.

Hoitink, H.,Madden, L., & Dorrance, A. (2006). Systemic resistance induced by Trichoderma spp.: interactions between the host, the pathogen, the biocontrol agent, and soil organic matter quality. *Phytopathology*, *96*(2), 186-189.

Howard, K. L.,Seymour, R., & Johnson Jr, T. (1970). Aquatic fungi of Iceland: Saprolegniaceae. *Journal of the Elisha Mitchell Scientific Society*, *86*(2), 63-79.

Huang, W.-Y.,Cai, Y.-Z.,Hyde, K. D.,Corke, H., & Sun, M. (2007). Endophytic fungi from Nerium oleander L (Apocynaceae): main constituents and antioxidant activity. *World Journal of Microbiology Biotechnology Letters*, *23*, 1253-1263.

Hung, P. M.,Wattanachai, P.,Soytong, K., & Poeaim, S. (2015). Efficacy of Chaetomium species as biological control agents against *Phytophthora nicotianae* root rot in citrus. *Mycobiology*, *43*(3), 288-296.

Ishii, H., & Holloman, D. (2015). *Fungicide resistance in plant pathogens* (Vol. 10). Springer.

Ishiuchi, K. i.,Nakazawa, T.,Yagishita, F.,Mino, T.,Noguchi, H.,Hotta, K., & Watanabe, K. (2013). Combinatorial generation of complexity by redox enzymes in the chaetoglobosin A biosynthesis. *Journal of the American Chemical Society*, *135*(19), 7371-7377.

Jin, X.,Guo, L.,Jin, B.,Zhu, S.,Mei, X.,Wu, J., He, X. (2020). Inhibitory mechanism of 6-Pentyl-2H-pyran-2-one secreted by *Trichoderma atroviride* T2 against Cylindrocarpon destructans. *Pesticide Biochemistry Physiology*, *170*, 104683.

Kaewchai, S., & Soytong, K. (2010). Application of biofungicides against Rigidoporus microporus causing white root disease of rubber trees. *Internation Journal of Agricultural Technology*, *6*(2), 349-363.

Kai, K.,Shimizu, B.-i.,Mizutani, M.,Watanabe, K., & Sakata, K. (2006). Accumulation of coumarins in Arabidopsis thaliana. *Phytochemistry Reviews*, *67*(4), 379-386.

Kamat, S.,Kumari, M.,Sajna, K. V., & Jayabaskaran, C. (2020). Endophytic fungus, Chaetomium globosum, associated with marine green alga, a new source of Chrysin. *Scientific Reports*, *10*(1), 1-17.

Kang, S.,Mansfield, M. A.,Park, B.,Geiser, D. M.,Ivors, K. L.,Coffey, M. D., Blair, J. E. (2010). The promise and pitfalls of sequence-based identification of plant-pathogenic fungi and oomycetes. *Phytopathology*, *100*(8), 732-737.

Kanokmedhakul, S.,Kanokmedhakul, K.,Nasomjai, P.,Louangsysouphanh, S.,Soytong, K.,Isobe, M., Suksamrarn, A. (2006). Antifungal Azaphilones from the fungus *Chaetomium cupreum* cc3003. *Journal of Natural Products*, *69*(6), 891-895.

Kasem, S.,Kanokmedhakul, S.,Kukongviriyapan, V., & Isobe, M. (2001). Application of Chaetomium species (Ketomium((R))) as a new broad spectrum biological fungicide for plant disease control: A review article. *Fungal diversity*, *7*, 1-15.

Kasem, S.,Srinon, W.,Rattanacherdchai, K.,Kanokmedhakul, S., & Kanokmedhakul, K. (2005). Application of antagonistic fungi to control

This material is reserved for educational use only, not allowed for commercial use.

Forbidden to modify the content, and cite the document when use.

anthracnose disease of grape. *International Journal of Agricultural Technology*, *1*(1), 33-41.
Kean, S.,Soytong, K., & To-anun, C. (2010a). Application of biological fungicides to control citrus root rot under field condition in Cambodia. *Internation Journal of Agricultural Technology*, *6*(2), 219-230.
Kean, S.,Soytong, K., & To-Anun, C. (2010b). Application of biological fungicides to control citrus root rot under field condition in Cambodia. *International Journal of Agriculture Technology*, *6*(2), 219-230.
Ketsa, S. (2018). Durian—Durio zibethinus. In *Exotic Fruits* (pp. 169-180). Elsevier.
Khan, J.,Ooka, J.,Miller, S.,Madden, L., & Hoitink, H. (2004). Systemic resistance induced by *Trichoderma hamatum* 382 in cucumber against Phytophthora crown rot and leaf blight. *Plant Disease*, *88*(3), 280-286.
Khan, R. A. A.,Najeeb, S.,Hussain, S.,Xie, B., & Li, Y. (2020). Bioactive secondary metabolites from Trichoderma spp. against phytopathogenic fungi. *Microorganisms*, *8*(6), 817.
Khatri, D. K.,Tiwari, D. N., & Bariya, H. S. (2017). Chitinolytic efficacy and secretion of cell wall-degrading enzymes from Trichoderma spp. in response to phytopathological fungi. *Journal of Applied BIology and Biotechnology 5*(6), 1-8.
Khonglah, D., & Kayang, H. (2018). Antagonism of indigenous fungal isolates against Botrytis cineria the causal of gray mold disease of tomato (Solanum lycopersicum L.). *International Journal of Current Research in Life Sciences*, *7*(1), 806-812.
Kohl, J.,Molhoek, W.,Van der Plas, C., & Fokkema, N. (1995). Effect of Ulocladium atrum and other antagonists on sporulation of Botrytis cinerea on dead lily leaves exposed to field conditions. *Phytopathology*, *85*(4), 393-400.
Kongtragoul, P.,Ishikawa, K., & Ishii, H. (2021). Metalaxyl resistance of *Phytophthora palmivora* causing durian diseases in Thailand. *Horticulturae*, *7*(10), 375.
Kroon, L. P.,Brouwer, H.,de Cock, A. W., & Govers, F. (2012). The genus Phytophthora anno 2012. *Phytopathology*, *102*(4), 348-364.
Kumar, R.,Kundu, A.,Dutta, A.,Saha, S.,Das, A., & Bhowmik, A. (2021). Chemo-profiling of bioactive metabolites from Chaetomium globosum for biocontrol of Sclerotinia rot and plant growth promotion. *Fungal biology*, *125*(3), 167-176.
Kumar, V., & Prasher, I. (2023). Phytochemical Analysis and Antioxidant Activity of Endophytic Fungi Isolated from Dillenia indica Linn. *Applied Biochemistry Biotechnology*, 1-18.
Lanzuise, S.,Manganiello, G.,Guastaferro, V. M.,Vincenzo, C.,Vitaglione, P.,Ferracane, R., Lorito, M. (2022). Combined biostimulant applications of Trichoderma spp. with fatty acid mixtures improve biocontrol activity, horticultural crop yield and nutritional quality. *Agronomy*, *12*(2), 275.
Lazazzara, V.,Vicelli, B.,Bueschl, C.,Parich, A.,Pertot, I.,Schuhmacher, R., & Perazzolli, M. (2021). Trichoderma spp. volatile organic compounds protect grapevine plants by activating defense‐related processes against downy mildew. *Physiologia Plantarum*, *172*(4), 1950-1965.

This material is reserved for educational use only, not allowed for commercial use.
Forbidden to modify the content, and cite the document when use.

Levy, Y.,Levi, R., & Cohen, Y. (1983). Buildup of a pathogen subpopulation resistant to a systemic fungicide under various control strategies: a flexible simulation model [Plant diseases]. *Phytopathology*, *73*(11), 1475-1480.

Li, R.-X.,Cai, F.,Pang, G.,Shen, Q.-R.,Li, R., & Chen, W. J. P. o. (2015). Solubilisation of phosphate and micronutrients by Trichoderma harzianum and its relationship with the promotion of tomato plant growth. *J PloS one*, *10*(6), e0130081.

Liu, M.,Niu, Q.,Wang, Z.,Qi, H.,Liang, X.,Gai, Y., Yin, S. (2023). Comparative physiological and transcriptome analysis provide insights into the inhibitory effect of 6-pentyl-2H-pyran-2-one on Clarireedia jacksonii. *Pesticide Biochemistry Physiology*, *193*, 105456.

Liu, S.,Ruan, W.,Li, J.,Xu, H.,Wang, J.,Gao, Y., & Wang, J. (2008). Biological control of phytopathogenic fungi by fatty acids. *Mycopathologia*, *166*, 93-102.

Longoni, P.,Rodolfi, M.,Pantaleoni, L.,Doria, E.,Concia, L.,Picco, A. M., & Cella, R. (2012). Functional analysis of the degradation of cellulosic substrates by a *Chaetomium globosum* endophytic isolate. *Applied Environmental Microbiology*, *78*(10), 3693-3705.

M, T., & MB, M. (1954). Isolates of Chaetomium that protect oats from *Helminthosporium-vitoriae*. *Phytopathology*, *44*(12), 686-689.

Madbouly, A. K., & Abdel-Wareth, M. T. (2020). The use of Chaetomium taxa as biocontrol agents. In *Recent Developments on Genus Chaetomium* (pp. 251-266). Springer.

Manandhar, J.,Thapliyal, P.,Cavanaugh, K., & Sinclair, J. (1987). Interaction between pathogenic and saprobic fungi isolated from soybean roots and seeds. *Mycopathologia, 98*(2), 69-75.

Mao, T.,Chen, X.,Ding, H.,Chen, X., & Jiang, X. (2020). Pepper growth promotion and Fusarium wilt biocontrol by *Trichoderma hamatum* MHT1134. *Biocontrol Sci Technol.*, *30*(11), 1228-1243.

Marlatt, M.,Correll, J.,Kaufmann, P., & Cooper, P. (1996). Two genetically distinct populations of *Fusarium oxysporum f. sp. lycopersici* race 3 in the United States. *Plant Disease*, *80*(12), 1336-1342.

Marra, R.,Lombardi, N.,d'Errico, G.,Troisi, J.,Scala, G.,Vinale, F., Lorito, M. (2019). Application of Trichoderma strains and metabolites enhances soybean productivity and nutrient content. *Journal of agricultural food chemistry*, *67*(7), 1814-1822.

Martin, F. N.,Abad, Z. G.,Balci, Y., & Ivors, K. (2012). Identification and detection of Phytophthora: reviewing our progress, identifying our needs. *Plant disease*, *96*(8), 1080-1103.

Masoud, H. M.,Megahed, A. A.,Helmy, M. S. E.,Ibrahim, M. A.-A.,El-Mougy, N. S., & Abdel-Kader, M. M. (2023). Phytopathological and biochemical impacts of *Trichoderma harzianum* and certain plant resistance inducers on faba bean root rot disease. *Egyptian Journal of Biological Pest Control*, *33*(1), 63.

Masyahit, M.,Sijam, K.,Awang, Y., & Satar, M. (2009). The first report of the occurrence of anthracnose disease caused by *Colletotrichum gloeosporioides* (penz.) penz. & sacc. On dragon fruit (hylocereus spp.) in peninsular Malaysia. *American Journal of Applied Sciences*, *6*.

Matthews, G.,Bateman, R., & Miller, P. (2014). *Pesticide application methods*. John Wiley & Sons.

This material is reserved for educational use only, not allowed for commercial use.

Forbidden to modify the content, and cite the document when use.

Mergawy, M. M.,Hassanin, M. M. H.,Ali, A. A. M., & Yousef, H. (2023). Morphological characterization, fungicidal alternatives and biological control of Peronospora farinosa on chamomile. *Egyptian Journal of Biological Pest Control*, *33*(1), 68.

Molina, A.,Roa, V.,Bay-Petersen, J.,Carpio, A., & Joven, J. (1998, 14-16 october 1998). Managing banana and citrus diseases. Proceedings of a regional workshop on disease management of banana and citrus through the use of disease-free planting materials held in Davao City, Philippines,

Morrissey, J. P., & Osbourn, A. E. (1999). Fungal resistance to plant antibiotics as a mechanism of pathogenesis. *Microbiology Molecular Biology Reviews*, *63*(3), 708-724.

Murray, R. D. H.,Méndez, J., & Brown, S. A. (1982). The natural coumarins. In (pp. 161). Elsevier.

Narayanasamy, P. (2013). Abiotic Biological Control Agents for Crop Disease Management. In *Biological Management of Diseases of Crops* (pp. 511-632). Springer.

Nguyen, T. T. T.,Le, H. H.,Ho, T. M. H.,Dogot, T.,Burny, P.,Bui, T. N., & Lebailly, P. (2020). Efficiency Analysis of the Progress of Orange Farms in Tuyen Quang Province, Vietnam Towards Sustainable Development. *Sustainability*, *12*(8), 3170.

O'Brien, P. A. (2017). Biological control of plant diseases. *Australasian Plant Pathology*, *46*(4), 293-304.

Osorio-Hernández, E.,Hernández, D.,Morales, G.,Rodriguez, R., & Castillo, F. (2011). In-vitro behavior of Trichoderma spp. against *Phytophthora capsici* Leonian. *African Journal of Agricultural Research*, *6*.

Park, J.,Park, B.,Veeraraghavan, N.,Jung, K.,Lee, Y.-H.,Blair, J. E., Nikolaeva, E. (2008). Phytophthora database: a forensic database supporting the identification and monitoring of Phytophthora. *Plant Disease*, *92*(6), 966-972.

Paxton, J. D. (1988). Fungal elicitors of phytoalexins and their potential use in agriculture. In (Vol. 80, pp. 109-119). ACS Publications.

Phal, P.,Soytong, K., & Poeaim, S. (2023a). Natural product nanofibers derived from *Trichoderma hamatum* K01 to control citrus anthracnose caused by Colletotrichum gloeosporioides. *Open Agriculture*, *8*(1), 20220193.

Phal, P.,Soytong, K., & Poeaim, S. (2023b). A new nanofibre derived from *Trichoderma hamatum* K01 to control durian rot caused by *Phytophthora palmivora*. *Asian Journal of Agriulture and Biology*(1), 1-14.

Phal, P.,Soytong, K.,Tangon, R., & Jiaojiao, S. (2021). Antimicrobial Activity of Metabolites from Chaetomium to Control Root Rot (*Phytophthora parasitica*) and *Colletotrichum gloeosporioides* (anthracnose) in Citrus. International Seminar on Promoting Local Resources for Sustainable Agriculture and Development (ISPLRSAD 2020),

Phong, N. H.,Pongnak, W.,Kasem, S., & Luu, N. T. (2014). Antimicrobial substances from Chaetomium spp. against Pestalotia spp. causing grey blight disease of tea. *International Journal of Agricultural Technology*, *10*(4), 863-874.

Phong, N. H.,Pongnak, W., & Soytong, K. (2015). Antifungal activities of Chaetomium spp. against Fusarium wilt of tea. *Plant Protection Science*, *52*(1), 10-17.

This material is reserved for educational use only, not allowed for commercial use.

Forbidden to modify the content, and cite the document when use.

Phong, N. H.,Pongnak, W., & Soytong, K. (2016). Antifungal activities of Chaetomium spp. against Fusarium wilt of tea. *Plant Protection Science*, *52*(1), 10-17.

Phoulivong, S.,Cai, L.,Chen, H.,McKenzie, E.,Abd-Elsalam, K.,Chukeatirote, E., & Hyde, K. (2010). *Colletotrichum gloeosporioides* is not a common pathogen on tropical fruits. *Fungal diversity*, *44*(3), 33-43.

Phoulivong, S.,McKenzie, E., & Hyde, K. (2012). Cross infection of Colletotrichum species; a case study with tropical fruits. *Curr. Res. Environ. Appl. Mycol*, *2*(2), 99-111.

Phung, M.,Pongnak, W.,Soytong, K., & Supatta, P. (2014). Biological control of Pomelo diseases using Chaetomium spp. *International Journal of Agricultural Technology*, *10*(4), 833-844.

Phung, M.,Pongnak, W.,Soytong, K., & Supatta, P. (2015a). Biological Control of *Phytophthora palmivora* Causing Root Rot of Pomelo Using Chaetomium spp. *Mycobiology*, *43*(3), 63-70.

Phung, M.,Pongnak, W.,Soytong, K., & Supatta, P. (2015b). Biological Control of *Phytophthora palmivora* Causing Root Rot of Pomelo Using Chaetomium spp. *Mycobiology*, *43*(1), 63-70.

Phung, M.,Pongnak, W.,Soytong, K., & Supatta, P. (2015c). Efficacy of Chaetomium species as biological control agents against *Phytophthora nicotianae* root rot in citrus. *Mycobiology*, *43*(3), 288-296.

Ploetz, R. (2003). Diseases of Tropical Fruit Crops. In *Diseases of Citrus* (pp. 163-195). CABI.

Prabha, T.,Revathi, K.,Vinod, M.,Shanthakumar, S., & Bernard, P. (2013). A simple method for total genomic DNA extraction from water moulds. *Current Science*, *104*(3), 345-347.

Pragasam, S. J., & Rasool, M. (2013). Dietary component p-coumaric acid suppresses monosodium urate crystal-induced inflammation in rats. *Inflammation research : official journal of the European Histamine Research Society*, *62*(5), 489-498.

Prokhorov, V., & Armenskaya, N. (2001). Coprotrophic perithecioid ascomycetes of the European part of Russia. *Byul. MOIP. Otd. Biol*, *106*(2), 78-82.

Rajani, P.,Rajasekaran, C.,Vasanthakumari, M.,Olsson, S. B.,Ravikanth, G., & Shaanker, R. U. (2021). Inhibition of plant pathogenic fungi by endophytic Trichoderma spp. through mycoparasitism and volatile organic compounds. *Microbiological Research*, *242*, 126595.

Rajendran, L.,Durgadevi, D.,Kavitha, R.,Divya, S.,Ganeshan, K.,Vetrivelkalai, P. M., . . . Raguchander, T. (2023). Characterization of chaetoglobosin producing Chaetomium globosum for the management of Fusarium–Meloidogyne wilt complex in tomato. *Journal of Applied Microbiology*, *134*(2), lxac074.

Rao, Y.,Zeng, L.,Jiang, H.,Mei, L., & Wang, Y. (2022). *Trichoderma atroviride* LZ42 releases volatile organic compounds promoting plant growth and suppressing Fusarium wilt disease in tomato seedlings. *BMC Microbiology*, *22*(1), 1-12.

Reino, J. L.,Guerrero, R. F.,Hernández-Galán, R., & Collado, I. G. (2008). Secondary metabolites from species of the biocontrol agent Trichoderma. *Phytochemistry Reviews*, *7*(1), 89-123.

Rodríguez, K.,Stchigel, A., & Guarro, J. (2002). Three new species of Chaetomium from soil. *Mycologia*, *94*(1), 116-126.

This material is reserved for educational use only, not allowed for commercial use.

Forbidden to modify the content, and cite the document when use.

Ruppavalli, M. V.,Muthamilan, M.,Sevugapperumal, N., & Subramanian, K. (2019). Phenotypic and Molecular Characterization of *Chaetomium globosum* (Gustav Kunze) from different microhabitats of Tamil Nadu. *International Journal of Current Microbiology and Applied Sciences*, *8*(6), 1496-1506.

Shaker, K. H.,Zohair, M. M.,Hassan, A. Z.,Sweelam, H.-t. M., & Ashour, W. E. (2022). LC–MS/MS and GC–MS based phytochemical perspectives and antimicrobial effects of endophytic fungus *Chaetomium ovatoascomatis* isolated from Euphorbia milii. *Archives of Microbiology*, *204*(11), 661.

Shaw, D. (1998). Phytophthora Diseases Worldwide. *Journal of Agricultural Science*, *131*(2), 245-249.

Shi, Q. (2015). *Flg22-triggered immunity correlates with canker resistance and Huanglongbing tolerance; the role of FLS2 in the improvement of citrus bacterial disease resistance* University of Florida].

Sibounnavong, P.,Charoenporn, C.,Kanokmedhakul, S., & Soytong, K. (2011a). Antifungal metabolites from antagonistic fungi used to control tomato wilt fungus *Fusarium oxysporum f. sp. lycopersici*. *African Journal of Biotechnology*, *10*(85), 19714-19722.

Sibounnavong, P.,Charoenporn, C.,Kanokmedhakul, S., & Soytong, K. (2011b). Antifungal metabolites from antagonistic fungi used to control tomato wilt fungus *Fusarium oxysporum f. sp. lycopersici*. *African Journal of Biotechnology*, *10*(85), 19714-19722.

Singh, A.,Singh, V. K.,Dwivedy, A. K.,Tiwari, S.,Dwivedi, A., & Dubey, N. K. (2020). Biological Control of Plant Diseases: Opportunities and Limitations. In *Plant Microbiome Paradigm* (pp. 121-146). Springer.

Somdej, K.,Somlit, V.,Kaunchai, K., & Soytong, K. (2018). Nano-particle derived from *chaetomium cuprem* cc3003 against Anthracnose of coffee var. Arabica. *International Journal of Plant Biology*, *9*(1), 47-51.

Somsri, S. (2011). Current status of durian breeding program in Thailand. International Symposium on Tropical and Subtropical Fruits 1024,

Song, J.,Soytong, K., & Kanokmedhakul, S. (2017). Fungal metabolites of Chaetomium lucknowense for inhibition of a rice blast pathogen, Pyricularia oryzae. *International Journal of Agricultural Technology*, *13*(7.2), 1621-1626.

Song, J.,Soytong, K.,Kanokmedhakul, S.,Kanokmedhakul, K., & Poeaim, S. (2020). Antifungal activity of microbial nanoparticles derived from Chaetomium spp. against *Magnaporthe oryzae* causing rice blast. *Plant Protection Science*, *56*(3), 180-190.

Sour, V.,Phonpho, S., & Soytong, K. (2015). Antifungal activities of endophytic fungi isolated from orchids against *Colletotrichum gloeosporioides* caused anthracnose in orchids. *Internal Journal of Agricultural Technology*, *11*(8), 1949-1961.

Soytong, K. (2010). Evaluation of Chaetomium-biological fungicide to control Phytophthora stem and root rot of durian. *Research Journal*, *3*, 117-124.

Soytong, K. (2015). Testing bioformulation of Chaetomium elatum ChE01to control Fusarium wilt of tomato. *Intenational Journal of Agriculture and Technology*, *11*(4), 975-996.

Soytong, K.,Chamaiporn, C., & Somdej, K. (2013). Evaluation of microbial elicitors to induce plant immunity for tomato wilt. *African Journal of Microbiology Research*, *7*(19), 1993-2000.

This material is reserved for educational use only, not allowed for commercial use.

Forbidden to modify the content, and cite the document when use.

Soytong, K.,Kanokmedhakul, S.,Kukongviriyapa, V., & Isobe, M. (2001). Application of Chaetomium species (Ketomium) as a new broad spectrum biological fungicide for plant disease control. *Fungal diversity*, *7*, 1-15.

Soytong, K., & Quimio, T. (1989). Antagonism of *Chaetomium globosum* to the rice blast pathogen, *Pyricularia oryzae*. *Agricuture and Natural Resources*, *23*(2), 198-203.

Soytong, K., & Quimio, T. (1992). Antagonism of Chaetomium cupreum to Pyricularia oryzae. *Journal of Plant Protection in the Tropics*, *9*(1), 17-23.

Soytong, K., & Ratanacherdchai, K. (2005). Application of mycofungicide to control late blight of potato. *Intenational Journal of Agriculture and Technology*, *1*(1), 19-32.

Steffens, J.,Pell, E., & Tien, M. (1996). Mechanisms of fungicide resistance in phytopathogenic fungi. *Current Opinion in Biotechnology*, *7*, 348-355.

Stephan, D.,Schmitt, A.,Carvalho, S. M.,Seddon, B., & Koch, E. (2005). Evaluation of biocontrol preparations and plant extracts for the control of *Phytophthora infestans* on potato leaves. *European Journal of Plant Pathology*, *112*(3), 235-246.

Studholme, D. J.,Harris, B.,Le Cocq, K.,Winsbury, R.,Perera, V.,Ryder, L., Grant, M. (2013). Investigating the beneficial traits of *Trichoderma hamatum* GD12 for sustainable agriculture insights from genomics. *Frontiers in Plant Science*, *4*, 258.

Suksiri, S.,Laipasu, P.,Soytong, K., & Poeaim, S. (2018). Isolation and identification of Phytophthora sp. and Pythium sp. from durian orchard in Chumphon Province, Thailand. *International Journal of Agricultural Technology*, *14*, 389-402.

Sun, H.,Yang, J.,Lin, C.,Huang, X.,Xing, R., & Zhang, K.-Q. (2006). Purification and properties of a β-1, 3-glucanase from Chaetomium sp. that is involved in mycoparasitism. *Biotechnology Letters*, *28*(2), 131-135.

Talubnak, C., & Soytong, K. (2010). Biological control of vanilla anthracnose using *Emericella nidulans*. *International Journal of Agricultural Technology*, *6*(1), 47-55.

Tamura, K., & Nei, M. (1993). Estimation of the number of nucleotide substitutions in the control region of mitochondrial DNA in humans and chimpanzees. *Molecular Biology Evolution*, *10*(3), 512-526.

Tathan, S.,Sibounnavong, P.,Sibounnavong, P.,Soytong, K., & To-anun, C. (2012). Biological metabolites from Chaetomium spp to inhibit *Drechslera oryzae* causing leaf spot of rice. *Intenational Journal of Agriculture and Technology*, *8*(5), 1691-1701.

Thongkham, D.,Soytong, K., & Kanokmedhakul, S. (2017a). Efficacy of nano particles from *Chaetomium cupreum* to control Phytophthora spp. causing root rot of durian. *International Journal of Agricultural Technology*, *13*(7.1), 1295-1300.

Thongkham, D.,Soytong, K., & Kanokmedhakul, S. (2017b). Efficacy of nano particles from Chaetomium cupreum to control Phytophthora spp. causing root rot of durian. *Intenational Journal of Agriculture and Technology*, *13*(7.1), 1295-1300.

Thongkham, D.,Soytong, K., & Kanokmedhakul, S. (2017c). Efficacy of nano particles from *Chaetomium cupreum* to control Phytophthora spp. causing root rot of durian. *Internal Journal of Agricultural Technology*, *13*(7.1), 1295-1300.

This material is reserved for educational use only, not allowed for commercial use.

Forbidden to modify the content, and cite the document when use.

Thongkham, D.,Soytong, K.,Kanokmedhakul, S., & Kanokmedhakul, K. (2018). Nanoparticles derived from Chaetomium elatum against Phytophthora rot of durian. *Internatiomnal Journal of Agricultural Technology*, *14*(7), 2115-2124.

Tongon, R., & Soytong, K. (2021). Application of *Chaetomium cochliodes* CTh02 to against durian root rot cause by *Phytophthora palmivora* RT01. *International Journal of Agricultural Technology*, *17*(2), 753-766.

Tongon, R., & Soytong, K. (2022). Nanoparticles Derived from Active Metabolites of *Chaetomium cupreum* CC3003 against Phytophthora Rot of Durian. *International Journal of Agriculture and Biology*, *27*(1), 19-27.

Tongon, R.,Soytong, K.,Kanokmedhakul, S., & Kanokmedhakul, K. (2018). Nano-particles from *Chaetomium brasiliense* to control *Phytophthora palmivora* caused root rot disease in durian var Montong. *International Journal of Agricultural Technology*, *14*, 2163-2170.

Treetong, W.,Soytong, K., & Kanokmedhakul, S. (2000). Integrated biological control of Shogun orange (Citrus reticulata Blanco cv. Shogun) root and stem rot. *Wichai lae Songsoem Wichakan Kaset*, *17*(2), 31-42.

Tveit, M., & Moore, M. (1954). Isolate of Chaetomium That Protect Oats from Helminthosporium-Victoriae. *Phytopathology*, *44*(12), 686-689.

U.G. (1990). PCR protocols a guide to methods and applications. *Trends in Biochemical Sciences*, *15*, 405–406.

Udagawa, S.,Muroi, T.,Kurata, H.,Sekita, S.,Yoshihira, K.,Natori, S., & Umeda, M. (1979). The production of chaetoglobosins, sterigmatocystin, O-methylsterigmatocystin, and chaetocin by Chaetomium spp. and related fungi. *Canadian Journal of Microbiology*, *25*(2), 170-177.

Udompongsuk, M.,Kanokmedhakul, S., & Soytong, K. (2017). Efficacy of nano particles from Chaetomium cochliodes to control Pythium spp. causing root rot of tangerine (Citrus reticulata). *International Journal of Agricultural Technology*, *13*(7.1), 1251-1257.

Van der Plaats-Niterink, A. (1981). Monograph of the genus Pythium. *Studies in Mycology*(21).

Vanneste, J. L.,Farrell, R. L., & Holland, P. T. (2002). Biological control of sapstain fungi with natural products and biological control agents: a review of the work carried out in New Zealand. *Mycological Research*, *106*(2), 228-232.

Vawdrey, L.,Langdon, P., & Martin, T. (2005). Incidence and pathogenicity of *Phytophthora palmivora* and *Pythium vexans* associated with durian decline in far northern Queensland. *Australasian Plant Pathology*, *34*(1), 127-128.

Vidyalakshmi, A., & Divya, C. V. (2013). New report of *Colletotrichum gloeosporioides* causing anthracnose of Pisonia alba in India. *Archives of Phytopathology and Plant Protection*, *46*(2), 201-204.

Walters, D.,Walsh, D.,Newton, A., & Lyon, G. (2005). Induced resistance for plant disease control: maximizing the efficacy of resistance elicitors. *Phytopathology*, *95*(12), 1368-1373.

Wang, W.,De Silva, A. G. D.,Moslemi, A.,Edwards, J.,Ades, P.,Crous, P. W., & Taylor, P. (2021a). *Colletotrichum* species causing anthracnose of citrus in Australia. *Journal of Fungi*, *7*(1), 47.

Wang, W.,de Silva, D. D.,Moslemi, A.,Edwards, J.,Ades, P. K.,Crous, P. W., & Taylor, P. W. (2021b). Colletotrichum species causing anthracnose of citrus in Australia. *Journal of Fungi*, *7*(1), 47.

This material is reserved for educational use only, not allowed for commercial use.

Forbidden to modify the content, and cite the document when use.

Wang, X.,Houbraken, J.,Groenewald, J.,Meijer, M.,Andersen, B.,Nielsen, K., Samson, R. (2016). Diversity and taxonomy of Chaetomium and chaetomium-like fungi from indoor environments. *Studies in Mycology*, *84*, 145-224.

WorldAtlas. (2017). *The World's Top Citrus Producing Countries*. Retrieved 27 April from

Yahia, E. M. (2011). Postharvest biology and technology of tropical and subtropical fruits: Mangosteen to white sapote (Vol. 4). Elsevier.

Younesi, H.,Bazgir, E.,Darvishnia, M., & Chehri, K. (2021). Selection and control efficiency of Trichoderma isolates against *Fusarium oxysporum* f. sp. ciceris in Iran. *Physiological Molecular Plant Pathology*, *116*, 101731.

Yun , Z.,Yang, Y.,Wang, A.,Xue, C.,Zhao, M., & Zhang, J. (2023). Transcriptome reveals the molecular mechanism of chaetoviridin A inhibiting the spore germination of *Verticillium dahliae*. *Journal of Plant Pathology*, 1-13.

This material is reserved for educational use only, not allowed for commercial use.
Forbidden to modify the content, and cite the document when use.

AUTHOR BIOGRAPHY

Name: Mr. Pheaktra Phal

Date of Birth: 06/07/1990

Address: Pheam village, Bovel commune, Bovel district, Battambang province, Cambodia

Email: 62604009@kmitl.ac.th

Education Background

2018 Bachelor of Science (Plant Production Technology), Faculty of Agricultural Technology, Rajamongala University of Technology Tawan-OK Chanthaburi.

2024 Master and Doctor of Philosophy in Agriculture, School of Agricultural Technology, King Mongkut's Institute of Technology Ladkrabang.

This material is reserved for educational use only, not allowed for commercial use.
Forbidden to modify the content, and cite the document when use.

APPENDIX

Publication

Phal P, Soytong K and Poeaim S, 2023. Natural product nanofibers derived from *Trichoderma hamatum* K01 to control citrus anthracnose caused by *Colletotrichum gloeosporioides*. Open Agric., 8(1): 1-15. Available from https://doi.org/10.1515/opag-2022-0193.

Phal P, Soytong K and Poeaim S. A new nanofibre derived from *Trichoderma hamatum* K01 to control durian rot caused by *Phytophthora palmivora*. Asian J. Agric. Biol. 2024(2): 2023182. DOI: https://doi.org/10.35495/ajab.2023.182.

This material is reserved for educational use only, not allowed for commercial use.
Forbidden to modify the content, and cite the document when use.